

## Vessel Noise Correlation Study

### ECHO Program Study Summary

This study was undertaken for Vancouver Fraser Port Authority's (VFPA) Enhancing Cetacean Habitat and Observation (ECHO) Program to use the large dataset of vessel source level measurements collected by the program to better understand underwater radiated noise from marine vessels. The ECHO Program Acoustic Technical Committee developed a list of vessel design characteristics expected to be correlated with vessel source levels, which could be compared to the existing source level dataset to look for trends.

This summary document describes how and why the project was conducted, its key findings and conclusions.

### What questions was the study trying to answer?

The vessel noise correlations study investigated three main questions:

- Which key vessel design characteristics drive noise differences between different vessels independently and as a vessel class?
- Which key vessel design characteristics result in the lowest noise emissions?
- Does a vessel's operational draft affect its underwater noise emissions?

In addition to the key questions above, a high-level comparison of vessel noise emissions against the Existing Vessel Design Index (EVDI) database, which contains greenhouse gas emissions data, was conducted.

### Who conducted the project?

To address these research questions, Vancouver Fraser Port Authority retained a team led by JASCO Applied Sciences (Canada) Ltd., the developer of the automated vessel source level measurement software used by the ECHO Program. JASCO worked with ERM to develop a statistical model to associate vessel design characteristics with underwater radiated noise measurements. Aspects of the statistical model were developed in consultation with a subject matter expert team, consisting of an experienced noise control engineer from Acentech and an experienced naval architect from Bay Marine Inc.

### What methods were used?

This project used data from four different databases to investigate correlations between vessel noise emissions, design characteristics and operating conditions for six major commercial vessel categories: bulker/general cargo carriers; container ships; large passenger/cruise ships; tankers; tugboats; and vehicle carriers.

The databases used for the correlation analysis included:

- ECHO Program vessel source level database from September 2015 to April 2018 (3671 accepted measurements collected from 1618 unique vessel)
- Database of general vessel characteristics from Lloyd's List Intelligence for the 1618 unique vessels
- Pacific Pilotage Authority transit logs articulating actual draft of the vessel at the time of measurement
- EVDI database containing greenhouse gas (GHG) emissions data and ratings from RightShip

From the combined datasets, variables which may have influenced noise emissions were grouped into three categories:

- Design: variables that relate to design characteristics of a marine vessel, such as gross tonnage or overall length, and remain constant over time
- Operational: variables that relate to operational characteristics of a marine vessel, such as speed through water and actual draft, which change between repeat measurements of the same vessel
- Method: variables that relate to the measurement methods, such as distance from hydrophone, which may also change between repeat measurements of the same vessel

A statistical model of the relationships between vessel design characteristics, vessel operational characteristics, and vessel noise emissions was developed. Graphs and summary statistics (scatter plots and correlation matrices) revealed the relationships between the variables and helped identify the vessel design and operational characteristics with the strongest influence on vessel radiated noise. The identified characteristics were carried forward and used at the statistical modelling stage. Analysis (principal components analysis) of the inter-relationships between vessel design characteristics revealed clusters of vessels, and vessel types, with similar design characteristics. The information from these initial analyses was used to build the statistical model (functional regression) of the relationships between vessel design and operational characteristics, and frequency-dependent vessel noise emissions. Physical models for wind and ocean currents were included in the regression model to control for the effects of environmental conditions. Then, a more complex functional regression model was developed to determine which combinations of design and operational variables best predicted variations in underwater radiated noise level for different frequency bands and vessel categories.

A detailed investigation was completed to look for commonalities between the loudest and quietest vessels, using high-resolution spectrum data for a sample of 30 of the loudest and 30 of the quietest vessel measurements.

## What were the key findings?

The main findings of the vessel noise correlation analysis are summarized as follows:

- Vessel size (length) was ranked as the design characteristic with the strongest correlation to underwater radiated noise. Other design characteristics related to vessel size, such as displacement, gross tonnage and beam, were strongly correlated with length, making it difficult to separate their influence on underwater radiated noise.
- Main engine RPM, main engine power, auxiliary engine power and design speed were also correlated with underwater radiated noise, but to a lesser degree than vessel size. Furthermore, the relative strengths of these correlations were not always consistent between vessel categories.
- None of the individual design characteristics investigated in this study were found to be associated with those vessels having the lowest noise emissions. Instead, specific vessel operating conditions, including reduced speed through water and reduced draft, were most strongly associated with the lowest noise emissions.
- Of the operational parameters, actual draft was found to be very influential on vessel noise emissions, second only to speed through water. Actual draft had a strong positive correlation with radiated noise above 100 Hz, where deeper drafts were associated with higher noise emissions. The greatest influence of draft was above 1000 Hz, where cavitation dominates the noise spectrum.
- Statistical analysis of noise correlations for the tug category was challenging as there were many predictors with a large fraction of missing data in the Lloyd's List database, and no information on whether vessels were involved in towing while under measurement (which is expected to affect propeller loading and thus influence noise emissions).
- For cruise vessels, the small number of unique vessels and relatively small number of total measurements meant that this category was data-deficient from a statistical perspective, limiting the ability to infer significant correlations with design characteristics.
- Analysis of high-resolution spectrum data for a sample of 30 loud and 30 quiet vessel measurements indicated that the loud vessels exhibited a distinct cavitation noise hump near 50 Hz whereas the quiet vessels exhibited a flatter spectrum below 100 Hz.
- The high-resolution spectrum data also showed that the loud vessels generally exhibited a smaller number of discrete tones than the quiet vessels, which was attributed to masking of machinery tones by

wide-band cavitation noise. No clear differences in design characteristics were evident between the loud and quiet vessels, other than the loud vessels tended to be larger in size in some (but not all) categories.

- When investigating CO<sub>2</sub> emissions against noise emissions using the EVDI ranking, the containers and vehicle carriers with a higher intensity of CO<sub>2</sub> emissions were slightly quieter, whereas for the bulkers and tankers category vessels with higher CO<sub>2</sub> emissions intensity also had slightly higher underwater noise. In both instances, these trends were relatively weak, and do not indicate a conclusive correlation between EVDI and underwater noise emissions.

## Conclusions and next steps

The investigation of vessel design characteristics and their influence on underwater radiated noise, as represented by the ECHO Program vessel source level database, found that vessel size was the design characteristic most strongly related to underwater radiated noise. The two main operational characteristics investigated, speed through water and actual draft, had the strongest correlation with underwater radiated noise in all vessel categories.

With the exception of vessel size (as represented by length overall in the statistical model), no other general design characteristics that are publicly available through Lloyd's List Intelligence were found to have a significant correlation to vessel noise emissions. It should be noted that other design characteristics that are known to influence transmission of machinery noise through the hull (such as hull insulation and resilient mounting or rafting of engines) were not available for this study. Additionally, other vessel design characteristics likely to influence cavitation and underwater noise emissions (such as number and diameter of propeller blades or wake flow modifiers) were also not publicly available.

Future iterations of the vessel noise correlations project will seek to use the ECHO Program's vessel source level database to confirm the findings of this study, and to further investigate correlations with design characteristics not available through the Lloyd's List Intelligence database used for this study.



# ECHO Vessel Noise Correlations Study

---

## Final Report

Submitted to:  
Krista Trounce  
Vancouver Fraser Port Authority ECHO Program  
*Contract: 19-0071(01)*

Authors:

Alexander MacGillivray<sup>1</sup>  
Laurie Ainsworth<sup>2</sup>  
Joanna Zhao<sup>2</sup>  
Heloise Frouin-Mouy<sup>1</sup>  
Joshua Dolman<sup>1</sup>  
Michael Bahtiarian<sup>3</sup>

19 May 2020

P001475-001  
Document 02025  
Version 2.1

<sup>1</sup>**JASCO Applied Sciences (Canada) Ltd**  
Suite 2305, 4464 Markham St.  
Victoria, BC V8Z 7X8 Canada  
Tel: +1-250-483-3300  
Fax: +1-250-483-3301  
[www.jasco.com](http://www.jasco.com)

<sup>2</sup>**ERM**  
1111 West Hastings St.  
Vancouver, BC V6E 2J3 Canada  
Tel: +1-604-689-9460  
Fax: +1-604-687-4277  
[www.erm.com](http://www.erm.com)

<sup>3</sup>**Acentech**  
33 Moulton St.  
Cambridge, MA 02138 USA  
[www.acentech.com](http://www.acentech.com)



Suggested citation:

MacGillivray, A.O., L. Ainsworth, J. Zhao, H. Frouin-Mouy, J. Dolman, and M. Bahtiarian. 2020. *ECHO Vessel Noise Correlations Study: Final Report*. Document 02025, Version 2.1. Technical report by JASCO Applied Sciences, ERM, and Acentech for Vancouver Fraser Port Authority ECHO Program.

Disclaimer:

The results presented herein are relevant within the specific context described in this report. They could be misinterpreted if not considered in the light of all the information contained in this report. Accordingly, if information from this report is used in documents released to the public or to regulatory bodies, such documents must clearly cite the original report, which shall be made readily available to the recipients in integral and unedited form.

# Contents

1. INTRODUCTION .....	1
2. METHODS.....	5
2.1. Dataset Overview .....	5
2.1.1. Predictor variables .....	6
2.1.2. Vessel source levels .....	8
2.2. Data Review and Evaluation .....	10
2.2.1. Data cleanup and conditioning .....	10
2.2.2. Missingness .....	10
2.2.3. Exploratory Analysis .....	12
2.3. Physical models and derived quantities .....	13
2.4. Data Imputation .....	18
2.5. Statistical Model Development .....	21
2.5.1. Repeat Measurements .....	21
2.5.2. Principal Components Analysis (PCA) .....	22
2.5.3. Functional Data Analysis .....	23
2.5.4. Functional PCA .....	23
2.5.5. Vessel Category Groupings .....	23
2.5.6. Variable Selection .....	23
2.5.7. Functional Regression .....	24
2.6. Spectrum Analysis .....	25
3. RESULTS .....	27
3.1. Exploratory Analysis .....	27
3.2. Correlation Analysis .....	28
3.3. Principal Component Analysis of Design Characteristics .....	29
3.4. Functional Principal Component Analysis of Source Levels .....	31
3.5. Single-Predictor Functional Regression .....	32
3.6. Variable Selection .....	34
3.7. Multiple-Predictor Functional Regression .....	35
3.8. Correlations with Greenhouse Gas Emissions .....	40
3.9. Spectrum Analysis .....	43
4. DISCUSSION .....	46
4.1. RNL versus MSL .....	46
4.2. Influence of Speed and Draft .....	47
4.3. Influence of Design Characteristics .....	48
5. SUMMARY AND CONCLUSIONS .....	50
GLOSSARY .....	52
LITERATURE CITED .....	56
APPENDIX A. DESCRIPTION OF VARIABLES IN MERGED DATABASE .....	A-1
APPENDIX B. CORRELATION MATRICES .....	B-1

APPENDIX C. MULTIPLE-PREDICTOR FUNCTIONAL REGRESSION RESULTS.....	C-1
APPENDIX D. SPECTRUM PLOTS .....	D-1

## Figures

Figure 1. Map showing location of Strait of Georgia underwater listening station (ULS) and Haro Strait slowdown trial Autonomous Multichannel Acoustic Recorders (AMARs). .....	1
Figure 2. Diagram of databases utilized in the present study.....	6
Figure 3. Spectrogram of a single vessel measurement from ShipSound .....	8
Figure 4. Plot of decade Monopole Source Level (MSL) (top) and Radiated Noise Level (RNL) (bottom) versus frequency from ECHO source level database .....	9
Figure 5. Missingness of candidate predictor variables considered in this study, by vessel category. ....	11
Figure 6. Missingness of Monopole Source Level (MSL) and Radiated Noise Level (RNL) data, in decade bands. ....	12
Figure 7. Diagram of speed through water calculation .....	13
Figure 8. Plot of heading coefficient used in wind resistance calculation .....	14
Figure 9. Diagram of apparent wind speed calculation.....	14
Figure 10. Calculated wind resistance factor versus wind speed for all measurements in the merged vessel noise database. ....	15
Figure 11. Diagram of surface angle calculation.....	15
Figure 12. Violin plot of block coefficient, per vessel category. ....	16
Figure 13. Violin plot of fractional speed through water, per vessel category. ....	17
Figure 14. Violin plot of fractional draft, per vessel category. ....	17
Figure 15. Illustration of spline imputation method for intermediate frequencies. ....	20
Figure 16. Plot showing the results of the high-frequency imputation method (spectral slope extrapolation), applied to 10 random measurements of container ships. ....	20
Figure 17. Histogram of number of repeat measurements per vessel .....	21
Figure 18. Diagram illustrating how to interpret a biplot. ....	22
Figure 19. Example showing stepwise addition of predictors to a multiple-predictor functional regression model. ....	25
Figure 20. Illustration of the tone detection method.....	26
Figure 21. Illustration of slope calculation method.....	26
Figure 22. Density plots (smoothed histograms) of operational variables, by vessel category. ....	27
Figure 23. Correlation matrix, showing correlations between pairs of variables for the Bulker category. ....	28
Figure 24. Scree plot showing proportion of variance versus PC number (all categories).....	30
Figure 25. Biplot of first two principal components (PC1 versus PC2) of vessel design parameters (all vessel categories). ....	30
Figure 26. Functional principal component analysis (FPCA) of vessel Monopole Source Level (MSL) versus $\log_{10}$ frequency (all categories). ....	31
Figure 27. Biplot of first two functional principal components (PC1 versus PC2) of vessel source levels (all vessel categories). ....	32
Figure 28. Coefficient of determination ( $r^2$ ) versus $\log(\text{frequency})$ for single-predictor functional regression of actual draft and Monopole Source Level (MSL) (left) and Radiated Noise Level (RNL) (right), for Bulklers and Tankers.....	33

Figure 29. Regression function $\beta(f)$ (i.e., frequency-dependent slope coefficient) versus log(frequency) for actual vessel draft (Bulkers and Tankers).....	33
Figure 30. Plots showing collinearity of size-related predictors: LOA.LLI, BREADTH.MOULDED.LLI, GROSS.LLI, and DISPLACEMENT.LLI.....	36
Figure 31. Coefficient of determination ( $r^2$ ) versus log(frequency) obtained from incrementally adding predictors to the multiple-predictor functional regression model for Bulkers and Tankers (Monopole Source Level (MSL)).....	38
Figure 32. Monopole Source Level (MSL) regression functions $\beta(f)$ (i.e., frequency-dependent slope coefficients) versus log(frequency) for all predictors for the Bulker and Tanker group.....	39
Figure 33. Plots of predicted Monopole Source Level (MSL) (dB re 1 $\mu$ Pa m) versus log(frequency) from the multiple-predictor functional regression model, for Bulkers and Tankers. ....	40
Figure 34. Left: scatter plots of adjusted decade-band RNL (dB re 1 $\mu$ Pa m) versus EVDI (grams CO <sub>2</sub> per tonne nautical mile).....	42
Figure 35. Plot of source spectrum density level versus frequency for Bulkers .....	43
Figure 36. Total number of tones per decade band identified in the loud and quiet vessel spectrum measurements. ....	44
Figure 37. Plot of Radiated Noise Level (RNL) versus frequency of all tones identified in spectra of loud and quiet vessels. ....	45
Figure 38. Comparison of Radiated Noise Level (RNL) and Monopole Source Level (MSL) versus frequency for the same containership measurement. ....	47

## Tables

Table 1. Summary of source level measurements collected by the ECHO Program during the period September 2015 through April 2018.....	2
Table 2. Vessel design and other characteristics recommended by the ECHO Acoustic Technical Committee (ATC) as being most likely to affect vessel underwater radiated noise. ....	3
Table 3. Summary of merged vessel noise database.....	6
Table 4. Candidate predictor variables from the merged vessel noise database.....	7
Table 5. Summary of imputation methods for predictor variables. ....	19
Table 6. Results of variable selection for multivariate analysis. ....	34
Table 7. Best-fit trend line parameters of adjusted RNL versus EVDI data as determined by linear regression analysis. ....	43
Table 8. Statistics of numbers of tones and spectral slope (mean $\pm$ standard deviation) for the loud and quiet vessel spectrum measurements. ....	44
Table 9. Ranking of design parameters, based on a qualitative review of the functional multiple regression analysis results for Bulkers & Tankers, Containers & Vehicle Carriers, and Tugs. ....	49
Table A-1. Description of all the variables captured in the merged vessel noise database. ....	A-1
Table D-1. Operating and design characteristics of the vessels shown in the spectrum plots.....	D-1

## List of Annexes

- Annex 1: Vessel Noise Exploratory Analysis  
(FINAL\_01\_ECHO-noise-vessel\_exploratory-analysis\_2020-03-30.html)
- Annex 2: Vessel Characteristic PCA Analysis  
(FINAL\_02\_ECHO-noise-vessel\_pca-analysis\_2020-03-30.html)
- Annex 3: Vessel Noise Profile Functional Principal Components Analysis  
(FINAL\_03\_ECHO-vessel-noise\_fpca-analysis\_2020-05-07.html)
- Annex 4: Vessel Noise Profile Functional Regression Analysis  
(FINAL\_04\_ECHO\_Vessel\_Noise\_functional-reg-review\_2020-01-07.html)
- Annex 5: Vessel Noise Profile Multiple Functional Regression Analysis  
(FINAL\_05\_ECHO-vessel-noise\_functional-regression-mva\_2020-05-07.html)

*Note: Annexes 1-5 contain information that is confidential to the Vancouver Fraser Port Authority. They are not publicly available documents.*

# 1. Introduction

Understanding underwater radiated noise from marine vessels is a priority study area for the Vancouver Fraser Port Authority's (VFPA) Enhancing Cetacean Habitat and Observation (ECHO) Program. Thus, between September 2015 and April 2018, a comprehensive database of vessel source level measurements was collected by the ECHO Program, in partnership with JASCO Applied Sciences (JASCO), Ocean Networks Canada, and Transport Canada. Source level measurements were collected on the Strait of Georgia Underwater Listening Station (ULS), as well as on two Autonomous Multichannel Acoustic Recorder (AMAR) systems deployed during the 2017 voluntary slowdown trial in Haro Strait (Figure 1). The ECHO database was collected using JASCO's ShipSound system and includes measurements of multiple commercial vessel types, identified through correlation of acoustic measurements to the automated identification system (AIS) (by Maritime Mobile Service Identity (MMSI) or International Maritime Organization (IMO) number). The ECHO database includes each vessel's Radiated Noise Level (RNL)<sup>1</sup>, Monopole Source Level (MSL), closest point of approach (CPA) to the station, speed, and other key parameters. Table 1 provides a summary of the numbers of accepted source level measurements from each site.

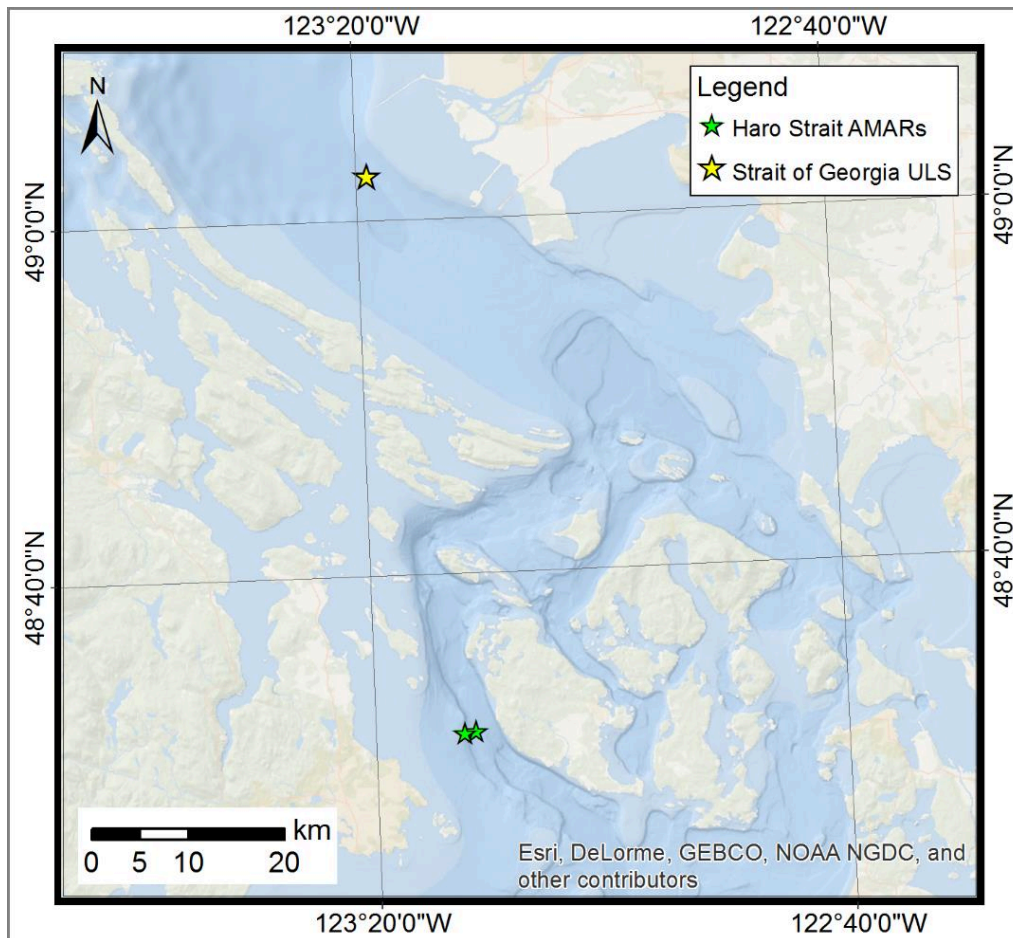


Figure 1. Map showing location of Strait of Georgia underwater listening station (ULS) and Haro Strait slowdown trial Autonomous Multichannel Acoustic Recorders (AMARs). The ECHO vessel noise database contained source level data from instruments situated at these three measurement locations.

<sup>1</sup> RNL was measured approximately to ANSI S12.64 standard (ANSI/ASA S12.64/Part 1 2009).

Table 1. Summary of source level measurements collected by the ECHO Program during the period September 2015 through April 2018.

	<b>Strait of Georgia ULS</b>	<b>Haro Strait slowdown trial</b>
Dates	Sep 2015 to Apr 2018	7 Aug 2017 to 6 Oct 2017
Number of QC accepted measurements	2351 (northbound only)	725 (northbound) 847 (southbound)
Transits with operational data from PPA	1717 (northbound only)	636 (northbound) 709 (southbound)

In February 2018, ECHO convened a meeting of their Acoustic Technical Committee (ATC) to identify how these measurements could be used to better understand factors driving underwater radiated noise from vessels. The goal of the ATC meeting was to identify those design characteristics that were expected to be correlated with vessel source levels (Table 2), and to recommend methods for investigating their influence on underwater radiated noise using the ECHO database. Following the meeting, a scope of work was defined by the ECHO team, based on the recommendations of the ATC: to analyze the ECHO source level measurements, in conjunction with a database of vessel design characteristics from Lloyd's List Intelligence (LLI), to identify key design components or trends in vessel-generated underwater noise.

Table 2. Vessel design and other characteristics recommended by the ECHO Acoustic Technical Committee (ATC) as being most likely to affect vessel underwater radiated noise. Some of these characteristics were not available in the databases that were made available for this study. The stars (\*) denote predictors that were moved from Rank 2 to Rank 1 following the ATC review.

Ranked 1	Ranked 2	Ranked 3
Ship type	Main engine type	Number of auxiliary engines
Gross Tonnage	Number of main engines	Number of thrusters
Draught	Speed max	Propulsion type
Length overall (LOA)	Hull type code	Thrusters descriptive narrative
Date of build	Main engine number of cylinders	Total power of auxiliary engines
Hull shape code	Main engine stroke type	
Propeller type	Number of all engines	
Propulsion type code	Number of propulsion units	
Speed service		
Total kilowatts of main engines		
Displacement*		
Breadth moulded*		
Main engine RPM*		
Total power of all engines*		
<i>Additional vessel design data to consider/calculate</i>		
Block coefficient		
Propeller coefficient		
Propeller diameter		
Propeller RPM		
Shaft depth		
Type of engine integration mountings		
<i>Operational and other data to consider</i>		
Weather data		
Propeller pitch (if CPP)		
Operational status of auxiliary machinery		

The goal of this vessel noise correlation study was to use the ECHO and LLI databases to seek answers to the following questions:

1. Which key vessel design characteristics drive noise differences between different vessels independently and as a vessel class?
2. Which key vessel design characteristics result in the lowest noise emissions?
3. Does a vessel's operational draught affect its underwater noise emissions?

To address these research objectives, JASCO and ERM developed a statistical model to associate vessel design characteristics with underwater radiated noise measurements. Aspects of the statistical model were developed in consultation with a subject matter expert (SME) team, consisting of an experienced noise control engineer (Michael Bahtiaran, Acentech) and an experienced naval architect

(David Bonney, Bay Marine Inc.). The statistical model controls for operational characteristics of the vessels (i.e., speed and draft) and the measurement conditions (i.e., currents, wind resistance, and distance from hydrophone). The statistical model was used to identify how frequency-dependent source levels varied with design characteristics in six different categories: cruise ships, container ships, bulk carriers & general cargo ships, tankers, tugs, and vehicle carriers. This report describes the methods used to develop the statistical model and presents results of a detailed statistical analysis of the vessel source level database.

The noise correlation analysis involved the following steps:

1. Merging the four databases (ECHO, LLI, PPA, EVDI) into a single database, and identifying relevant predictor and response variable for statistical analysis.
2. Conditioning the data for analysis by removing outliers, correcting invalid data, and quantifying missingness in the predictor and response variables.
3. Performing exploratory analysis (e.g., using scatter plots and distribution plots) to identify features and trends in the data and to identify the need for data transformations.
4. Applying imputation procedures, where appropriate, to fill in missing values in the database (required for multiple-predictor models).
5. Calculating derived quantities, such as wind resistance and block coefficient, using physical models.
6. Subsampling repeat vessel measurements to ensure frequently measured vessels are not over-represented in the database.
7. Performing principal component analysis (PCA) to identify relationships between predictor variables.
8. Performing functional principal component analysis (FPCA) to identify modes of variability in source level measurements (RNL and MSL).
9. Grouping vessel categories and selecting predictor variables (including both operational conditions and design characteristics) for the functional regression analysis.
10. Performing functional regression analysis to identify frequency-dependent relationships between predictors and source level measurements (RNL and MSL), using both single-predictor and multiple-predictor models.
11. Performing correlation analysis between GHG emissions data and source level measurements adjusted for vessel operating conditions (using the functional regression model).
12. Qualitatively reviewing detailed spectrum level data for a selected subset of measurements to identify commonalities between loud and quiet vessels.

Section 2 of this report describes the methods for each step of the data analysis. Section 3 presents results from each step of the data analysis. Section 4 provides a discussion of the results, focusing on the stated research objectives of the project. Finally, Section 5 provides a summary and the conclusions from this research.

## 2. Methods

### 2.1. Dataset Overview

This project utilized data from four different databases to investigate correlations between vessel noise emissions, design characteristics, and operating conditions (Figure 2). This research project was limited to commercial vessels in the following six categories:

- Bulker carriers and general cargo ships,
- Container ships,
- Cruise ships (i.e., passenger vessels greater than 100 m length, excluding ferries<sup>2</sup>)
- Tankers
- Tugs
- Vehicle carriers

Each measurement in the ECHO database was matched to records from the LLI, EVDI, and PPA databases based on IMO number, whenever possible. The IMO number is a 7-digit code that uniquely identifies large cargo vessels (>300 gross tons) and large passenger vessels (>100 gross tons). In cases where a IMO number was unavailable, or was recorded incorrectly, records were instead matched on the basis of MMSI or by vessel name. IMO numbers, MMSI numbers, and vessel names in the ECHO database were obtained from the Automated Information System (AIS), as broadcast at the time of measurement. Data from all four databases were merged into a single vessel noise database for subsequent analysis. Appendix A provides descriptions of all the variables captured in the merged vessel noise database.

Vessels that could not be matched to an entry in the LLI database were excluded from the analysis (22 total). Only measurements that passed a manual quality review (i.e., with qcStatus = "Accepted") were retained for subsequent statistical analysis. A total of 3671 accepted measurements of 1618 unique vessels met these criteria and were retained in the merged vessel noise database (Table 3).

---

<sup>2</sup> ULS measurements of BC Ferries and Seaspun Ferries vessels were analyzed in detail during two prior ECHO studies (MacGillivray and Li 2016, MacGillivray et al. 2017).

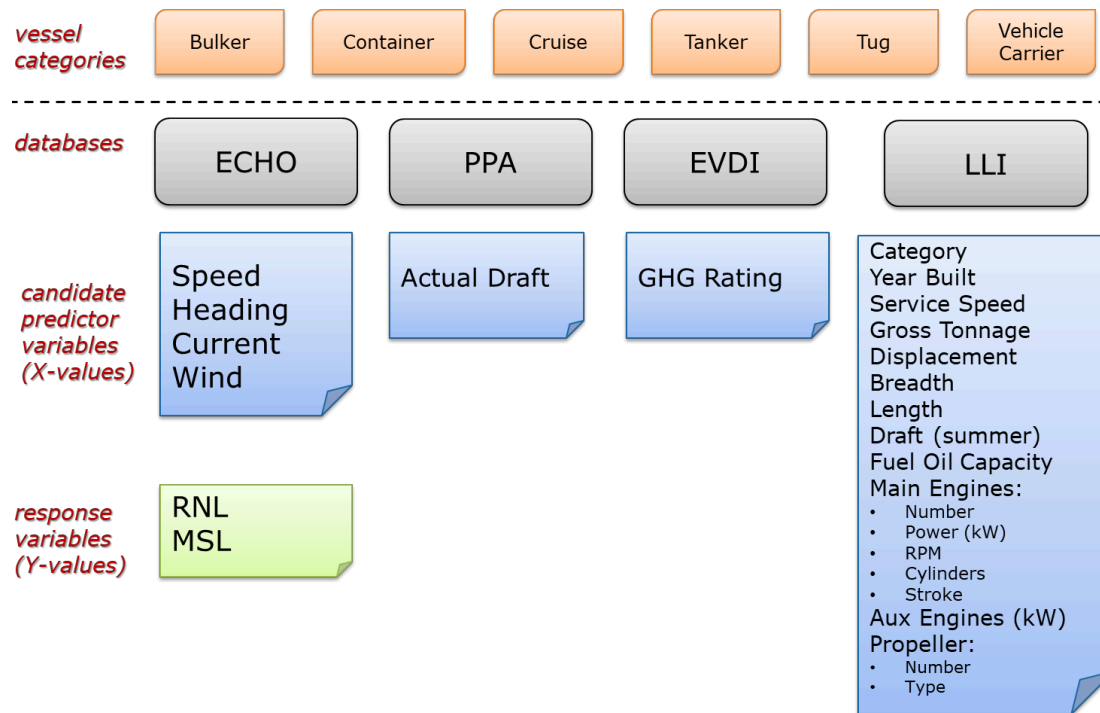


Figure 2. Diagram of databases utilized in the present study. Blue boxes contain predictors variables, and green box contains response variables. ECHO = Enhancing Cetacean Habitat and Observation Program vessel noise database includes the source level measurements and measurement conditions (including wind and currents). PPA = Pacific Pilotage Authority transit logs provide records of actual vessel draft at the time of transit, as recorded by on-duty pilots. EVDI = Existing Vessel Design Index database: contains greenhouse gas (GHG) emissions data and emissions ratings from RightShip. LLI = Lloyd's List Intelligence database: contains those vessel design characteristics identified by the ATC that were available from Lloyd's Register of Shipping.

Table 3. Summary of merged vessel noise database.

Accepted measurements	Unique vessels	Total variables (not all used)
3671	1618	183

### 2.1.1. Predictor variables

Predictor variables are those variables that may have influenced underwater noise emissions (these are often referred to as independent variables, or x-values, in a statistical context). Three types of predictor variables were considered in this study:

- **Design:** Variables that relate to design characteristics of a marine vessel (e.g., gross tonnage). These variables remain constant between repeat measurements of the same vessel.
- **Operational:** Variables that relate to operational characteristics of a marine vessel (e.g., speed through water). These variables may change between repeat measurements of the same vessel.
- **Method:** Variables that relate to the measurement method (e.g., distance from hydrophone). These variables may also change between repeat measurements of the same vessel.

Candidate predictors were identified from all data sources captured in the merged vessel noise database (Table 4). These candidate predictors were evaluated during the data review and evaluation (Section 2.2), to determine which variables should be retained for subsequent statistical analysis.

Table 4. Candidate predictor variables from the merged vessel noise database.

Variable	Variable type	Description
actualVesselDraft	Operational	Actual vessel draft at time of measurement (m)
sow*		Speed through water (STW) (knots)
wind.resistance		Factor measuring resistance on the vessel due to apparent wind ( $m^2/s^2$ )
TYPE.LLI	Design	A Lloyds List code signifying the vessel type (categorical)
GROSS.LLI†		Gross tonnage
DRAFT.LLI		Maximum draft at summer load lines (m)
LOA.LLI		Overall length of the vessel (m)
YEAR.OF.BUILD.LLI		Year the vessel was built
SPEED.LLI		Design speed (knots)
DISPLACEMENT.LLI		Maximum displacement of the vessel, measured at summer load line (tonnes)
BREADTH.MOULDED.LLI		Maximum breadth of the vessel, measured at the moulded line of the frame (m)
MainEngine_Type.LLI		Engine type (categorical)
MainEngines_No.LLI		Number of main engines in the vessel
MainEngine_kW.LLI		Maximum rated power output of the main engines (kW)
MainEngine_RPM.LLI		Maximum rated RPM of the main engine
MainEngine_Cylinders.LLI		Number of cylinders in the main engine
MainEngine_StrokeType.LLI		Number of strokes the engine performs (2 or 4)
PropellerType.LLI		The type of propeller (categorical)
No_of_propulsion_units.LLI		Number of propulsive engines (corresponds to number of propellers)
AuxiliaryEngine_kW.LLI		Maximum rated power output of the auxiliary engines (kW)

\* Throughout this report "sow" refers to the name of the variable in the database, whereas "speed through water" or "STW" is used to refer to the quantity represented by this variable.

† Gross tonnage is a non-dimensional measure of the total internal volume of a vessel, calculated according a formula specified by the International Convention on Tonnage Measurement of Ships. It is not a measure of mass or weight of a ship.

## 2.1.2. Vessel source levels

Source levels from the ECHO vessel noise database were previously calculated in decidecade (i.e., 1/3-octave) bands by JASCO's ShipSound software (Hannay et al. 2016). ShipSound monitors sound level measurements and AIS broadcasts from passing vessels. It identifies vessels that traverse a predefined transit area and then automatically extracts the corresponding acoustic data for analysis. It uses a vessel's broadcast speed combined with an analysis of the Lloyd mirror pattern to determine the timing and location of closest point of approach (CPA) of the vessel's acoustic centre. The data window is defined by the period over which the acoustic centre is within  $\pm 30^\circ$  of the CPA (following ANSI/ASA S12.64). ShipSound automatically determines the data window and processes a single acoustic channel in 1-second periods stepped in 0.5-second intervals (Figure 3). ShipSound only accepts measured source band levels if they exceed the background levels by 3 dB or more. ShipSound corrects the band levels if they exceed background levels by 3–10 dB, but rejects them if they are less than 3 dB above background. Source levels that cannot be measured due to background noise are treated as missing data (i.e., NA values).

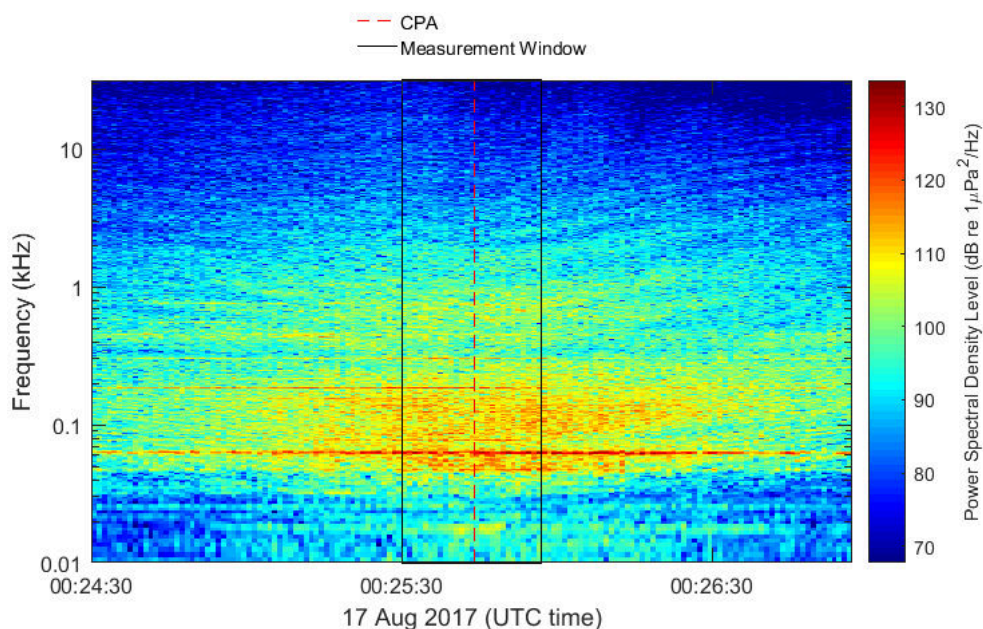


Figure 3. Spectrogram of a single vessel measurement from ShipSound, showing the closest point of approach (CPA) time (dashed red line) and the measurement window (black box) used for calculating vessel source levels. The spectrogram shows the spectrum of the underwater sound pressure recorded on the underwater listening station (ULS) hydrophone versus time and frequency.

Two types of vessel source levels are stored in the ECHO database: Radiated Noise Level (RNL) and Monopole Source Level (MSL). RNL is equal to the measured sound pressure level, scaled according to the distance between a source and the hydrophone (i.e., using the spherical spreading propagation method of  $20 \times \log_{10}(R)$ ). MSL is equal to the measured sound pressure level scaled according to a numerical acoustic propagation loss (PL) model that accounts for the effect of the local environment on sound propagation (i.e., sea-surface reflection, water column refraction and absorption, and bottom loss). MSL back-propagation is performed using predictions of the Parabolic Equation model RAM, modified to treat shear wave reflection losses, in 1/3-octave-bands to 5 kHz, and an image reflectivity model at higher frequencies. MSL back-propagation requires a source depth, which is defined in ShipSound as a Gaussian distribution centred at half the reported vessel draft. RNL is the source level calculation method specified by the ANSI standard S12.64 whereas most acoustic models used for assessing shipping noise effects on marine fauna use MSL. RNL and MSL measurements, in decidecade frequency bands, were available for the frequency range 10 Hz to 63,000 Hz (Figure 4).

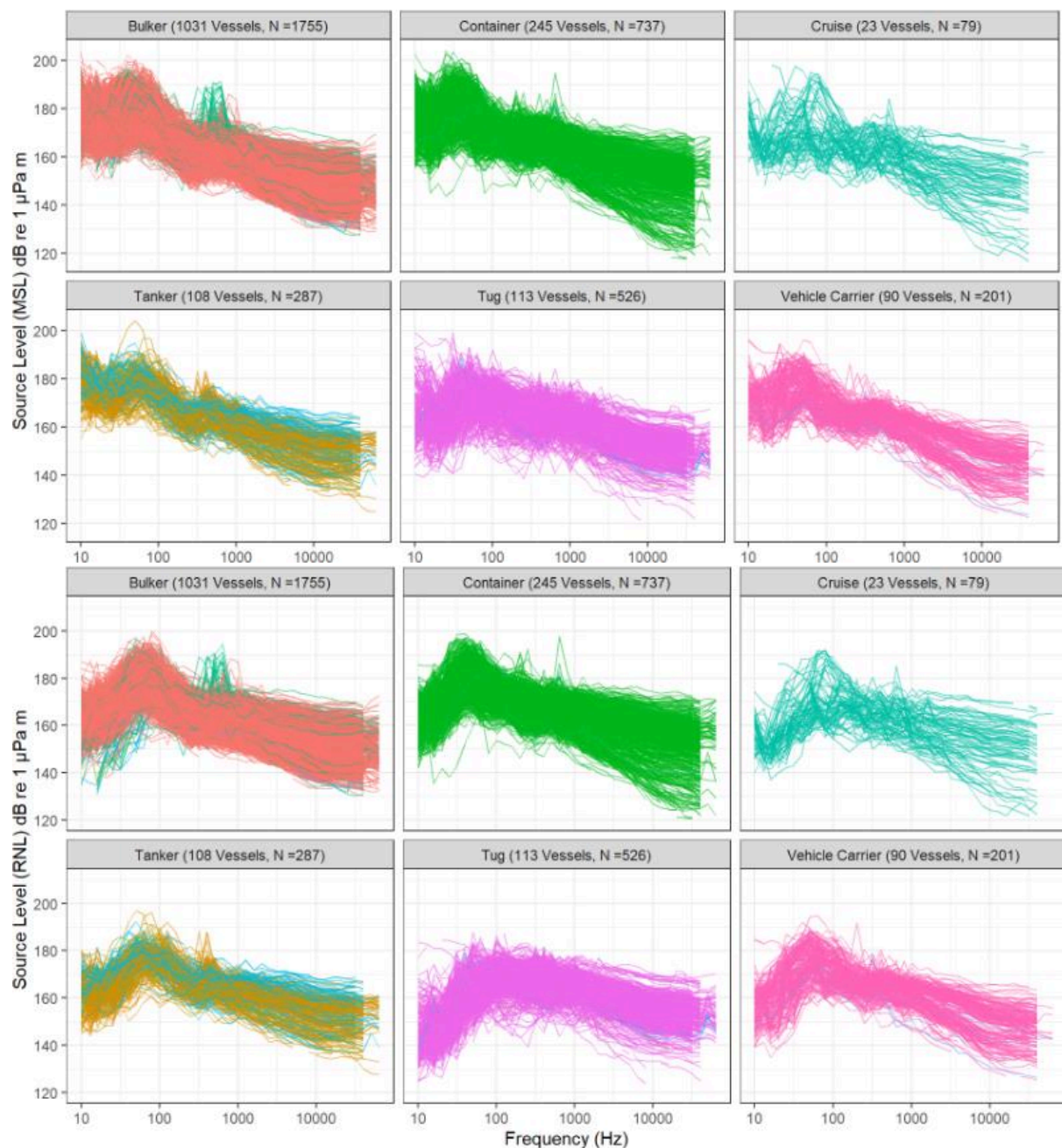


Figure 4. Plot of decade Monopole Source Level (MSL) (top) and Radiated Noise Level (RNL) (bottom) versus frequency from ECHO source level database (each curve represents a unique measurement). Different color curves reflect different vessel sub-types in the LLI database (i.e., according to VESSEL.TYPE.LLI). See Annex 1, Section 6.2.

## 2.2. Data Review and Evaluation

### 2.2.1. Data cleanup and conditioning

A manual review was carried out to clean the merged database and remove outlying values (outliers). Invalid data were corrected when possible (e.g., using online databases) or flagged as missing if they could not be corrected. The following corrections were applied to the database:

- Several IMO and MMSI numbers in the ECHO database were missing or incorrectly formatted (e.g., containing the wrong number of digits). IMO numbers were corrected for 69 vessels, and MMSI numbers were corrected for 19 vessels.
- Manual checks of the spectrum data identified 19 measurements that were affected by clipping (i.e., due to the measured pressure signal exceeding the voltage range of the hydrophone). These clipped measurements were removed from the database.
- A previous review of high-frequency source levels for some ships (in the 16 to 31.5 kHz range) identified several measurements contaminated by sonar-like signals. Data in frequency bands affected by this issue were flagged as missing data (i.e., value set to NA).
- Some measurements were found to match multiple vessel records in the EVDI database. These corresponded to 11 vessels that changed name or MMSI number but retained the same IMO. Duplicate entries were removed.
- Scatter plots and box-and-whisker plots of vessel characteristics identified several vessels with outlying design characteristics (e.g., design speed, draft, gross tonnage, and engine power). Most outliers corresponded to vessels that were incorrectly classified in the LLI database (14 vessels were reclassified as a result of the manual review). The remaining outlying design characteristics (e.g., unrealistic dimensions or engine characteristics) were corrected using online databases or flagged as missing data.
- Measurements obtained at horizontal distances less than 10 m were discarded (25 total), as the MSL calculation method was found to be unreliable directly above the hydrophone.

The cleaned version of the merged database was used for all subsequent statistical analysis.

### 2.2.2. Missingness

The merged database contained missing (NA) values where information for a specified predictor was unavailable in the LLI, PPA, and EVDI databases. The percentage of missing data was calculated for each of the candidate predictors, broken down by vessel category (Figure 1). Tugs were found to be most affected by missing data, with eight of the predictors having greater than 50% missingness. The design characteristic most affected by missingness across all categories was fuel oil capacity (FO.Capacity.LLI), but this variable was not expected to affect underwater noise emissions. For the remaining predictors, imputation was used to fill in missing values for the functional regression analysis (Section 2.5.7).

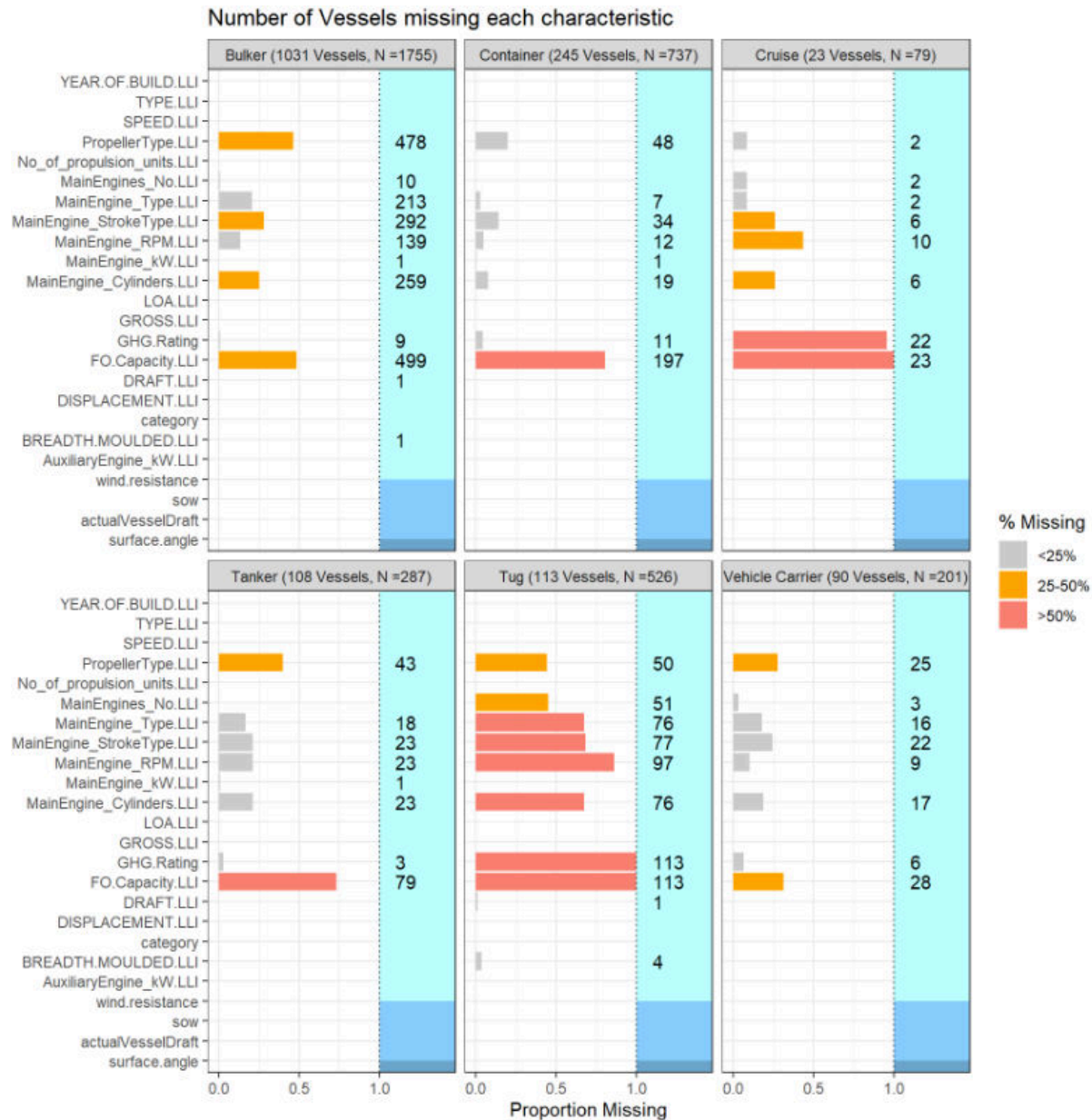


Figure 5. Missingness of candidate predictor variables considered in this study, by vessel category. The horizontal bars indicate the fraction of missing data. The numbers to the right of the bars indicate the total number of missing values.

Source levels were treated as missing (NA) when ShipSound determined that background noise levels were within 3 dB of received signal levels during a vessel measurement. Additionally, source levels for the 40,000, 50,000, and 63,000 Hz bands were only available for a small fraction of the measurements, as most ULS data were collected at an audio sampling rate of 64 kHz (which limited the maximum sampling frequency of most of the data to 32 kHz). As with the predictors, the percentage of missing data was calculated for each of the decidecade source levels, broken down by vessel category (Figure 6). Tugs had the most missing source level data, since they are generally smaller and quieter than the larger cargo vessels. Missingness was generally greatest at the lowest and highest frequencies for all vessel categories. As for the predictor variables, imputation was used to fill in missing source levels values for the functional regression analysis (Section 2.4).

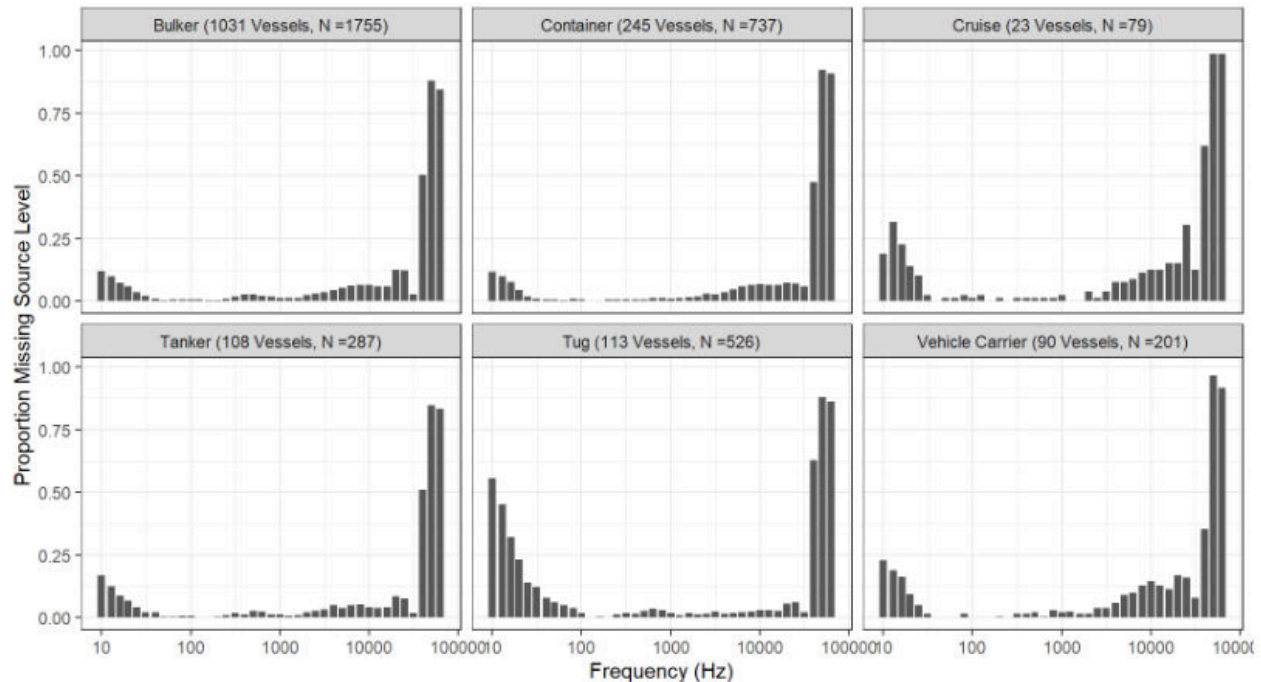


Figure 6. Missingness of Monopole Source Level (MSL) and Radiated Noise Level (RNL) data, in decidecade bands. Note that missingness of RNL and MSL data was identical because they were calculated from the same hydrophone measurements.

### 2.2.3. Exploratory Analysis

Univariate, bivariate, and multivariate statistical methods were used to explore the inter-relationships among the ship characteristics and operational parameters and noise across frequency bands. Initial exploratory data analyses were carried out for quality assurance and quality control, to identify outliers, to determine appropriate data transformations, and to identify the most important ship characteristics and operational parameters relative to noise in three key frequency bands (see below).

Bivariate scatter plots, density plots, and correlation matrix plots were used to investigate relationships between pairs of variables (source levels and predictors) and to guide development of the statistical model. To simplify exploratory analysis of the source level data, decade band source levels (RNL and MSL) were calculated for the following three frequency ranges:

- 10–100 Hz
- 100–1000 Hz
- 1000–10,000 Hz

Decade band source levels were calculated by summing the decidecade band RNL and MSL source factors inside these three frequency ranges (with appropriate weighting at the band edges where the decidecade bands partially overlapped the decade bands).

Bivariate scatter plots (i.e., X-Y plots) were created for all pairs of numerical variables. These were used to identify trends between pairs of variables and to identify outliers. For categorical (i.e., non-numerical) quantities, box-and-whisker plots were used instead of scatter plots.

Histograms and density plots (smoothed histograms) were used to assess the distributions of numerical variables. These plots were also used for identifying outliers and for determining which variables should be transformed for subsequent regression analysis (Section 2.5.7). A logarithmic transformation was identified as the most suitable transformation for most predictor variables, since source levels also measure radiated noise on a logarithmic (i.e., decibel) scale.

Correlation matrix plots were created to show correlation coefficients between pairs of (numerical) variables. The correlation coefficient,  $r$ , is a dimensionless number, in the range  $-1 < r < 1$ , that indicates the strength of linear correlation between two variables. Positive  $r$ -values indicate a positive relationship between two parameters and negative  $r$ -values indicate a negative relationship between two parameters. Standard statistical thresholds for correlation values are as follows:

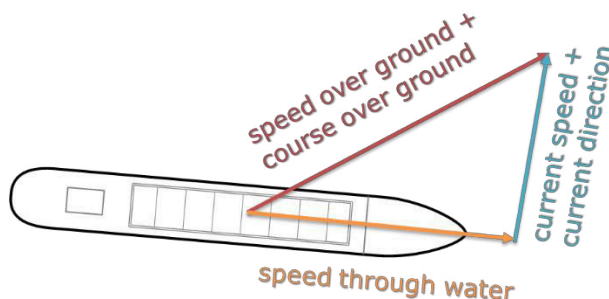
- Strong correlation:  $|r| \geq 0.8$
- Moderate correlation:  $0.8 > |r| \geq 0.5$
- Weak correlation:  $|r| \leq 0.5$

When pairs of predictor variables are strongly correlated (i.e., when they are linearly dependent), it is often necessary to drop one of the predictors from a multiple regression model because the effects of those predictors cannot easily be separated from one another and may lead to numerical instability and inaccurate regression estimates. The correlation matrix analysis was thus used to identify which sets of independent predictors should be retained for the multiple-predictor statistical model.

## 2.3. Physical models and derived quantities

Physical models were used to capture the effect of water currents, wind, and source-receiver geometry on measured source levels. The magnitude and direction of wind and water currents were captured by ShipSound, at the time of measurement, and stored in the ECHO vessel noise database. Meteorological data for Haro Strait and Georgia Strait were obtained from the Environment Canada weather stations at Kelp Reefs and Sands Head Light Station, respectively (Environment Canada 2020). Ocean current data for the Georgia Strait ULS were obtained from an Acoustic Current Doppler Profiler (ADCP) on the VENUS East node. Direct ocean current measurements were unavailable for Haro Strait, so ocean current data at the Haro Strait ULS were obtained from the WebTide Tidal Prediction Model (v 0.7.1), provided by Fisheries and Oceans Canada (Bedford Institute of Oceanography 2015).

Speed through water was used in the statistical analysis as it directly accounts for the effect of water current and speed and direction on underwater radiated noise. This is because the moving reference frame of the water itself is the preferred frame for physically analyzing underwater noise generated by a marine vessel<sup>3</sup>. The speed through water vector was computed as the difference between the speed over ground vector (from AIS) and the ocean current vector (Figure 7). The magnitude of the resulting speed through water vector was used as a predictor in the subsequent statistical analysis. Speed over ground and ocean current were not used as predictors because they are implicitly included in the speed through water calculation.



$$STW \text{ vector} = SOG \text{ vector} - \text{current vector}$$

Figure 7. Diagram of speed through water calculation (STW = speed through water, SOG = speed over ground).

<sup>3</sup> Note that the Doppler shift, due to the relative motion of the vessel and the hydrophone, is not expected to affect the measured source levels. This is because, on a frequency scale, the decade bands used for the source level analysis are much larger than the possible Doppler shift (i.e., 23% of frequency versus <1% of frequency).

The effect of wind on vessel source levels was captured by calculating a wind resistance factor that depended on the speed and course over ground of the vessel and on the magnitude and direction of the wind at the time of measurement. The cross section of a vessel's hull that sits above the water line experiences an aerodynamic drag force that depends on the speed of airflow around the hull (i.e., apparent wind speed) and on the cross-sectional hull area that is exposed to the airflow. According to naval architecture literature, the propulsive power required to overcome this drag force is proportional to a constant known as the heading coefficient ( $C_Y$ ) (Lewis 1988). The heading coefficient is positive (representing a resistive force) when the apparent wind direction is toward the bow of the ship, and negative (representing a driving force) when the apparent wind direction is toward the stern of the ship (Figure 8).

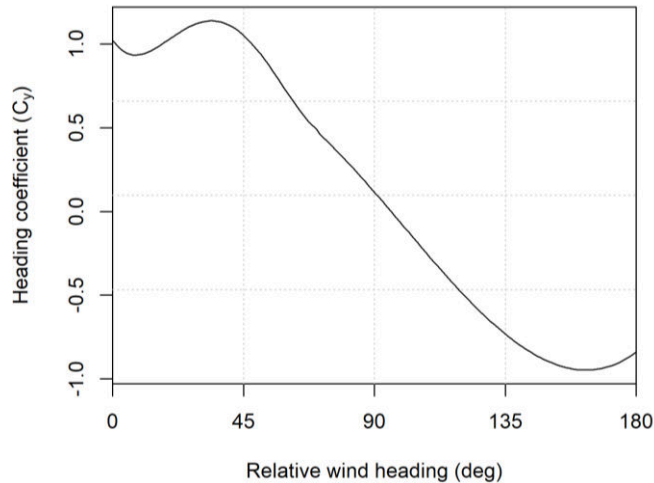
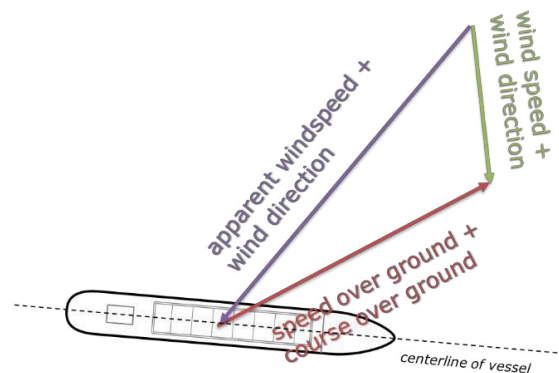


Figure 8. Plot of heading coefficient used in wind resistance calculation, as adapted from (Lewis 1988).

The apparent wind speed vector was calculated from the difference between the true wind speed vector and the speed over ground vector of the vessel (Figure 9). A wind resistance factor ( $K_w$ ), which was proportional to the power required to overcome the aerodynamic drag force, was then calculated from the product of the square of the apparent wind speed ( $V_R$ ) and the heading coefficient:

$$K_w = C_Y V_R^2.$$

This wind resistance factor was used as a predictor in the subsequent statistical analysis, rather than separate wind speed and direction (Figure 10), as it best reflected the increase in propulsion power (and, thus, associated noise and vibration) required to overcome wind-induced drag forces.



$$\text{apparent wind vector} = \text{true wind vector} - \text{SOG vector}$$

Figure 9. Diagram of apparent wind speed calculation.

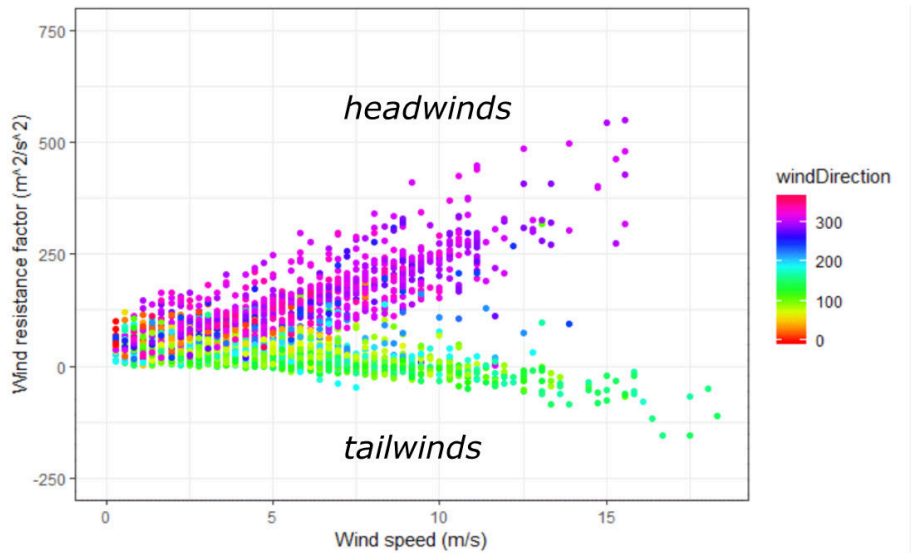


Figure 10. Calculated wind resistance factor versus wind speed for all measurements in the merged vessel noise database. The color of the plot symbols indicates the wind direction (degrees clockwise from north). The wind resistance is positive for headwinds and negative for tailwinds.

By following the methods defined by the ANSI S12.64 (Grade C) standard, the ULS was set up to generate repeatable measurements and to reduce, as much as practically possible, the influence of source-receiver geometry on measured source levels. Nonetheless, differences in the source-receiver geometry between measurements might still have a minor influence on the measured source levels, and it is desirable to control for such sampling differences in the statistical analysis. To this end, the surface angle was included as a predictor in the statistical analysis to control for geometric differences between measurements. The surface angle was calculated from the closest distance of approach of the vessel to the hydrophone and the depth of the hydrophone (Figure 11). The surface angle was preferred as it also captures the cancellation of radiated sound by the sea-surface (i.e., the Lloyd-mirror effect), which is proportional to the surface angle (this is mainly in relation to RNL, since MSL includes an explicit correction for this effect).

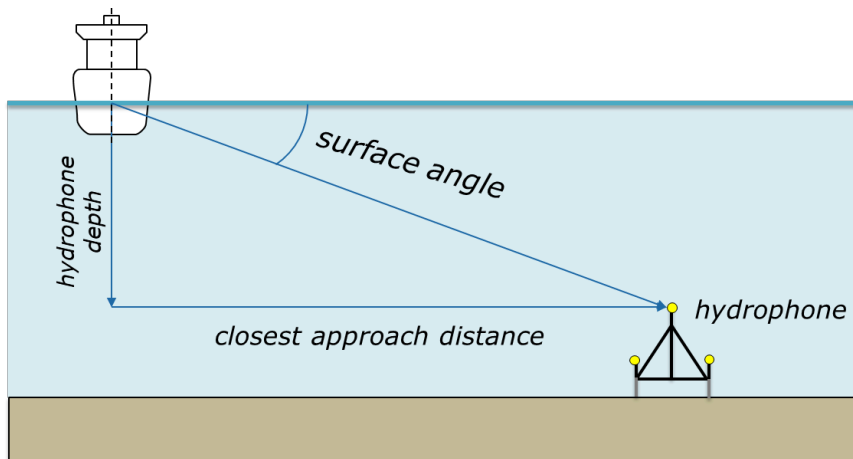


Figure 11. Diagram of surface angle calculation.

Three dimensionless derived quantities were also calculated from groups of predictors in the merged vessel noise database. The first derived quantity was the block coefficient (Figure 12), which is the ratio of the displacement to the submerged volume of the vessel:

$$C_b = \frac{\text{displacement}}{\text{beam} \times \text{length} \times \text{draft}}$$

Note that the block coefficient could only be calculated for the summer draft (i.e., as a static value), since the True displacement depends on the actual draft in a fashion that depends on the hull design.

The second derived quantity was the fractional speed (Figure 13), which was the ratio of the actual speed through water (STW) to the design speed of the vessel:

$$v_{\%} = \frac{\text{actual STW}}{\text{design speed}}$$

The third derived quantity was the fractional draft (Figure 14), which was the ratio of the actual draft to the summer draft:

$$d_{\%} = \frac{\text{actual draft}}{\text{summer draft}}$$

These derived quantities were evaluated during univariate analysis (Section 3.5) to determine whether they were more strongly correlated with vessel source levels than the constituent quantities on their own.

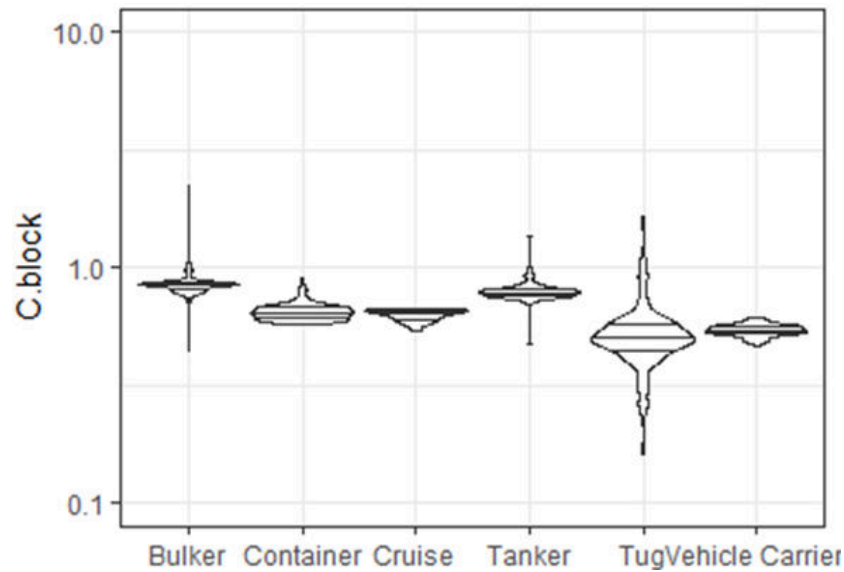


Figure 12. Violin plot of block coefficient, per vessel category. The width of the swath corresponds to the distribution of the data and the horizontal lines indicate the 25th, 50th, and 75th percentiles of the data.

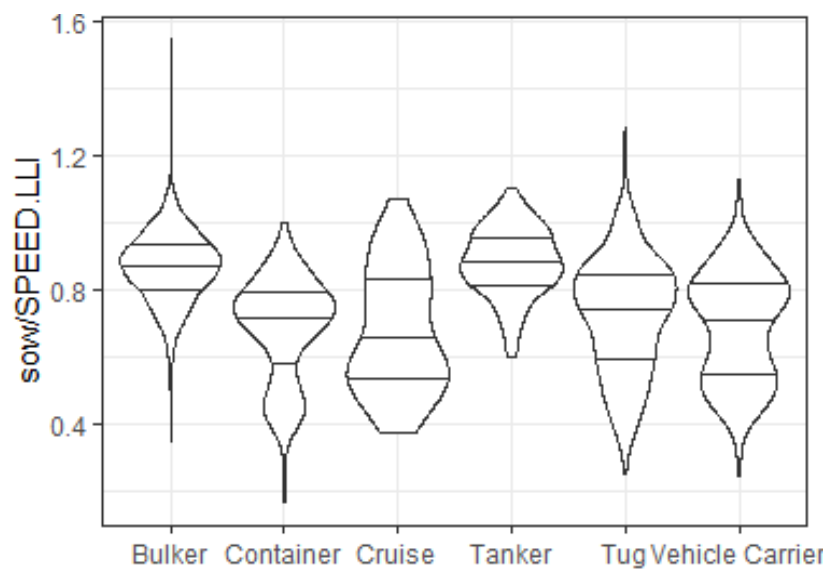


Figure 13. Violin plot of fractional speed through water, per vessel category. The width of the swath corresponds to the distribution of the data and the horizontal lines indicate the 25th, 50th, and 75th percentiles of the data.

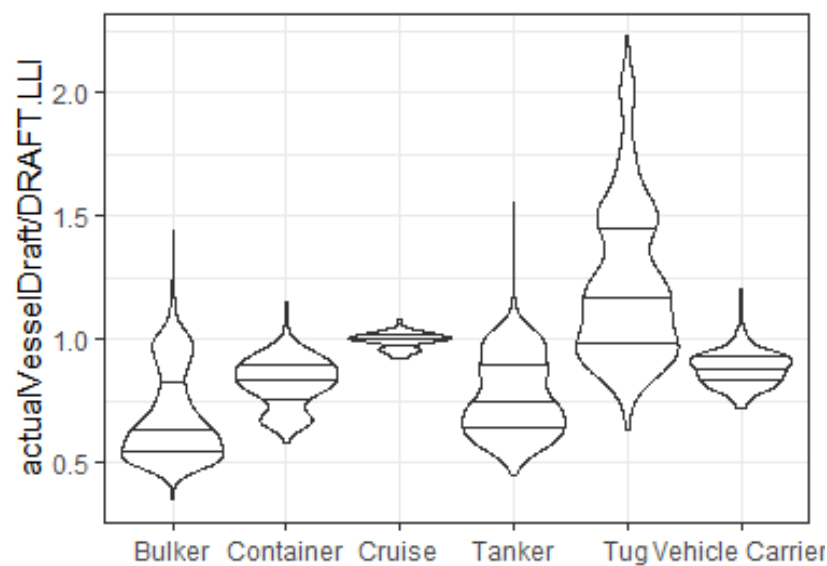


Figure 14. Violin plot of fractional draft, per vessel category. The width of the swath corresponds to the distribution of the data and the horizontal lines show the 25th, 50th, and 75th percentiles of the data.

## 2.4. Data Imputation

Imputation is the process whereby missing data associated with a measurement are estimated based on known data values from similar measurements. Imputation is often required when applying multi-variate statistical methods, since incomplete cases (i.e., measurements with missing data) may not otherwise be used. Imputation of missing data is generally performed using a combination of expert knowledge and statistical analysis. Separate imputation methods were applied for the predictor variables and the source level variables.

Missing predictor values were generally replaced using one of the following methods:

- Where redundant information was available in other database columns, missing values were imputed using those values. For example, when pilot draft was unavailable, it was replaced by active draft from AIS.
- Where redundant information was unavailable, missing values were imputed using either the median value or most-frequent value (i.e., the mode) of the non-missing data in the same column.

Table 5 summarizes the methods used for imputing missing predictors in the merged vessel noise database. The validity of the imputation assumptions for the vessel design characteristics were vetted by the SME team.

Table 5. Summary of imputation methods for predictor variables.

Variable	Variable type	Percent missing	Imputation
actualVesselDraft	Operational	1	Static draft from AIS If missing, impute with DRAFT.LLI
sow		3	Speed over ground
wind.resistance		7	Zero-wind resistance value, based on speed over ground
TYPE.LLI	Design	2	Mode value for category
GROSS.LLI		2	Median for category
DRAFT.LLI		2	Static draft from AIS
LOA.LLI		2	Length overall from AIS If missing, impute with median for category
YEAR.OF.BUILD.LLI		2	Year built from AIS If missing, impute with median for category
SPEED.LLI		2	Median for category
DISPLACEMENT.LLI		2	Median for category
BREADTH.MOULDED.LLI		2	Median for category
MainEngine_Type.LLI		24	'DSL' (diesel) for all categories
MainEngines_No.LLI		9	1 2 for tugs and cruise ships 1 for other categories
MainEngine_kW.LLI		2	Median for category
MainEngine_RPM.LLI		24	Median RPM of vessels with the same (or similar) gross tonnage (i.e., grouped by GROSS.LLI)
MainEngine_Cylinders.LLI		28	Median for category
MainEngine_StrokeType.LLI		31	Mode for category
PropellerType.LLI		38	'FP' (fixed pitch) for all categories
No_of_propulsion_units.LLI		2	2 for tugs and cruise ships 1 for other categories
AuxiliaryEngine_kW.LLI		2	Median for category

Decade band source levels (RNL and MSL) were imputed using one of three methods, depending on the frequency range of the missing data:

- At intermediate frequencies, where missing bands were bounded above and below by non-missing bands, imputation was performed by interpolation using a natural spline. A smooth and flexible piecewise polynomial was fit to each noise profile, and missing bands were imputed with the spline fitted values (Figure 15).
- At low frequencies, where missing bands were at the bottom end of the frequency range, source levels were imputed using the median source levels, in the same band, of similar measurements (i.e., with broadband RNL or MSL within  $\pm 1.25$  dB) in the same vessel category.

- At high frequencies, where missing bands were at the top end of the frequency range, source levels were imputed by extrapolating the lower frequency data according to a constant-slope spectral density curve (Figure 16). This method was motivated by the observation that the spectrum of cavitation noise at high frequencies generally has a constant slope (Ross 1976). The spectral slope used in the extrapolation was calculated on a per-category basis.

In all instances, the imputed values were constrained to be less than the measured background noise level. The imputation was used to fill in the missing source level measurements so that a functional regression analysis could be applied to the data (Section 2.5.7).

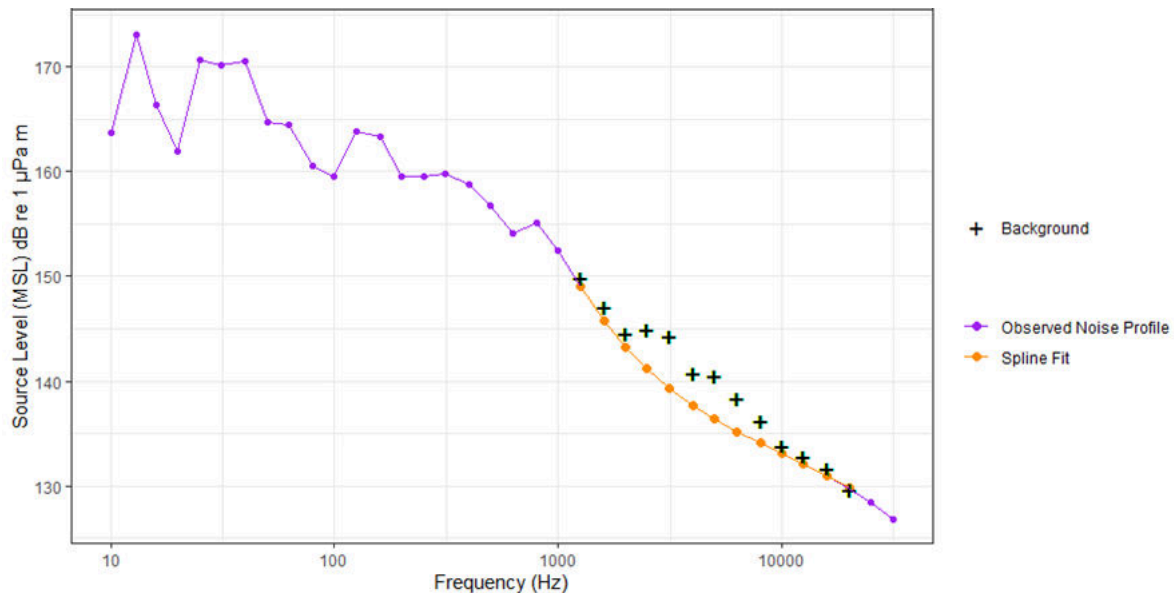


Figure 15. Illustration of spline imputation method for intermediate frequencies.

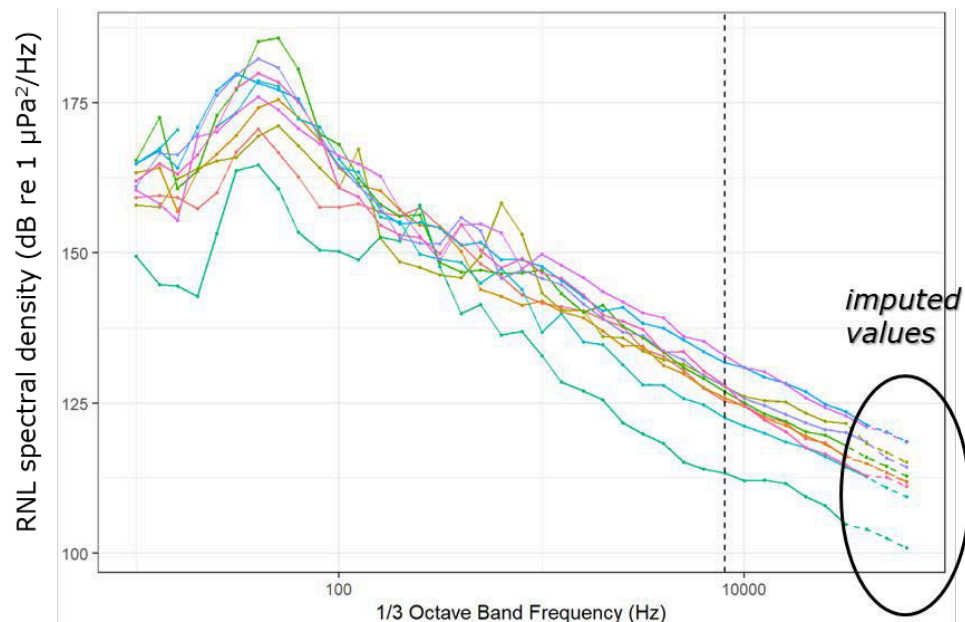


Figure 16. Plot showing the results of the high-frequency imputation method (spectral slope extrapolation), applied to 10 random measurements of container ships.

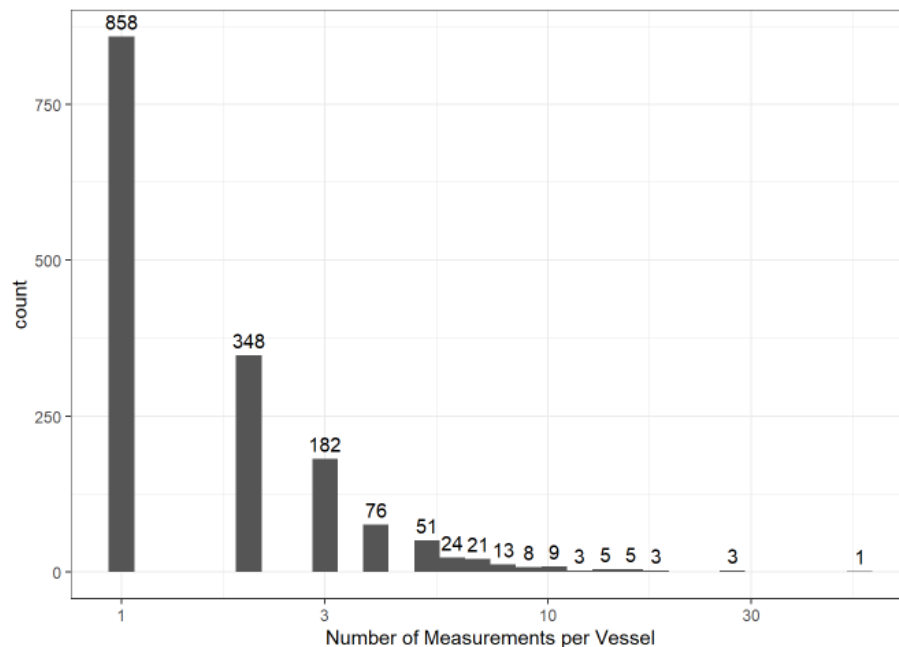
## 2.5. Statistical Model Development

### 2.5.1. Repeat Measurements

Many vessels in the ECHO vessel noise database had more than one measurement, with 30 vessels (of the 1618 total) having 10 or more measurements (Figure 17). Repeat measurements are valuable when they capture the same vessel under different operating conditions, but they can also bias the analysis by weighting the result toward the most frequently-sampled vessels. To balance these competing effects, repeat vessel measurements were randomly subsampled (without replacement) so that they were included only when the following three operating conditions were substantially different: speed through water, actual draft, and wind resistance. To perform the subsampling, repeat measurements of a vessel were binned according to these three variables and a single measurement was randomly selected from each bin, up to a maximum of 8 randomly-selected measurements per vessel. The following bin widths were used for the subsampling procedure:

- `sow` (speed through water) bin width equal to 20% of vessel design speed
- `actualDraft` bin width equal to 20% of vessel summer draft
- `wind.resistance` bin width equal to  $100 \text{ m}^2/\text{s}^2$  (corresponds to 10 m/s wind speed)

The subsampling ensured that different operating conditions were captured in the statistical analysis, without biasing the result too heavily to any single vessel.



## 2.5.2. Principal Components Analysis (PCA)

PCA is a commonly used data reduction and interpretation technique (Johnson and Wichern 2007). It takes high dimensional data (many variables) and projects them onto a smaller, more manageable space for analysis and visualization. The projected data are summarized by the new variables, called principal components (PCs). A carefully constructed analysis generally leads to a small number of important PCs with scientifically relevant interpretations. Investigation of the PC loadings can also be useful to identify the variables that capture the majority of the information in the data set. The PC scores, that represent a weighted average of the variable values, are often used to reduce the number of predictor variables, and address multi-collinearity in subsequent regression analyses. In addition to providing concise summaries of the multivariate data, investigation of the PCA results often reveal relationships that would not have been discovered by looking at the variables one at a time. The loadings that define the PCs can identify underlying constructs and how variables group together, and cluster analysis of the PC scores can identify groups of similar observations, that often align with physical categories such as vessel class.

- PCA was carried out on design parameters of all ship categories combined as well as separately for each ship category
- Appropriate data transformations were used to reduce the influence of outliers for skewed variables and to linearize the inter-relationships among variables
- Bivariate plots of the PC scores (biplots) were used to understand variable groupings and aid interpretation
- Cluster analysis of PC scores were used to assess correspondence of PC groups with vessel classes

The principal component analysis results are presented using biplots, which show the PC scores of the samples and the loadings of the variables onto the principal components (Figure 18).

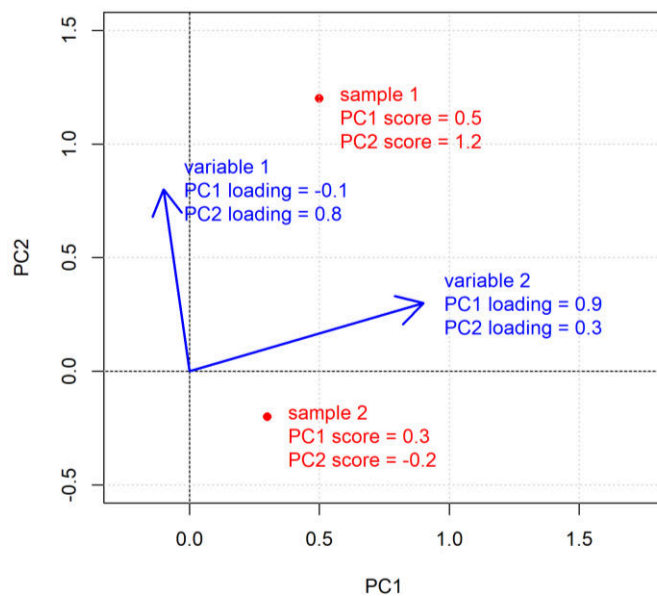


Figure 18. Diagram illustrating how to interpret a biplot. Horizontal axis represents the first principal component (PC1), and vertical axis represents the second principal component (PC2). The blue vectors indicate the loadings (i.e., weights) of the variables onto the principal components. The horizontal (x) component of the vector is the PC1 loading, and the vertical (y) component of the vector is the PC2 loading. The red circles indicate the PC scores of the samples. The PC scores express the sample values in terms of PC1 and PC2.

### 2.5.3. Functional Data Analysis

Functional data analysis is a modern statistical technique (Ramsay and Silverman 2005) used to analyze the characteristics of curves or profiles. Similar to PCA, functional principal components analysis (FPCA) is a data reduction technique. However, rather than summarizing the information in many variables, FPCA summarizes the information in measurements taken over time or, in the case of noise, across frequency bands. Similarly, functional regression analysis provides a means for carrying out regression analysis when the outcome or predictor variables are curves rather than individual data points. For example, Ainsworth et al. (2011) used functional data analysis techniques to relate daily river flow patterns to annual salmon returns. This approach identified the river flow patterns and seasonal variations in the smolt year that related to changes in salmon return rates. Here, functional regression analysis is used to identify how source level versus frequency curves are affected by the ship characteristics and operational parameter variables.

An advantage of functional data analysis is that it captures the information in the entire curve (i.e., the entire source level versus frequency profile). Rather than looking at individual correlations of ship characteristics and operational parameter variables with source levels in distinct frequency ranges, FPCA and functional regression analysis allows for a simultaneous analysis of ship characteristic associations with the entire source level curve. Thus, functional regression analyses were used to identify which ship characteristics and operational parameters were the best predictors of noise, and in which bands they were most predictive.

### 2.5.4. Functional PCA

Functional Principal Components Analysis (FPCA) of the source level versus frequency curves was used to understand the key features of the data, and the frequency bands that had the most noise variability across vessel categories.

- FPCA was carried out on source levels for all vessel classes combined as well as separately for each category
- Key features of the source level versus frequency curves were summarized graphically and related to vessel categories and characteristics

### 2.5.5. Vessel Category Groupings

For development of the statistical models, certain vessel categories were grouped together based on commonalities in their design and source level characteristics. These groupings were selected using principal component analysis and expert knowledge. Principal component analysis was applied to both the design predictors (PCA) and the source level data (FPCA) to identify where there was overlap between the different vessel categories (i.e., cluster analysis). Based on this analysis, and on discussion with the SME team, the six vessel categories were grouped as follows:

- Bulkers and Tankers (slow cargo vessels) were grouped together;
- Containers and Vehicle Carriers (fast cargo vessels) were grouped together;
- Cruise and Tugs were not grouped with any other category.

These groupings were subsequently used for functional regression analysis of the vessel noise data set, and development of the final statistical model (see Section 2.5.7).

### 2.5.6. Variable Selection

Not all predictors in the merged vessel noise database were retained for the regression analyses. Variables with a large amount of missing data or redundant variables were removed. Including redundant

predictor variables causes collinearity that can lead to numerical instability and inaccurate regression coefficient estimates. As well, fitting too many predictors, can lead to overfitting the data and reduce the generalizability of the statistical model. Some predictors were not immediately relevant to underwater radiated noise, and others did not exhibit a strong correlation with measured source levels, so they were excluded from the analyses.

Variable selection was carried out using a combination of statistical analysis and expert knowledge. Functional regression analysis (see Section 2.5.7) was used to investigate linear trends between individual (transformed) variables and source levels (both RNL and MSL) across decade bands. Those variables that had weak correlations were omitted, particularly if another variable captured a closely-related design characteristic of a vessel. A short-list of design predictors was reviewed in consultation with the SME team to identify which ones were to be retained for the final multiple-predictor functional regression analysis (see Section 2.5.7).

## 2.5.7. Functional Regression

Functional regression analysis is an extension of standard regression analysis. For each observation, the outcome variable value (or predictor variable values) can be a curve rather than a single number. This is a powerful technique for assessing source level data as it allows the simultaneous assessment of the relationship between predictor variables and noise emissions at all frequencies that avoids the need to run multiple regression analysis on noise levels aggregated across frequency bands.

Standard regression analysis leads to a single regression coefficient for each predictor. On the other hand, functional regression analysis provides a regression coefficient function for each predictor variable. This function indicates which frequencies are most correlated with a predictor variable, and the direction of the relationship. For example, a predictor variable may have a positive relationship with source levels at low frequencies, no relationship at mid frequencies, and a negative relationship with source levels at high frequencies.

Similar to standard regression analysis, functional regression analysis models can include a single predictor or multiple-predictor variables (single-variable and multiple-variable cases). Functional regression analyses were used as follows:

- Ship operational and design characteristics were used to predict source level profiles
- Graphical summaries of the functional regression analysis were used to determine the subset of ship characteristics and operational parameters that were most important for predicting noise emissions

Both single-predictor and multiple-predictor functional regression models were used to investigate the relationship between predictors and vessel source levels (MSL and RNL) in decade bands. Single-predictor functional regression models were used to independently analyze the correlation of all predictors with vessel source levels. These results informed the variable selection procedure for the multiple-predictor functional regression analysis (Section 2.5.6). Multiple-predictor functional regression models were then used to simultaneously analyze the correlation of a subset of the predictors with vessel source levels. The multiple-predictor functional regression models were developed in a forward-stepwise fashion, by incrementally adding predictors to the model and evaluating the coefficient of determination ( $r^2$ ), versus frequency, at each step (Figure 19).

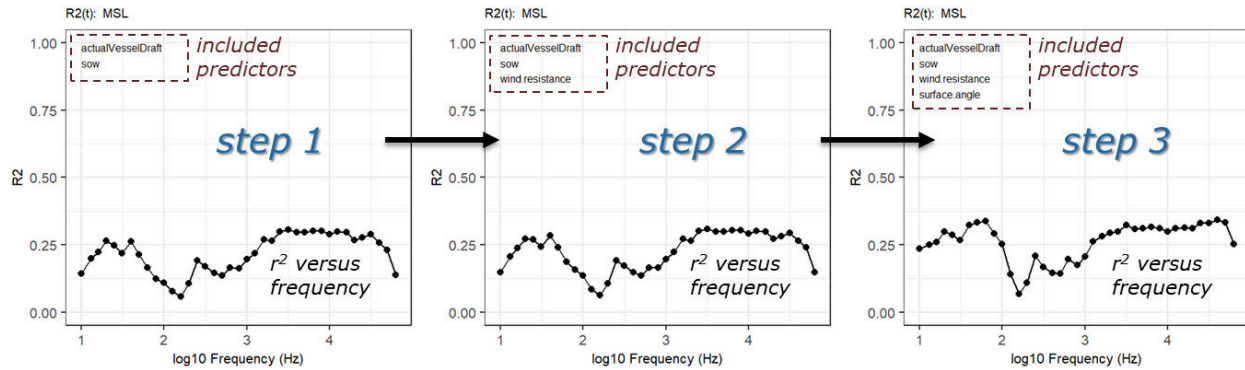


Figure 19. Example showing stepwise addition of predictors to a multiple-predictor functional regression model. Each plot shows the coefficient of determination ( $r^2$ ), versus frequency, as predictors are incrementally added to the model. The coefficient of determination ( $r^2$ ) is a number in the range 0–1 that indicates the strength of correlation with a response variable. The  $r^2$  values increase gradually as predictors are added to the model.

## 2.6. Spectrum Analysis

JASCO has access to raw spectral data from the ShipSound measurements, as calculated directly from pressure waveforms recorded on the ULS hydrophones. Noise spectrum data (in 1/8 Hz and 1 Hz frequency bands, referenced to 1 m range) were extracted from the ShipSound database, for a subset of 60 different vessel measurements, in order to investigate whether the loudest and quietest vessels in each category shared common spectral characteristics. The main benefit of spectral analysis is that it can be used to identify tonal noise sources that cannot be resolved by decade band analysis. Tones usually originate from rotating or vibrating machinery and are often the dominant source of vessel noise below 1000 Hz.

Measurements were selected for spectral analysis by ranking all measurements in each vessel category according to their adjusted broadband RNL value. The adjusted RNL for each measurement was calculated by scaling the measured RNL according to a reference STW and actual draft (equal to the category-average values), using the multiple-predictor functional regression model (see Section 2.5.7). The top five (i.e., loud) and bottom five (i.e., quiet) ranked measurements in each category were then chosen for spectral analysis. Repeat measurements were excluded, so as to consider ten different vessels in each category. Furthermore, measurements with unusually low STW (i.e., <8 knots for vessels other than tugs) were excluded from consideration, so as not to apply excessive adjustments to slow-steaming vessels.

The 60 selected spectra were plotted versus frequency to provide a visual comparison of loud and quiet vessel measurements in each category (Appendix D). A tone detection algorithm was applied to the spectrum data, to measure the frequency and RNL of discrete tones present in the vessel measurements (Figure 20). The slope of each measured spectrum was calculated from the trend of the spectral decay with frequency, after smoothing was applied to remove the influence of tones on the trend analysis (Figure 21).

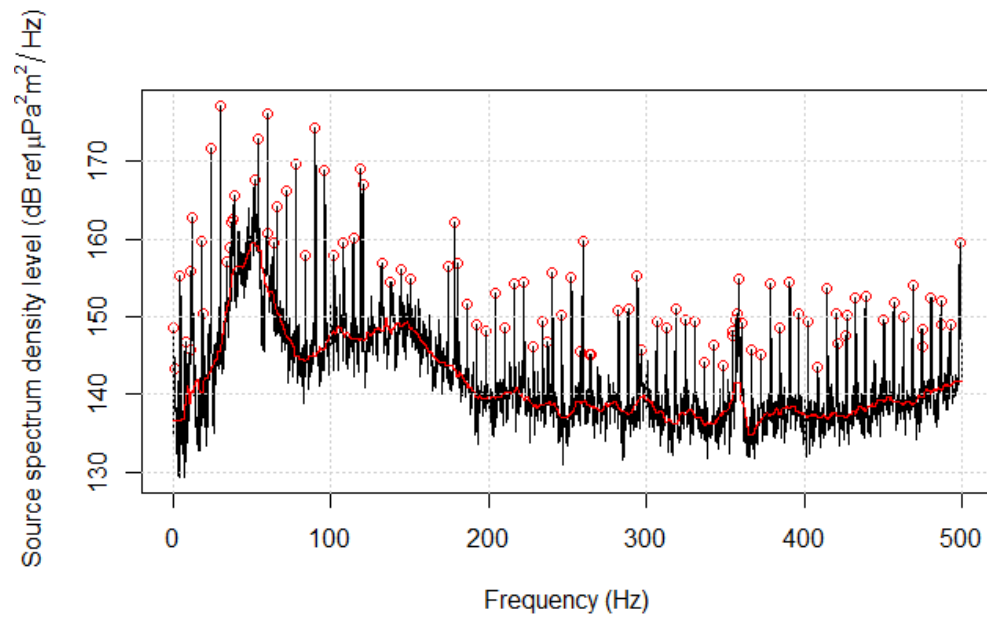


Figure 20. Illustration of the tone detection method. The algorithm identifies tones as those features that exceed the median-smoothed spectrum by 6 dB. The black line is the raw vessel noise spectrum, and the red line is the smoothed spectrum obtained using an 81-point median filter. The red circles indicate the peak levels and frequencies of tones that were identified using a 6 dB threshold detector.

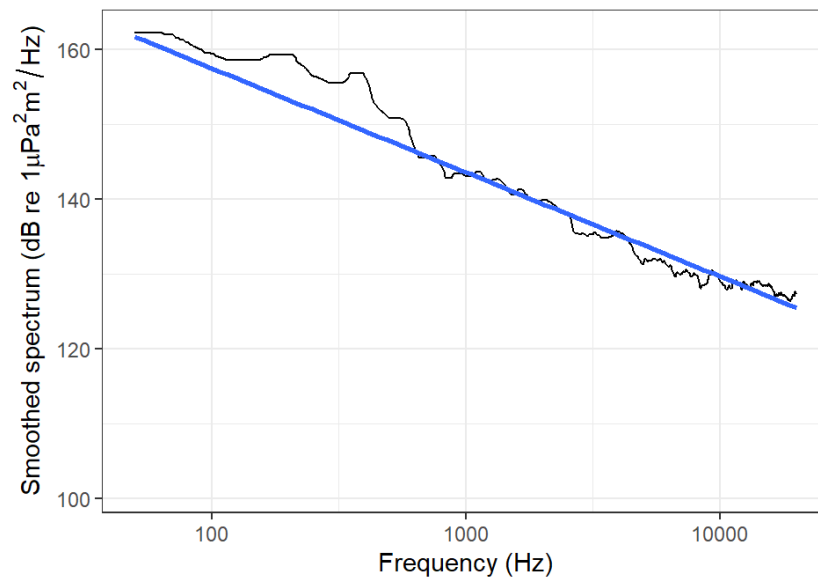


Figure 21. Illustration of slope calculation method. The spectral slope was calculated by applying linear regression (blue line) to the smoothed spectrum level versus log frequency curve (black line). Smoothing was applied using an 81-point median filter.

## 3. Results

### 3.1. Exploratory Analysis

Several notable observations resulted from the exploratory analysis of the merged vessel noise database:

- A range of operational and measurement conditions were sampled for each vessel category (Figure 22). The spread in speed through water (sow) values, and the bi-modal distributions of the vehicle carrier and container categories, were attributed to inclusion of the Haro Strait slowdown measurements in the data set.
- Scatter plots and density plots indicated that logarithmic transformations were appropriate for linearizing observed trends in most predictor variables. Exceptions were for variables containing negative values (e.g., wind resistance) and categorical variables (e.g., engine type). Surface angle was not subjected to a logarithmic transformation since it spanned a small range of values.
- Several design characteristics were dominated by a single value, which made them unsuitable for statistical analysis. For example, the overwhelming majority of vessels used conventional diesel propulsion (only 6 vessels used diesel-electric or gas turbine propulsion). Likewise, the overwhelming majority of vessels used fixed-pitch propulsion (8 or fewer vessels in each category used alternative propulsion methods). Also, the overwhelming majority of cargo vessels had a single 2-stroke engine. The homogeneity of these variables meant that meaningful correlations could not be detected from the data.
- In general, design characteristics of tugs and cruise vessels were considerably different from those of the other categories. This suggested that tugs and cruise vessels should be analyzed separately from other vessels in the functional regression analyses.

Annex 1 provides detailed results of the exploratory analysis, including scatter plots and density plots for all vessel categories.

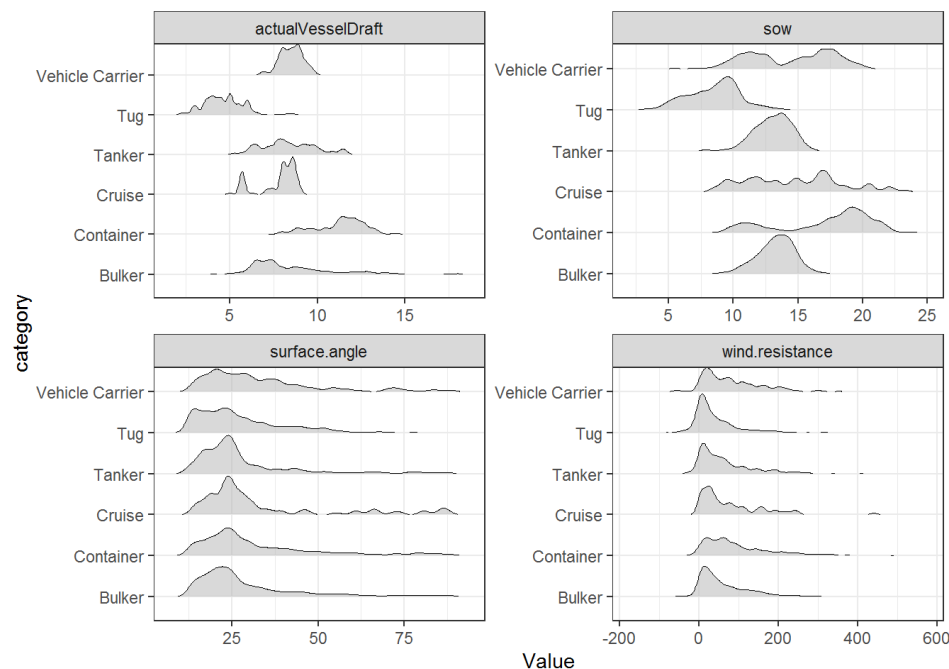


Figure 22. Density plots (smoothed histograms) of operational variables, by vessel category. The height of the density curve indicates the relative number of samples at each x value.

### 3.2. Correlation Analysis

Correlation matrices were used to identify strong correlations between pairs of variables (both predictors and decade-band source levels) in the merged vessel noise database. Figure 23 shows the correlation matrix for the Bulker category. The first three rows or columns of the correlation matrix can be used to visually identify correlations between RNL and the predictor variables. Subsequent rows and columns can be used to visually identify correlations between pairs of predictors. Large circles indicate strong positive or negative relationships and color indicates the direction of the relationship. Appendix B provides correlation matrix plots for all vessel categories.

The strength of the correlations between predictors and vessel source levels varied by category, but some commonalities were observed between all categories. Speed through water and wind resistance always exhibited a positive correlation with RNL. Actual vessel draft also exhibited a positive correlation with RNL for 4 of the 6 categories (cruise ships had a negative correlation, and vehicle carriers had a weak correlation). Correlations between vessel source levels and the various design parameters generally varied by category, but vessel size and engine power were generally correlated with source levels to some degree.

The correlation analysis also showed strong positive correlations between all the size-related design parameters for all vessel categories (gross tonnage, length, breadth, displacement, and summer draft). This indicates that their influence on underwater radiated vessel noise may not easily be distinguished from one another.

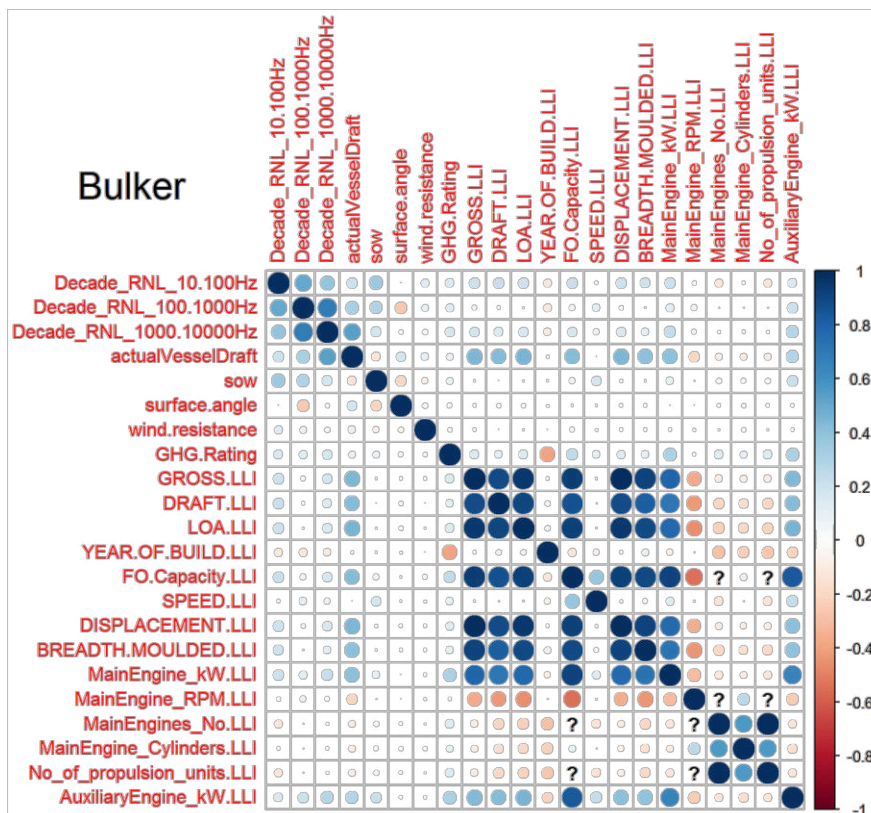


Figure 23. Correlation matrix, showing correlations between pairs of variables for the Bulker category. The size and color of the circles indicate the strength and magnitude of the correlation (blue = positive, red = negative, correlations along the diagonal are  $r=1$ ). The "?" indicates where the correlation cannot be computed between two variables (usually due to missing values, but sometimes due to a variable having a constant value).

### 3.3. Principal Component Analysis of Design Characteristics

Principal component analysis (PCA) was applied to the vessel design predictors to identify whether any natural groupings existed in the vessel design characteristics. PCA was first applied to all the data collectively then PCA was applied to each of the six vessel categories separately. Recall that PCA is a statistical procedure that uses strengths of correlations between predictor variables to summarize them into a small number of principal components (PCs). The principal components are linear combinations of the predictors (i.e., the design parameters, in this case), and are denoted "PC1", "PC2", etc., in order of their relative importance. Each principal component included all the vessel design characteristics from the correlation analysis (Section 3.2), but the loading (i.e., weighting) of each design characteristic was different for each principal component. The purpose of this analysis was to identify groups of related (i.e., strongly correlated) predictors. Annex 2 contains detailed PCA results for all vessel categories.

Scree plots were used to show the percentage of the data variability explained by the (ranked) principal components. For example, the scree plot for all data (Figure 24) shows that the first principal component describes 67% of the variability in the vessel design characteristic data, the second principal component describes 17% of the variability, etc. When the PCA was limited to vessels in a single category, the percent of data variance explained by the first two principal components was reduced. This is likely due to the increased variability and strength of relationships when looking at design characteristics across vessel categories.

Biplots (i.e., scatter plots of pairs of principal components) were used to show the data in terms of their PC scores and to show the loadings, or weights, of the predictors onto the principal components (see Section 2.5.2 for an explanation of the biplots). For example, the biplot of PC1 versus PC2 for all data (Figure 25) shows clear groupings of the design characteristics for the six different vessel categories:

- Design characteristics of Bulkers and Tankers have the greatest degree of overlap;
- Design characteristics of Containers and Vehicle Carriers also have substantial overlap, but with more scatter than Bulkers and Tankers;
- Cruise vessels partially overlap with Container vessels, but there are only a small number of vessels in this category;
- Tugs are outliers when compared to the other categories and generally have incomplete data on their design characteristics (see Figure 5).

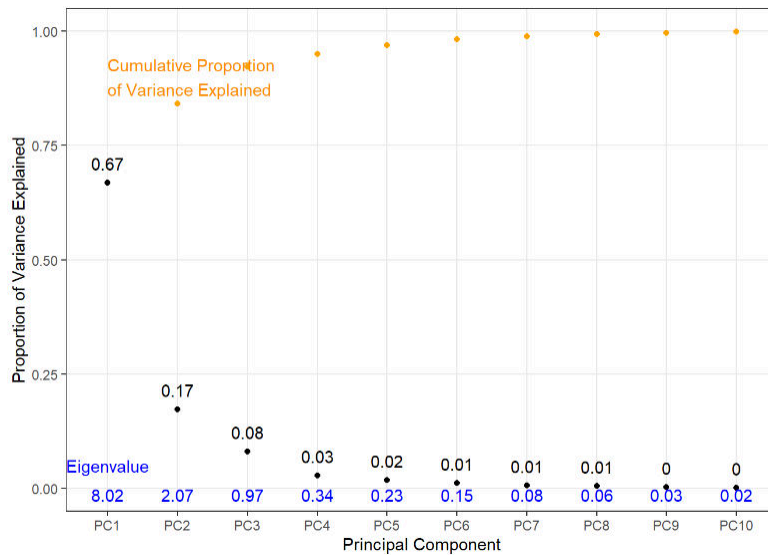


Figure 24. Scree plot showing proportion of variance versus PC number (all categories). Black points indicate the fraction of variability explained by each PC individually. Orange points indicate the fraction of variability explained by all PCs cumulatively. The eigenvalues indicate the relative magnitude of the PCs and are used in the variance calculation.

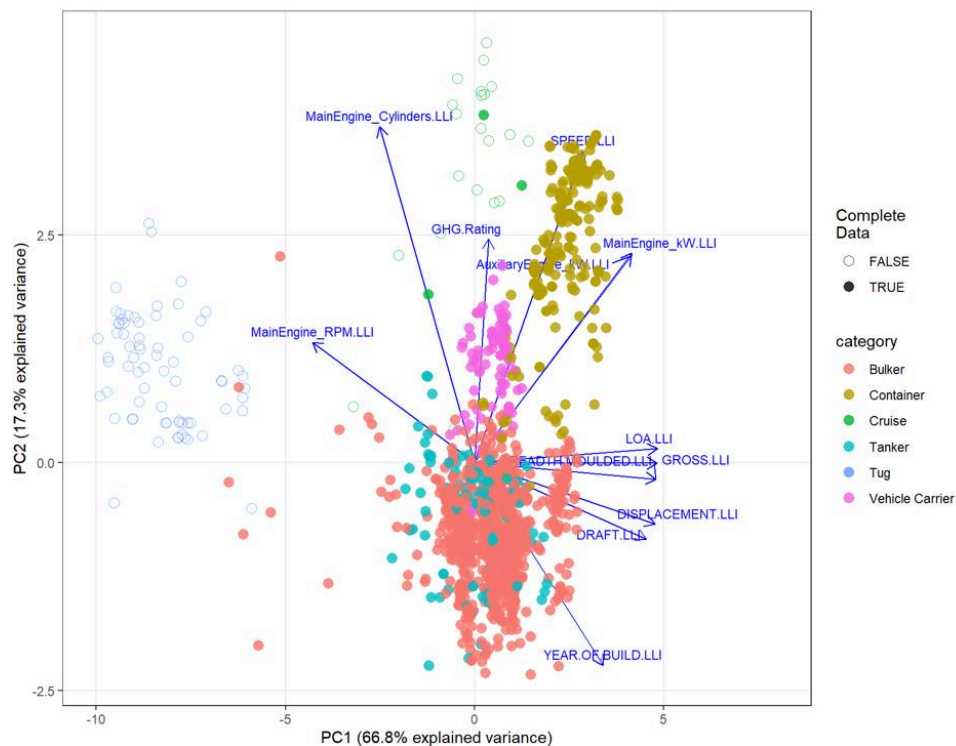


Figure 25. Biplot of first two principal components (PC1 versus PC2) of vessel design parameters (all vessel categories). The points on the scatter plot show the PC scores for each vessel in the data set. Together, PC1 and PC2 explain 84.4% of the variance in the design parameter data set. The spike lines indicate the loadings of each design parameter onto the first two PCs (i.e., the horizontal component of the spike is the PC1 loading and the vertical component of the spike is the PC2 loading). Open and closed circles indicate whether each data point corresponds to a complete case or not (i.e., FALSE = vessel is missing data in one or more columns).

### 3.4. Functional Principal Component Analysis of Source Levels

Functional principal component analysis (FPCA) was applied to source level versus-frequency curves for the entire vessel noise data set. This analysis was used to identify dominant modes of variation in the source level curves (i.e., where source levels at different frequencies varied together according to a common pattern). As with conventional PCA, each mode of variability is associated with a principal component (PC) and the components are ranked according to their relative importance. The purpose of carrying out the FPCA was to understand the variability in source level curves between vessel categories, which helped determine the vessel groupings.

This analysis showed that the majority of frequency-dependent variability in the source level data (93.4%) was captured by the first four principal components (Figure 26). The dominant modes of variation in the FPCA relate to variations both between vessel categories and between individual vessels. The first mode of variability reflects an overall increase or decrease in the MSL curve, with greatest variations observed at high frequencies (>1000 Hz) where cavitation dominates. The second mode of variability reflects specific changes in the low-frequency (<100 Hz) components of the MSL curve. This latter mode of variability relates to frequencies dominated by machinery noise, but also reflects changes in MSL due to the influence of vessel draft (i.e., via the surface dipole effect). Plotting the first two principal components against each other (Figure 27) showed that measurements in a specific vessel category tended to cluster together. However, there was more overlap between the data from different vessel categories than was observed in PCA of the design characteristics (cf. Figure 25). Annex 3 provides additional FPCA results obtained from this analysis.

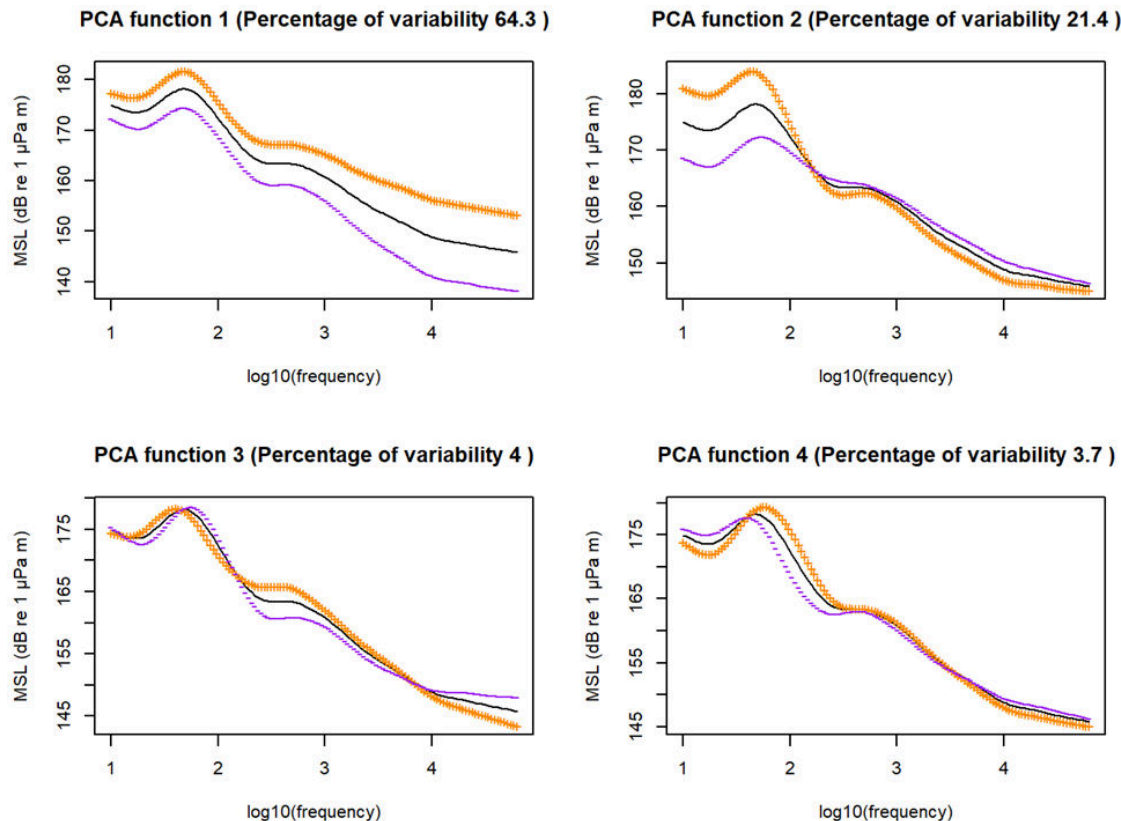


Figure 26. Functional principal component analysis (FPCA) of vessel Monopole Source Level (MSL) versus  $\log_{10}$  frequency (all categories). The middle line (black) corresponds to the mean curve, and the  $\pm$  symbols (orange and purple) show the standard deviation about the mean for the corresponding principal component. Each functional principal component corresponds to a frequency-dependent mode of variability of the data (ranked from strongest to weakest). The slope of variability is positive where the + symbol is above the – symbol and the slope of variability is negative where the + symbol is below the – symbol.

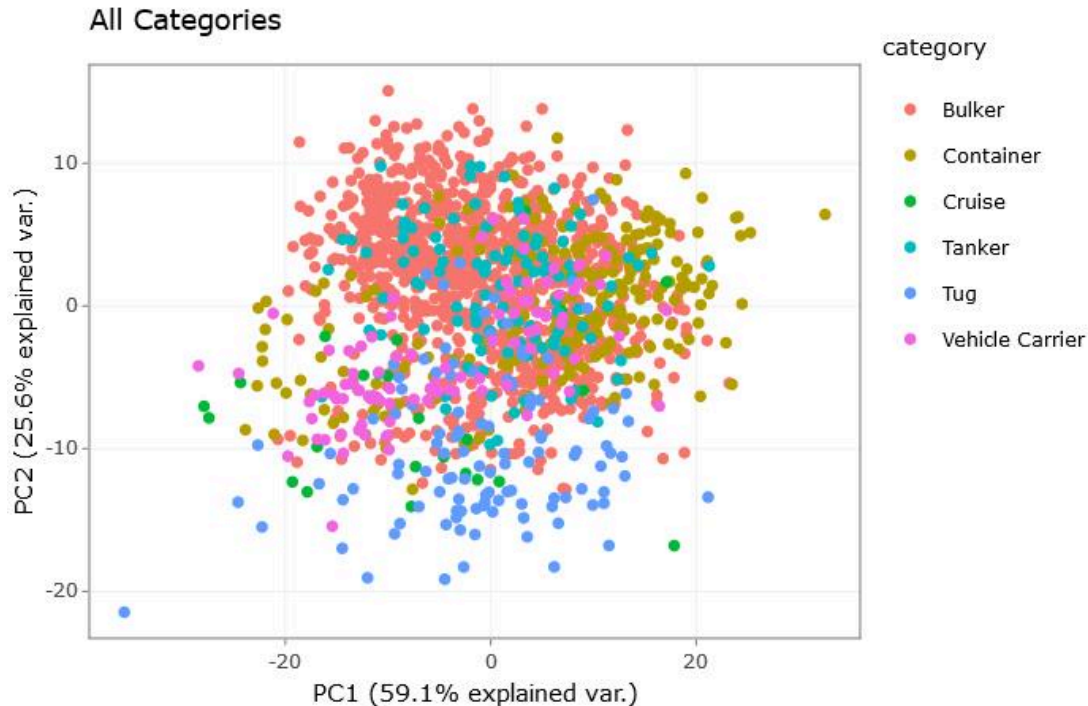


Figure 27. Biplot of first two functional principal components (PC1 versus PC2) of vessel source levels (all vessel categories). The points on the scatter plot show the PC scores for each measurement. Together, PC1 and PC2 explain 84.7% of the variance in the vessel source level data set.

### 3.5. Single-Predictor Functional Regression

Functional regression was applied to investigate the effect of single predictors on frequency-dependent source levels. This analysis was also used to aid in variable selection for the multiple-predictor model (Section 2.5.6). Results are summarized using the coefficient of determination ( $r^2$ ) and frequency-dependent slope coefficient ( $\beta(f)$ , where  $f$  = frequency) between single predictors and decade source level measurements. Annex 4 provides detailed single-predictor functional regression results for each predictor and vessel category.

Frequency-dependent  $r^2$  values (e.g., Figure 28) were used to identify which predictors had the strongest correlation with vessel source levels over a wide range of frequencies. Recall that  $r^2$  values measure the fraction of the source level variability (in the range 0-1) explained by a given predictor. In this analysis, the variance explained by each predictor varies with frequency. Regression function plots (e.g., Figure 29) were used to identify the slope of the trend between the (transformed) predictors and frequency dependent source levels (RNL and MSL). For example,  $r^2$  and slope coefficient estimates for Bulklers and Tankers showed that actual vessel draft was most influential at frequencies above 200 Hz. Differences between RNL and MSL at low frequencies were due to the influence of the draft on the MSL calculation. This is because MSL source depth is assumed to be half of vessel draft, and this in turn influences the MSL estimate because of the surface dipole effect at low frequencies. This is not the case for RNL so, in this instance, RNL better reflects the influence of draft on vessel noise emissions.

In general, the strongest correlations were observed for the two main operational parameters: speed through water and actual draft. Another notable result of this analysis was that the three derived quantities (fractional speed, fractional draft, and block coefficient) all had lower  $r^2$  values than their constituent variables. This indicates that including these derived quantities would not provide any more explanatory power in a statistical model. Thus, they were excluded from consideration in the multiple-predictor functional regression analysis.

Age of the vessel, as reflected by YEAR.OF.BUILD, also had a very weak correlation with RNL ( $r^2 < 0.05$ ) for bulkers, containers, tankers, and vehicle carriers. Although the correlation was slightly higher for tugs (cruise was data-deficient), the consensus of the SME team was that this was not strictly a vessel design parameter (i.e., much like EVDI). Thus, it was also excluded from the multiple-predictor functional regression analysis.

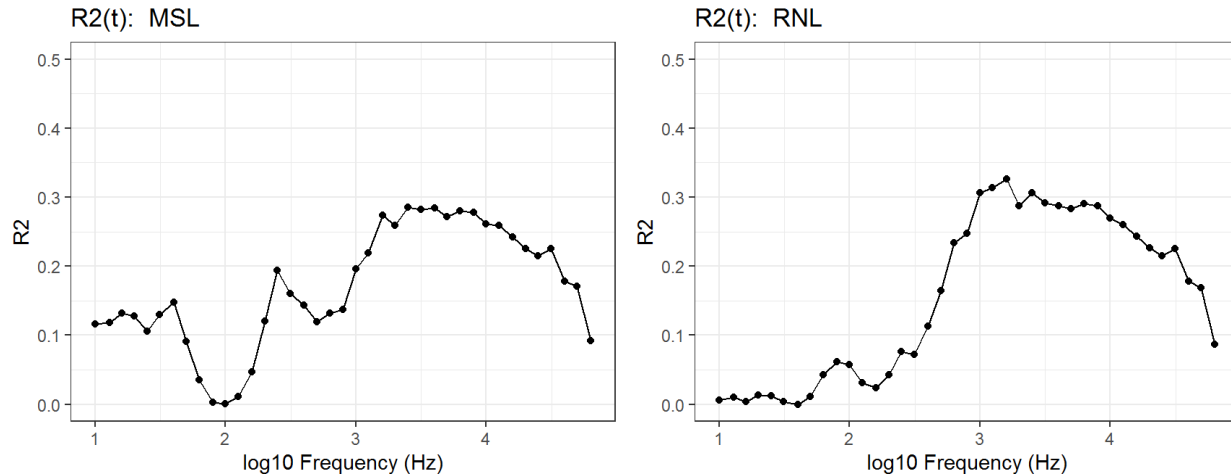


Figure 28. Coefficient of determination ( $r^2$ ) versus log(frequency) for single-predictor functional regression of actual draft and Monopole Source Level (MSL) (left) and Radiated Noise Level (RNL) (right), for Bulkers and Tankers.

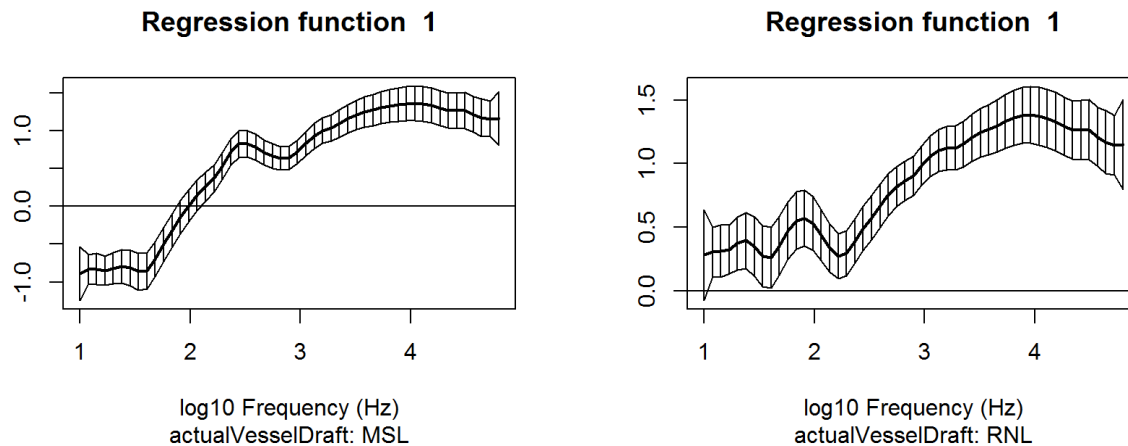


Figure 29. Regression function  $\beta(f)$  (i.e., frequency-dependent slope coefficient) versus log(frequency) for actual vessel draft (Bulkers and Tankers). Left plot is MSL, right plot is RNL. The solid line is the estimated regression coefficient across frequencies and the hatched area is the 95% confidence interval on the estimated regression coefficient. Positive values of  $\beta(f)$  indicate that increasing draft was associated with higher source levels, whereas negative values indicate that increasing draft was associated with lower source levels.

### 3.6. Variable Selection

Final variable selection was carried out after reviewing the single-predictor functional regression results with the SME team and ECHO team (Table 6). The short-list of predictors was used for developing the multiple-predictor functional regression model (Section 3.7).

Table 6. Results of variable selection for multivariate analysis. Keep/Toss refers to whether a predictor was retained for the multiple-predictor functional regression model (Section 2.5.7).

Variable Name	Description	Expected to impact URN	Keep/Toss	Rationale
GROSS.LLI	Gross tonnage, according to Lloyds.	No	Keep	ATC Rank 1
DRAFT.LLI	Maximum Draft of the vessel according to Lloyds. Measured at Summer load lines.	No	Toss	Redundant with PPA actual draft
YEAR.OF.BUILD.LLI	Year the vessel was built, from Lloyds.	No	Toss	Not a design parameter
DISPLACEMENT.LLI	Maximum displacement of the vessel, according to Lloyds. Measured at summer load line.	No	Keep	ATC Rank 1
BREADTH.MOULDED.LLI	Maximum breadth of the vessel, measured at the molded line of the frame.	No	Keep	ATC Rank 1
draft.fraction	Actual draft as fraction of summer draft.	No	Toss	Weak correlation with URN
actualVesselDraft	Actual vessel draft from PPA, AIS, and summer draft, in that order.	Minimal	Keep	
surface.angle	The depression angle from vessel to the hydrophone (calculated). Measured with respect to the sea surface.	Minimal	Keep	Accounts for single-hydrophone effects
LOA.LLI	Overall length of the vessel, according to Lloyds.	Minimal	Keep	
MainEngines_No.LLI	Number of main engines in the vessel.	Minimal	Toss	Insufficient range
MainEngine_RPM.LLI	Maximum rated RPM of the main engine.	Minimal	Keep	ATC Rank 1
MainEngine_Cylinders.LLI	Number of cylinders in the main engine.	Minimal	Toss	Unclear relationship to URN (specific to engine model)

Variable Name	Description	Expected to impact URN	Keep/Toss	Rationale
No_of_propulsion_units.LLI	Number of propulsive engines. Corresponds to number of propellers.	Minimal	Toss	Insufficient range (except tugs)
AuxiliaryEngine_kW.LLI	Maximum rated power output of the auxiliary engines.	Minimal	Keep	
block.coefficient	Ratio of displacement to submerged volume (calculated using summer draft & displacement).	Minimal	Toss	Weak correlation with URN and strongly correlated with length, breadth, and draft
sow	Speed through water. Calculated from speed over ground, course over ground, current speed, and current direction.	Direct	Keep	
wind.resistance	Resistance on the vessel due to the wind. Calculated from wind speed, wind direction, speed over ground and course over ground.	Direct	Keep	
SPEED.LLI	Service speed of the vessel, according to Lloyds. The speed the ship is designed to maintain, at the summer load waterline at maximum propeller RPM.	Direct	Keep	
MainEngine_kW.LLI	Maximum rated power output of the main engines.	Direct	Keep	
PropellerType.LLI	The type of propeller. Az = Azimuth Drive, CP = Controllable Pitch, DP = Directional Pitch, FP = Fixed Pitch, RP = Rudder Pitch, Z = Z type	Direct	Toss	Insufficient range of values
speed.fraction	Speed through water as fraction of service speed.	Direct	Toss	Captured by difference of log10(sow) and log10(SPEED.LLI)

### 3.7. Multiple-Predictor Functional Regression

Multiple-predictor functional regression models were developed to investigate the simultaneous correlation of vessel source level measurements (both RNL and MSL) with their design, measurement, and operational characteristics. Multiple-predictor functional regression models were developed for each category group by including predictors incrementally and calculating pointwise  $r^2$  values for each frequency band (for both RNL and MSL). First, operational characteristics were included as predictors, followed by design characteristics. As LOA.LLI, BREADTH.MOULDED.LLI, GROSS.LLI,

DISPLACEMENT.LLI were highly correlated (Figure 30), LOA.LLI (easiest to interpret and understand) was included first. The remaining size-related variables were included after all other variables were added. This was done as a final check to assess whether they provided additional improvement to the final model. Note that, due to the large number of Bulker measurements and the computational intensity of the analysis, only 30% of bulker observations (randomly selected) could be included for calculating confidence intervals for the multiple-predictor functional regression for the Bulker and Tanker group. Several sets of randomly selected bulker observations were assessed to ensure that the results were consistent across randomly selected subsets (Annex 5). All tanker measurements were included in the functional regression model. Annex 5 provides details of the multiple-predictor functional regression models for all vessel groupings.

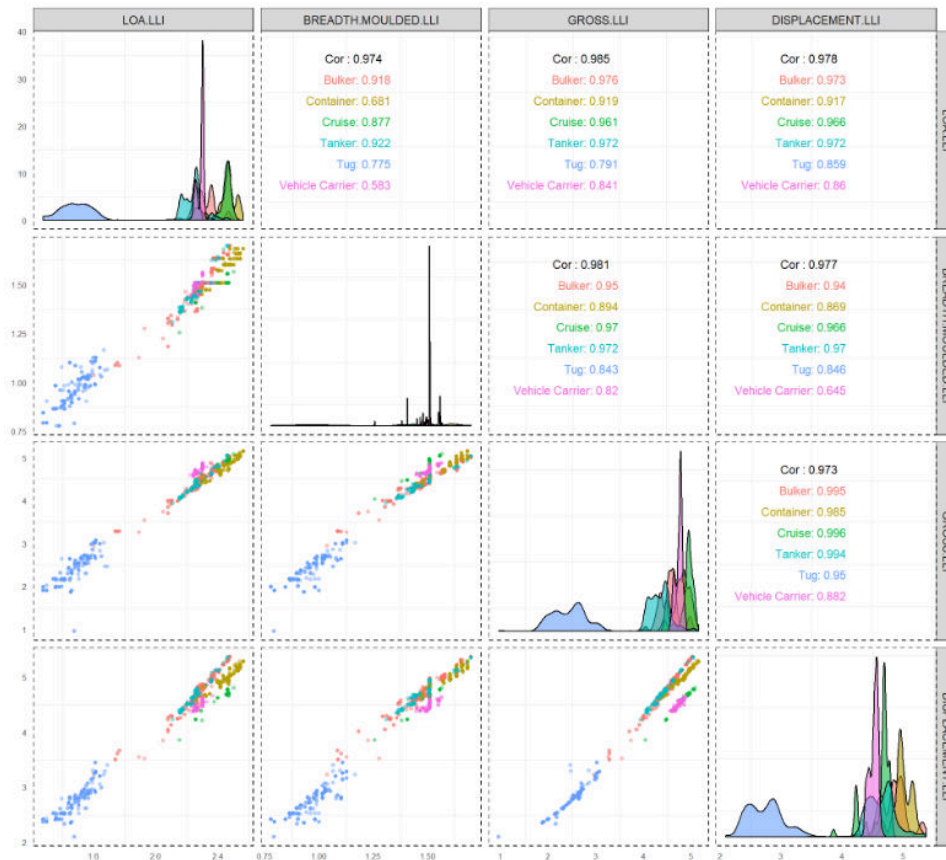


Figure 30. Plots showing collinearity of size-related predictors: LOA.LLI, BREADTH.MOULDED.LLI, GROSS.LLI, and DISPLACEMENT.LLI.

While the regression results were generally different for each vessel group, incremental analysis of the pointwise  $r^2$  values (e.g., Figure 31) showed that the operational variables (sow, actualVesselDraft) explained the largest fraction of the source level variability. The design parameters, by contrast, generally explained much less of the variability. In particular, the additional size related variables (BREADTH.MOULDED.LLI, GROSS.LLI, DISPLACEMENT.LLI) did not generally improve the fit of the models to the data. Thus, the final models included only the following nine predictors:

1. actualVesselDraft,
2. sow,
3. wind.resistance,
4. surface.angle,

5. LOA.LLI,
6. MainEngine\_RPM.LLI,
7. MainEngine\_kW.LLI,
8. AuxiliaryEngine\_kW.LLI, and
9. SPEED.LLI.

Regression function plots (e.g., Figure 32) were used to show the frequency-dependent slope of the trend between the (transformed) predictors and decibade source levels (RNL and MSL). The regression functions show how strongly the source levels at each frequency correlate with each predictor (either positive or negative). Confidence intervals (95%) were calculated for the regression functions. The correlation is not statistically significant where the confidence intervals intersect the zero line. Within the same group, regression functions for a given predictor were generally very similar for RNL and MSL, with the notable exception of actualVesselDraft. The reason for this latter discrepancy is that the draft is directly involved in the MSL calculation, whereas this is not the case for RNL (see discussion in Section 3.5).

To aid in the interpretation of the regression functions, predicted source level plots (e.g., Figure 33) were created to show the influence of individual predictors on source levels for an average vessel in each group. The curves show the predicted source levels obtained by changing the value of a single predictor (color-coded) while holding all other predictors at fixed average values. For predictors having more than 200 possible values in the data, 200 values were randomly selected, along with the minimum and maximum value. Narrow groups of lines correspond to cases where there was very little variation with a given predictor. Appendix C shows predicted source level plots for all vessel groups.

Note that the unusual trends observed for Cruise vessels, for some predictors, were likely due to the small number of measurements included in this category (only 50 were included, after subsampling for repeat measurements). Unlike other categories, Cruise vessels were extremely heterogeneous, so large deviations from the mean could be due to a single vessel. More data would likely be needed to better understand the relationships between predictors and source levels for this category.

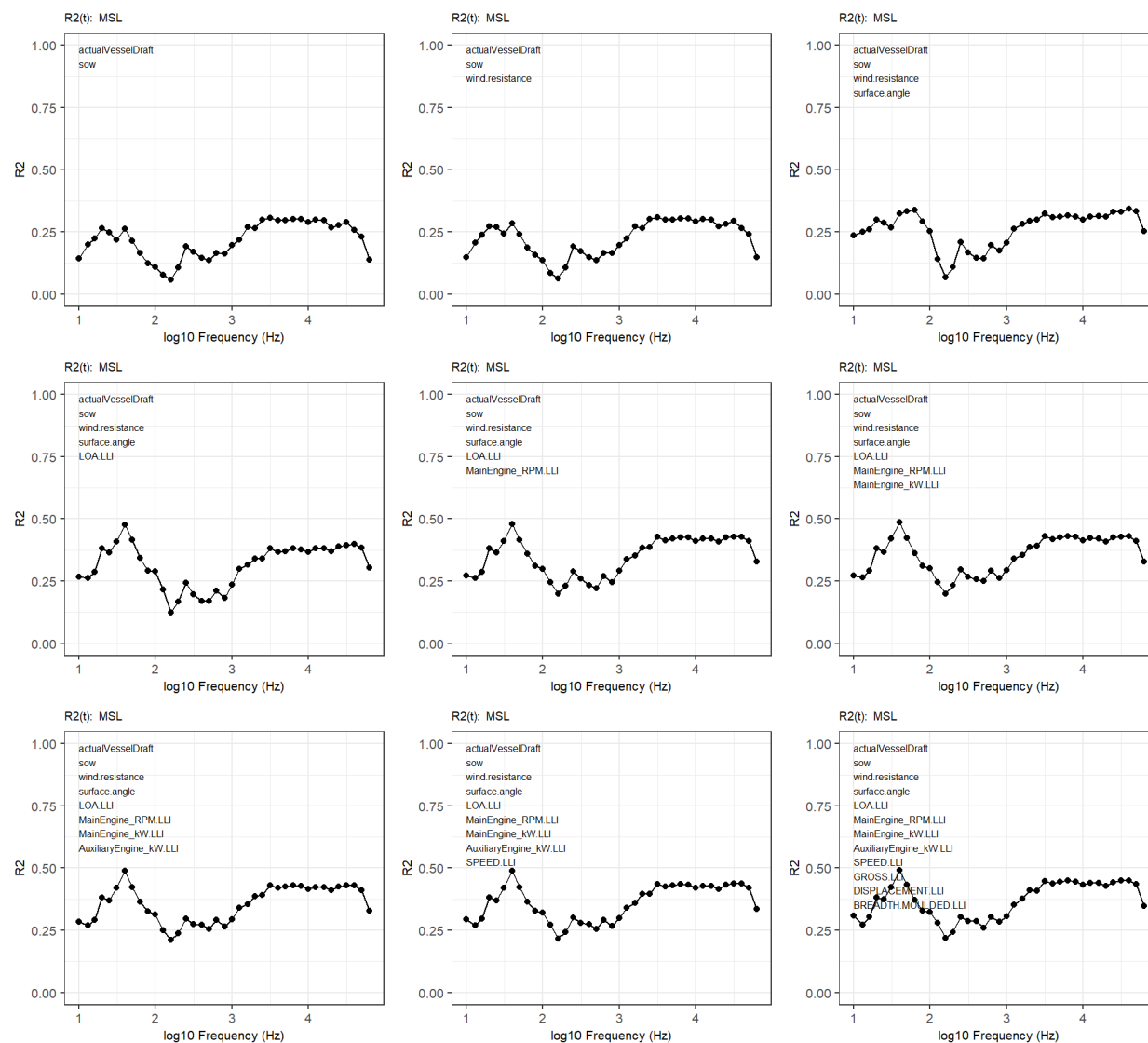


Figure 31. Coefficient of determination ( $r^2$ ) versus  $\log(\text{frequency})$  obtained from incrementally adding predictors to the multiple-predictor functional regression model for Bulkers and Tankers (Monopole Source Level (MSL)). The  $r^2$  value indicates the fraction of the source level variability explained by the model in each frequency band. The annotation lists the variables included in the model at each step (from top-left to bottom-right). See Section 2.5.7 for additional explanation of these plots.

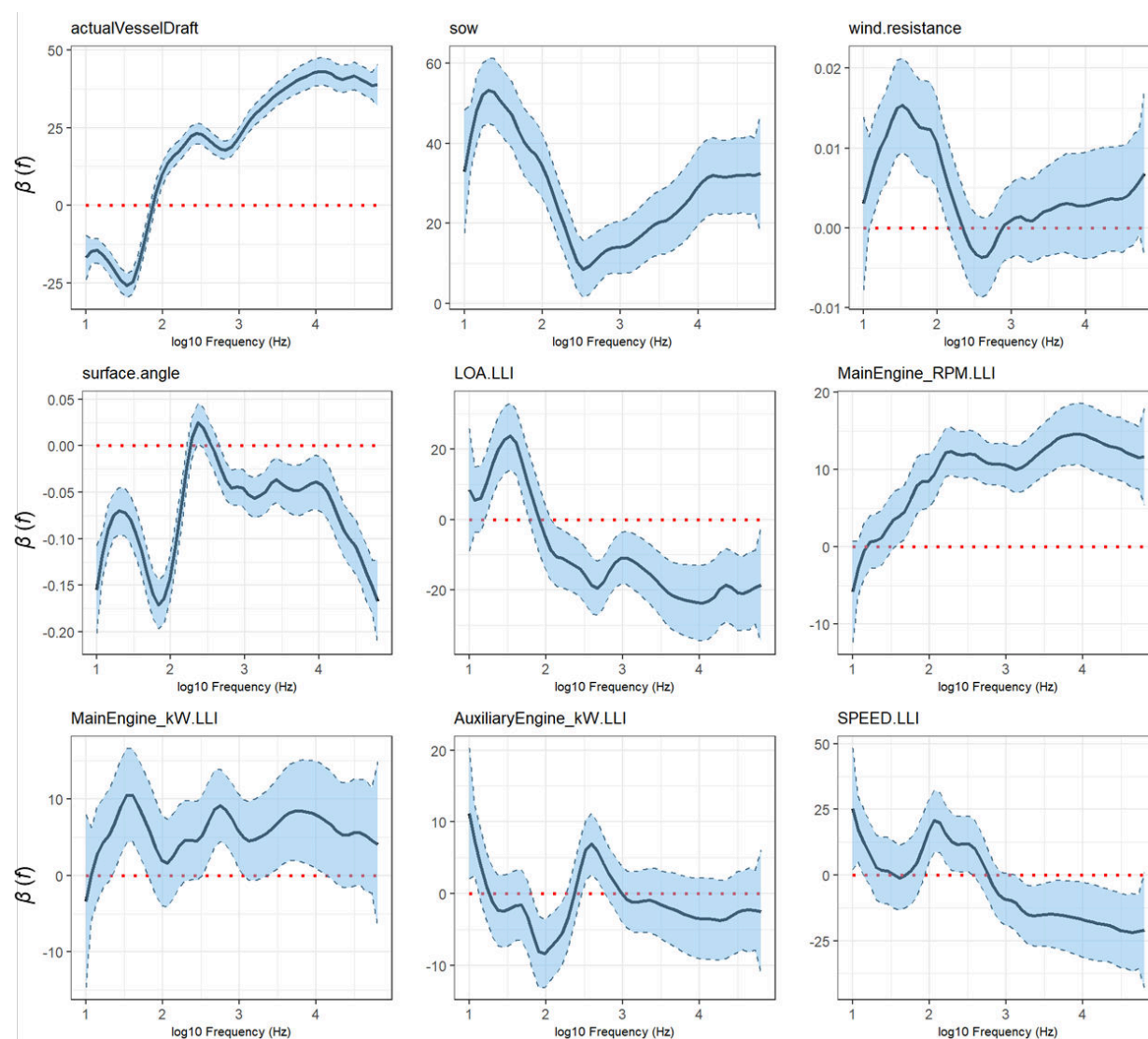


Figure 32. Monopole Source Level (MSL) regression functions  $\beta(f)$  (i.e., frequency-dependent slope coefficients) versus  $\log(\text{frequency})$  for all predictors for the Bulker and Tanker group. The solid line is the estimated regression coefficient and the blue area is the 95% confidence interval for the coefficient. Positive values of  $\beta(f)$  indicate that an increasing predictor value was associated with higher MSL, whereas negative values indicate that an increasing predictor value was associated with lower MSL.

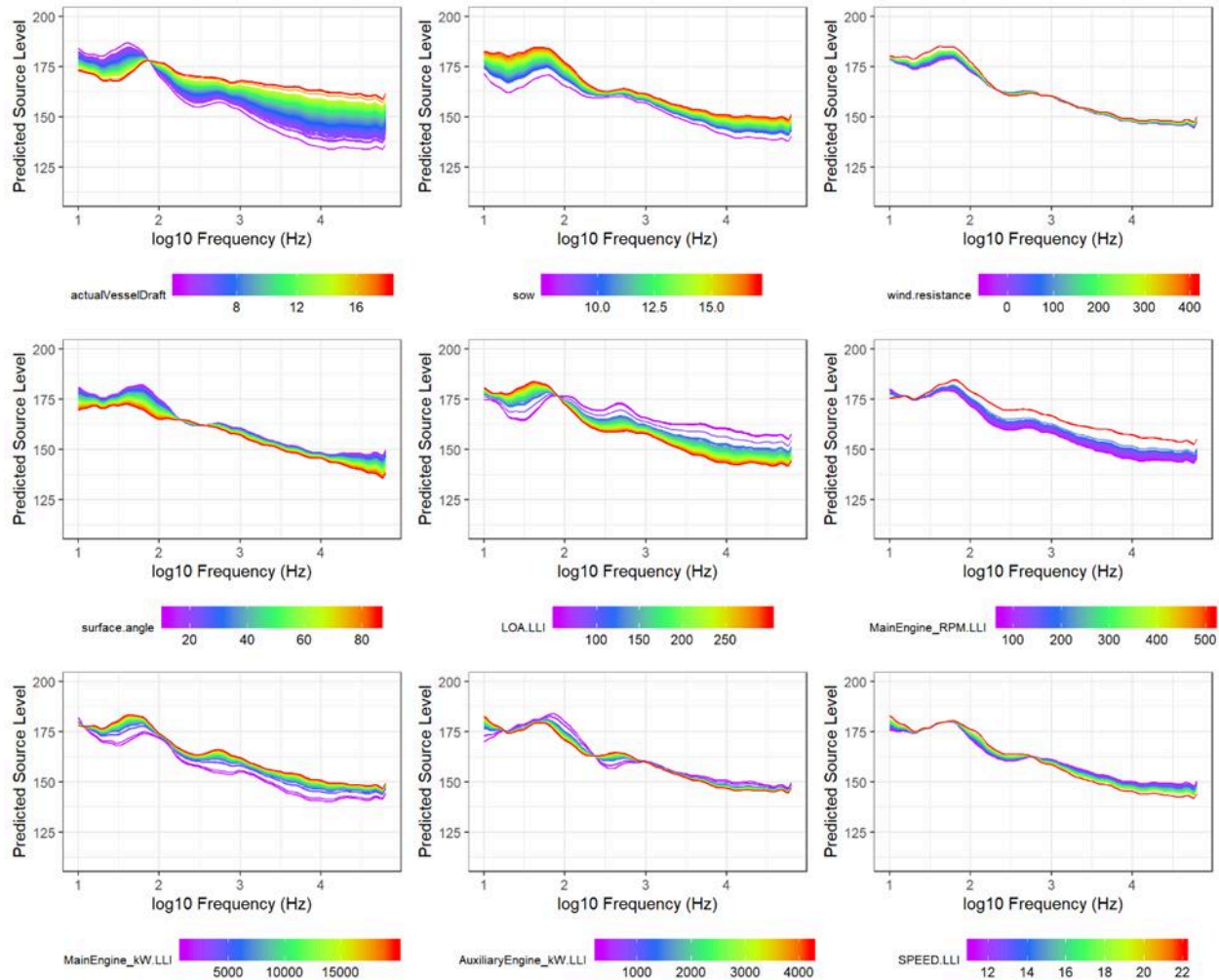


Figure 33. Plots of predicted Monopole Source Level (MSL) (dB re 1  $\mu\text{Pa m}$ ) versus  $\log(\text{frequency})$  from the multiple-predictor functional regression model, for Bulkers and Tankers. Each panel shows the effect of varying a different predictor in the model, while keeping the other predictors constant. The curves show the predicted deviation from the mean source level obtained by varying the predictor value over the range indicated by the color bar. The color of each curve corresponds to the associated predictor value.

### 3.8. Correlations with Greenhouse Gas Emissions

A graphical analysis was used to investigate whether vessel noise emissions were correlated with greenhouse gas (GHG) emissions. Emissions are not strictly a vessel design parameter, but they do relate to the installed machinery (engines and generators). Emissions data from RightShip were available in terms of two different variables:

- **EVDI (Existing Vessel Design Index)**: equal to the rate of  $\text{CO}_2$  emissions of a vessel, in grams per gross tonnage, per nautical mile travelled. A higher value represents higher intensity of emissions.
- **GHG.Rating**: a letter grade scale (A-G) ranking the  $\text{CO}_2$  efficiency of a vessel relative to its size and class cohort. The scale indicates the number of standard deviations from the mean score for a vessel class. A is the best, G the worst, and D is the centre.

GHG ratings were only available for cargo vessels, so tugs and cruise vessels were excluded from this analysis. Graphical comparisons were performed using decade band RNL (Figure 34), after adjusting for

speed through water and actual vessel draft using the multiple-predictor functional regression models. All measurements were adjusted to the average speed and draft value for the vessel group before performing the comparison. The adjustments were performed by scaling decidecade RNL values using the regression functions,  $\beta(f)$ , for the corresponding category group and predictor. Broadband adjusted RNL values were calculated from the power sum of the scaled decidecade bands.

The observed correlations between RNL and GHG emissions were weak, with a substantial degree of scatter, but some trends were evident (Table 7). Furthermore, the observed trends were markedly different for the two vessel groups:

- Containers and Vehicle Carriers exhibited a weak negative trend of decreasing RNL with increasing EVDI in the 10–100 Hz and 100–1000 Hz bands. The trend in the 1000–10000 Hz band was nearly flat. No clear trend was evident with the GHG rating data.
- Bulkers and Tankers exhibited a weak positive trend of increasing RNL with increasing EVDI in the 100–1000 Hz and 1000–10000 Hz bands. The trend in the 10–100 Hz band was nearly flat. A clear trend was evident in the GHG rating data, with A-grade vessels generally having the lowest RNL.

This discrepancy may be attributable to differences in the trends of RNL with vessel size in these two groups, and the tendency of GHG ratings to improve with increasing vessel size (see GHG.Rating correlations in Appendix B). For Bulkers and Tankers, larger vessels tended to have lower RNL (above 100 Hz), whereas for Containers and Vehicle Carriers, larger vessels tended to have higher RNL (at all frequencies). Thus, these trends are likely driven by differences in relative GHG emissions between large and small vessels in each group.

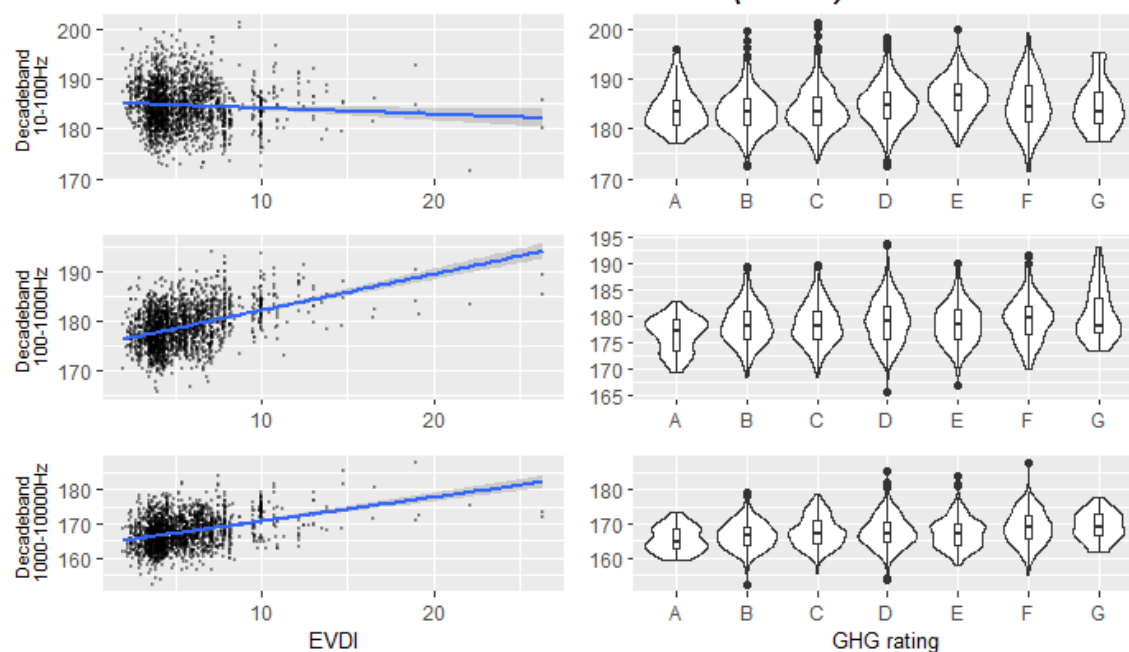
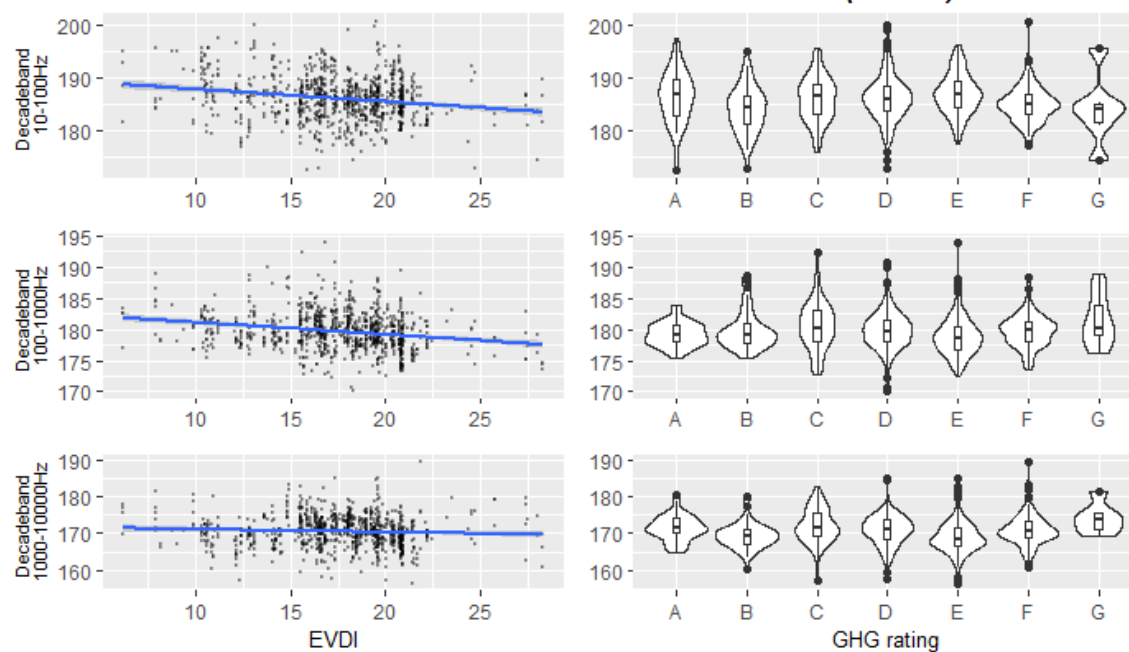
*Bulkers and Tankers (RNL)**Containers and Vehicle Carriers (RNL)*

Figure 34. Left: scatter plots of adjusted decade-band RNL (dB re 1  $\mu$ Pa m) versus EVDI (grams CO<sub>2</sub> per tonne nautical mile). The blue lines indicate the best-fit linear trend for the data. Right: violin plots of adjusted decade-band Radiated Noise Level (RNL; dB re 1  $\mu$ Pa m) versus GHG rating (ranked from A-G). The width of the swath corresponds the distribution of the data and interior boxes indicate the 25th, 50th, and 75th percentiles of the data (dots indicate outliers). The measured RNL values have been adjusted for operating speed and draft of the vessels.

Table 7. Best-fit trend line parameters of adjusted RNL versus EVDI data as determined by linear regression analysis. The coefficient of determination ( $r^2$ ) is a number in the range 0–1 that indicates the strength of correlation between RNL and EVDI (0 = no correlation, 1 = total correlation). Asterisks indicate the significance level of the slope (\* =  $p < .05$ , \*\* =  $p < .01$ , \*\*\* =  $p < .001$ ). Values without an asterisk are not statistically significant (i.e.,  $p \geq .05$ ).

Decade band	Slope of adjusted RNL versus EVDI (dB/g[CO <sub>2</sub> ] GT <sup>-1</sup> nmi <sup>-1</sup> )	Coefficient of determination ( $r^2$ )
<i>Bulkers and Tankers</i>		
10–100 Hz	-0.031**	0.003
100–1000 Hz	0.214***	0.156
1000–10000 Hz	0.170***	0.119
<i>Containers and Vehicle Carriers</i>		
10–100 Hz	-0.159***	0.036
100–1000 Hz	-0.249***	0.047
1000–10000 Hz	-0.050	0.002

### 3.9. Spectrum Analysis

In order to augment the statistical analysis of the ECHO database, fine-scale spectrum data were compared for the loudest five measurements and the quietest five measurements in each of the six vessel categories. The objective of the spectrum analysis was to identify whether the loudest and quietest measurements in each vessel category shared common spectral characteristics, and to determine how those characteristics relate to results of the multivariate analysis. Figure 35 shows the 10 selected vessel spectrum measurements for the Bulker category (0–200 Hz). Plots of the spectrum data for all 60 vessel measurements are presented in Appendix D.

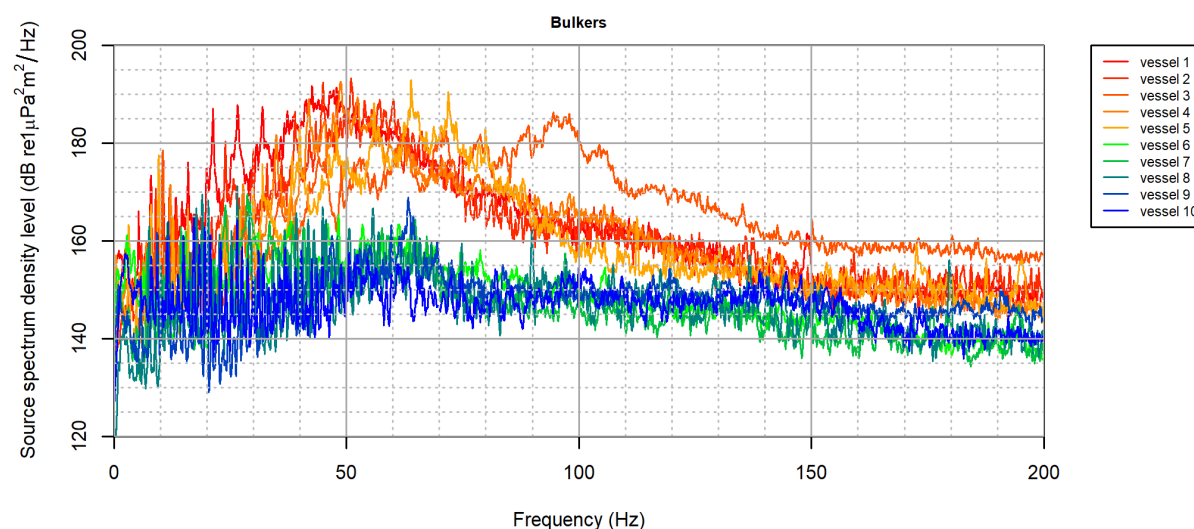


Figure 35. Plot of source spectrum density level versus frequency for Bulkers (0.125 Hz analysis bandwidth, 0–200 Hz). The vessel identities have been anonymized and are numbered in order of their ranked adjusted RNL (from loudest to quietest). The five loudest vessels are displayed using hot colors (red-orange) and the five quietest vessels are displayed using cool colors (green-blue).

Qualitative comparisons of noise level versus frequency plots indicated that the loud merchant vessels (i.e., bulkers, containers, tankers, and vehicle carriers) often exhibited a characteristic hump in their noise spectrum around 50 Hz, whereas the quiet vessels had a flatter spectrum below 100 Hz (e.g., Figure 35). This hump is believed to be related to propeller cavitation, though the specific noise generating mechanism is not entirely understood at present (Wittekind and Schuster 2016).

Both the loud and the quiet vessels in all classes exhibited a large number of discrete tones in their low-frequency spectrum (approximately below 500 Hz). Analysis of tones in the spectrum measurements indicated that the quiet vessels generally exhibited a greater number of distinct tones than the loud vessels (Table 8). This result, while seemingly counterintuitive, is likely due to masking of weaker machinery tones by wideband, low-frequency, cavitation noise. This is reflected by the fact that quiet vessels generally had more discrete tones between 10–100 Hz than loud vessels (Figure 36; see also Fig. 2 in Wittekind and Schuster (2016)). Nonetheless, tone levels for the loud vessels were about 10 dB higher, on average, than for the quiet vessels (Figure 37). The average spectral decay rate was also steeper for the loud vessels (Table 8), which is mostly attributable to the cavitation hump near 50 Hz.

The design characteristics of the loudest and quietest vessel measurements are provided in Table D-1. No clear differences in design characteristics were evident between loud and quiet vessels, other than that the loud vessels in the Bulker, Container, and Cruise vessel categories tended to be larger in size, which was consistent with the trends identified by the functional regression analysis. For the limited data set used for detailed spectrum analysis, the relationship of larger vessels being louder did not hold true for the other vessel categories including Tugs, Tankers, and Vehicle Carriers.

Table 8. Statistics of numbers of tones and spectral slope (mean  $\pm$  standard deviation) for the loud and quiet vessel spectrum measurements. The spectral slope was calculated by applying linear regression to the spectrum-level-versus-log-frequency data, after smoothing using an 81-point median filter.

Spectrum feature	Loud vessels	Quiet vessels
Number of tones	40.1 $\pm$ 34.3	54.2 $\pm$ 38.3
Slope (dB/decade)	-16.5 $\pm$ 4.3	-15.1 $\pm$ 4.4

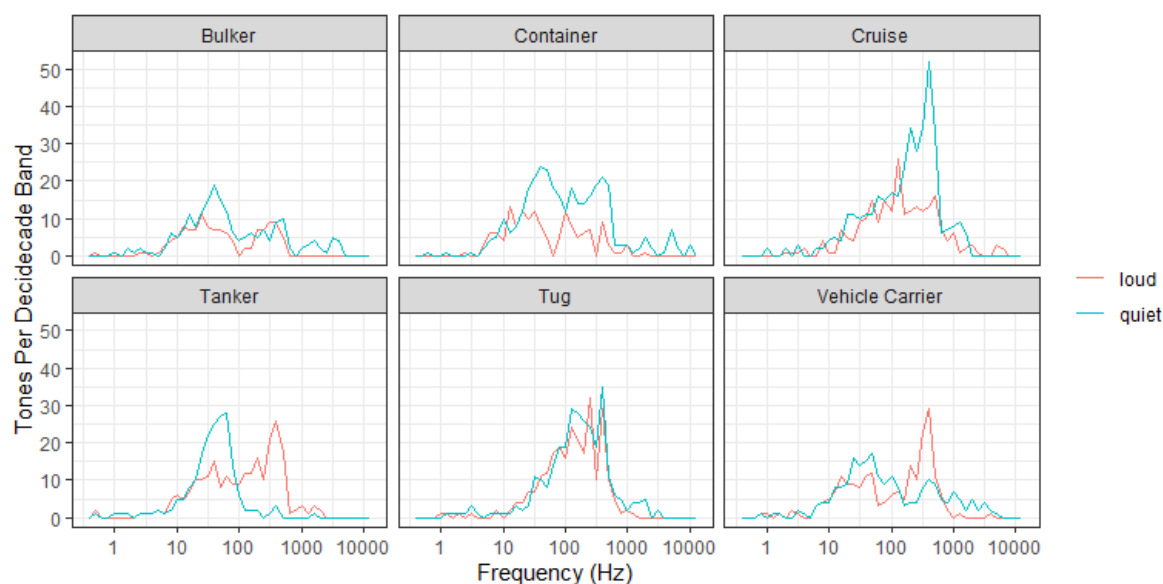


Figure 36. Total number of tones per decade band identified in the loud and quiet vessel spectrum measurements.

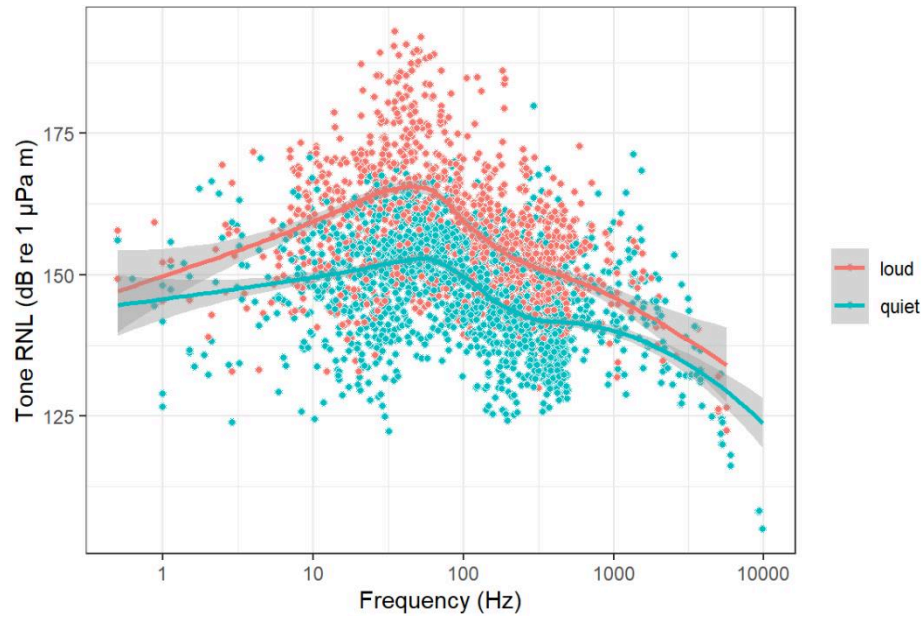


Figure 37. Plot of Radiated Noise Level (RNL) versus frequency of all tones identified in spectra of loud and quiet vessels. The points indicate the RNL and frequency of individual tones, and the lines show the smoothed trend versus frequency.

## 4. Discussion

### 4.1. RNL versus MSL

Radiated noise levels (RNL) and monopole source levels (MSL) both provide a useful method for measuring vessel noise emissions, but they have different limitations and are suited to different purposes. MSL is a more physically rigorous quantity and is the best choice for making accurate far-field sound level predictions (i.e., via sound propagation modelling). The MSL calculation explicitly corrects for the influence of the sea-surface (primary) and seabed (secondary) reflected sound energy on vessel source level measurements. There is, however, not yet a standard method for calculating MSL that is recognized by the major standards bodies (ANSI and ISO). Furthermore, the value of MSL is sensitive to the value of the assumed monopole source depth at low frequencies. The monopole source depth is not a directly measured dimension or otherwise determined quantity.

RNL is more directly related to measured vessel noise emissions (as received at short distances) and is repeatable when measured according to the ANSI S12.64 standard method. For an opportunistic measurement program, as undertaken by ECHO at the ULS, it is only possible to approximately adhere to the full S12.64 standard when computing RNL. Even with the simplest measurement method (Grade C), restrictions on repeat measurements, hydrophone geometry, and water depth must be relaxed when implementing a measurement program in vessel traffic lanes under practical conditions. Deviation from the strict standard is nonetheless offset by the large number of measurements available in the ECHO database.

RNL and MSL are both calculated from identical SPL data (by ShipSound) and differ only in the post-processing method used to adjust the received level to obtain a source level. Figure 38 shows a comparison of MSL and RNL for a typical vessel noise measurement at the ECHO ULS. The MSL is greater than RNL at lower frequencies and less than RNL at higher frequencies, with the crossover frequency between these two regimes determined by the assumed source depth (6.25 m in this case). The results of the noise correlation analysis (Sections 3.5 and 3.6) are not generally RNL- or MSL-dependent, with the exception of `surface.angle` and `actualVesselDraft`. MSL is sensitive to these last two parameters because they determine strength of influence of the sea-surface in the propagation loss calculation. Overall, the results of the statistical analyses are more easily related to underwater radiated noise via RNL since details of the propagation loss calculation do not need to be taken into account. Nonetheless, the MSL remains the preferred metric for detailed noise level prediction in other contexts.

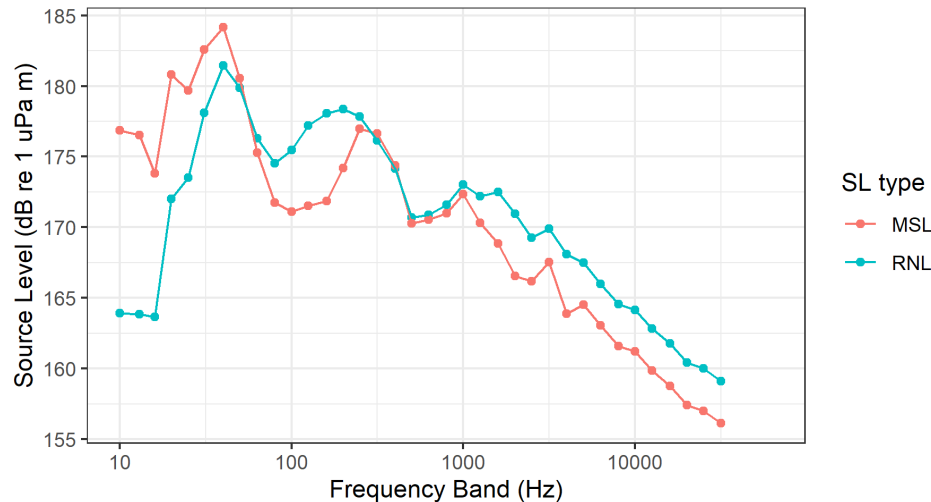


Figure 38. Comparison of Radiated Noise Level (RNL) and Monopole Source Level (MSL) versus frequency for the same containership measurement. The monopole source depth assumed in the MSL calculation was 6.35 m, which corresponds to a quarter-wavelength frequency of 60 Hz in water. Below this frequency, the dipole effect increases the calculated MSL above the RNL (i.e., due to increased propagation loss). Above this frequency, reflected sound energy reduces the calculated MSL below the RNL (i.e., due to reduced propagation loss).

## 4.2. Influence of Speed and Draft

The statistical analysis showed that speed through water and actual vessel draft (i.e., the two primary operational parameters) were generally the most influential predictors for underwater noise. While the specific influence of these predictors was slightly different between categories, the overall patterns of variability were nonetheless consistent (with the exception of Cruise vessels, which was a data-deficient group). Wind resistance and surface angle (measurement predictors) also had low-to-moderate influence on underwater radiated noise, but practically speaking neither parameter is an effective control of underwater radiated noise from a design standpoint.

Higher speed through water was associated with higher underwater radiated noise for all vessel groups. It had the greatest influence at high frequencies (>1000 Hz), where cavitation dominates, and the smallest influence at mid frequencies (100–1000 Hz), where machinery noise dominates. This observation was consistent with results obtained during the 2017 Haro Strait slowdown study (MacGillivray et al. 2019). This trend is to be expected for conventional fixed-pitch propellers, which is the predominant type of propulsion employed by vessels in this data set, but it is not necessarily the case for controllable-pitch propellers (e.g., as was shown for ferries in MacGillivray et al. (2017)).

Actual vessel draft also had a strong influence on underwater radiated noise, primarily at frequencies above 100 Hz. As with speed through water, the strongest influence of actual vessel draft was at high frequencies (>1000 Hz), where cavitation dominates the noise spectrum. Interestingly, actual vessel draft had a negligible, or slightly-negative influence on underwater radiated noise below approximately 100 Hz<sup>4</sup>. From a noise control perspective, draft can influence underwater radiated noise in the following different ways:

- Deeper draft results in more surface area in the water, and more surface area results in better coupling to underwater sound propagation;
- Deeper draft may be related to greater hydrodynamic drag, resulting in more power (and, thus, more vibration) needed to travel at the same speed; and

<sup>4</sup> Note that the influence of actual vessel draft on underwater radiated noise at low frequencies is better reflected by the RNL results, due to the reasons discussed in Section 4.1.

- Shallower draft can lower the cavitation inception speed (due to lower hydrostatic pressure), resulting in higher underwater radiated noise. This effect is pronounced for greater depths as is found with submarines.

Results of the statistical analysis may indicate that drag and surface area dominate above 100 Hz, whereas cavitation inception may dominate at low frequencies where blade-rate cavitation tonals are an important contributor to radiated vessel noise.

### 4.3. Influence of Design Characteristics

When considering ship design from a noise control perspective, the most relevant parameters are as follows:

- Airborne sound within machinery spaces,
- Vibration of mechanical equipment (mostly propulsion engines),
- Hull materials (whether steel, aluminum, or another material),
- Exposed surface area of a vibrating hull,
- Use of noise mitigating materials (i.e., machinery vibration isolators, insulation, hull dampening below the waterline).

None of these parameters are part of the LLI or other databases. However, machinery sound and vibration are related to engine power and ship speed. Exposed surface area is related to length (LOA), draft and beam.

Of the design parameters considered in the statistical analysis, length overall (LOA.LLI) was generally the design parameter most strongly associated with increased underwater noise emissions. Vessels with larger length overall have a greater surface area to propagate underwater sounds. It is also interesting to note that historical naval equations for source levels of surface ships include length and speed as direct indicators of higher sound (Ross and Alvarez 1964). An alternative formulation includes the displacement tonnage instead of length (Ross 1976), but, as demonstrated by the statistical analysis, length and displacement are strongly correlated parameters and cannot easily be disentangled. The observed univariate trends of RNL versus LOA.LLI and DISPLACEMENT.LLI were roughly consistent with the reported trends from the historical equations.

Table 9 provides a qualitative ranking of the relative influence on RNL of the five vessel design parameters included in the functional multiple regression analysis. It is clear that, apart from LOA.LLI, the rankings and correlations of the predictors are not generally consistent between categories. In addition, the design parameters do not seem to be as impactful as expected, especially MainEngine\_kW. All other things being equal, a ship with higher installed power should be louder. Likewise, AuxiliaryEngine\_kW.LLI should only be impactful in unusual situations (e.g., if it were hard mounted improperly to the hull below the waterline or potentially when the auxiliary engine is not operating properly).

Table 9. Ranking of design parameters, based on a qualitative review of the functional multiple regression analysis results for Bulkers & Tankers, Containers & Vehicle Carriers, and Tugs. Arrows indicate direction of association with Radiated Noise Level (RNL) and frequency dependence: ↑ = positive, ↓ = negative, ↑↓ = positive at low frequency, negative at high frequency, ↓↑ = negative at low frequency, positive at high frequency, – = negligible. For example, SPEED.LLI (↓) for tugs indicates that RNL decreases as design speed increases. Cruise vessels are not included, as this category did not have enough samples for high-confidence statistical estimates.

Ranking	Bulkers & Tankers	Containers & Vehicle	Tugs
Highest ↑ ↓ Lowest	LOA.LLI (↑↓)	LOA.LLI (↑)	LOA.LLI (↑)
	MainEngine_RPM.LLI (↑)	MainEngine_kW.LLI (↓)	SPEED.LLI (↓)
	MainEngine_kW.LLI (↑)	AuxiliaryEngine_kW.LLI (↑↓)	AuxiliaryEngine_kW.LLI (↑)
	SPEED.LLI (↑↓)	SPEED.LLI (↓)	MainEngine_kW.LLI (↓↑)
	AuxiliaryEngine_kW.LLI (–)	MainEngine_RPM.LLI (↑)	MainEngine_RPM.LLI (↓↑)

When interpreting these results, it is important to note that the statistical methods employed by the study only had the ability to examine correlation, not causation. The analysis was also limited by the sampling methods inherent to the data set, which was collected opportunistically for traffic coming in and out of the Port of Vancouver (i.e., not in fashion that controlled for design parameters). For example, the functional multiple regression showed that higher MainEngine\_kW was associated lower underwater radiated noise for the Containers and Vehicle Carriers group. This result defies common sense, unless one also considers that MainEngine\_kW was strongly correlated with LOA in this group, and larger LOA is more strongly associated with higher -RNL. The underlying relations of LOA and MainEngine\_kW with RNL are very difficult for a statistical analysis to pull apart because the underlying predictors are so strongly correlated. The univariate analysis, on the other hand, shows the expected result, which is that Containers and Vehicle Carriers with higher MainEngine\_kW tend to have higher RNL (see Annex 4).

The relationship of design predictors with RNL was generally weakest for the Tug category. This could be explained in part by the fact that tugs had more missing information in the LLI database than other categories. It could also be related to the fact that radiated tug noise depends on the operating mode of the vessel when transiting. For example, a tug performing escort duties (not towing or pushing) would have a different noise signature than a tug engaged in towing or part of an articulated-tug-barge unit. Information was not available in the ECHO database on whether tugs were involved in towing or pushing, which could significantly affect their radiated noise. Note, however, that tugs actively involved in escort duties would be excluded from the analysis, since ShipSound measurements are rejected when other AIS vessels are in close proximity to the hydrophone (as would be the case during tanker escort, for example).

Some categorical information related to engine design that was present in the LLI database (e.g., engine model and designer) did not easily fit into framework of functional regression analysis. Such information might be amenable to future analysis, if additional data related to the engine design (and noise and vibration) could be obtained, e.g., from the equipment vendors. Alternatively, categorical data on engine design might be investigated using descriptive statistics (similar to how EVDI was examined in Section 3.8) or by focusing on a smaller subset of the data. Such additional investigations were, however, outside the scope of the present study.

## 5. Summary and Conclusions

In terms of the key questions posed by this study, the main findings of the vessel noise correlations analysis are summarized as follows:

1. *Which key vessel design characteristics drive noise differences between different vessels independently and as a vessel class?*
  - Vessel size (represented via length overall) was ranked as the design parameter with the strongest correlation to underwater radiated noise. Other design characteristics related to vessel size (i.e., displacement, gross tonnage, and beam) were strongly correlated with length, making it difficult to separate their influence on underwater radiated noise.
  - Other parameters that were investigated (main engine RPM, main engine power, auxiliary engine power, and design speed) had weaker correlations with underwater radiated noise, which were furthermore not always consistent between vessel categories (see Table 9). This may have been due to lack of data related to other design characteristics that are known to influence transmission of machinery noise through the hull (e.g., insulating/damping of hull below the waterline, resilient mounting or rafting of engines, and airborne sound within machinery spaces).
  - Several important design characteristics (engine type, propeller type, engine stroke) lacked sufficient variation in their values to be able to assess their influence using statistical methods.
2. *Which key vessel design characteristics result in the lowest noise emissions?*
  - None of individual design characteristics investigated in this study were found to be associated with those vessels having the lowest noise emissions. Instead, vessel operating conditions (specifically, reduced speed through water and reduced draft) were most strongly associated with the lowest noise emissions.
  - Publicly available databases (e.g., Lloyds List) do not record many of the vessel design characteristics that are known to be more relevant for reducing underwater radiated noise (see Section 4.3). If such information could be made available (e.g., via ship classification societies), more detailed analyses of low-noise design characteristics could be conducted.
3. *Does a vessel's operational draft affect its underwater noise emissions?*
  - Operational draft was found to be a very influential parameter influencing vessel noise emissions, second only to speed through water. Operational draft had a strong positive correlation with radiated noise above 100 Hz, where deeper drafts were associated with higher noise emissions. The greatest influence of draft was above 1000 Hz, where cavitation dominates the noise spectrum. At low frequencies (below 100 Hz), operational draft had a weak negative correlation with radiated noise.

There were several other important findings of this study, which are summarized as follows:

- The two main operational parameters, speed through water and actual draft, were the predictors most strongly correlated with underwater radiated noise in all vessel categories. The influence of speed through water was found to be consistent with results obtained during the 2017 ECHO slowdown trial in Haro Strait.
- A principal component analysis showed that design characteristics of the Tanker and Bulker categories substantially overlapped, as did the Vehicle Carrier and Container categories (but to a lesser degree). Tugs were clearly outliers when their design characteristics were compared to those of the other categories.
- Block coefficient (which the ATC recommended investigating) had a weaker correlation with underwater noise than its constituent quantities (displacement, beam, length, draft). Similarly, the ratio of the actual speed through water (STW) to the design speed, and the ratio of the actual draft to the summer draft both had weaker correlations than STW and actual draft on their own.

- Greenhouse gas emissions exhibited a weak negative trend with underwater radiated noise for the Containers and Vehicle Carriers group in the 10–100 Hz and 100–1000 Hz bands. This means that for these vessel categories, vessels with a higher intensity of CO<sub>2</sub> emissions were slightly quieter. Greenhouse gas emissions exhibited a weak positive trend with underwater radiated noise for the Bulkers and Tankers category in the 100–1000 Hz and 1000–10000 Hz bands. This means that for these categories, vessels with higher CO<sub>2</sub> emissions intensity also had slightly higher underwater noise.
- Statistical analysis of noise correlations for the tug and cruise vessel categories proved challenging, due to limitations of the available data set. For tugs, there were many predictors with a large fraction of missing data in the Lloyd's List database. Furthermore, there was no information on whether vessels were involved in towing or pushing while under measurement (which is expected to affect propeller loading and thus influence noise emissions for tugs). For cruise vessels, the small number of unique vessels (and relatively small number of total measurements) meant that this category was data-deficient from a statistical perspective.
- Analysis of high-resolution spectrum data for a sample of 30 loud and 30 quiet vessel measurements indicated that the loud vessels exhibited a distinct cavitation noise hump near 50 Hz (e.g., as discussed by Wittekind and Schuster (2016)), whereas the quiet vessels exhibited a flatter spectrum below 100 Hz. The loud vessels generally exhibited a smaller number of discrete tones than the quiet vessels, which was attributed to masking of machinery tones by wide-band cavitation noise. No clear differences in design characteristics were evident between the loud and quiet vessels, other than that the loud vessels tended to be larger in size in some (but not all) categories.

## Glossary

**1/3-octave**

One third of an octave. Note: A one-third octave is approximately equal to one decidecade ( $1/3 \text{ oct} \approx 1.003 \text{ ddec}$ ; ISO 2017).

**1/3-octave-band**

Frequency band whose bandwidth is one one-third octave. Note: The bandwidth of a one-third octave-band increases with increasing centre frequency.

**Acoustic Current Doppler Profiler (ADCP)**

An active sonar system for measuring ocean currents, much like the weather Doppler systems used to map atmospheric winds and rain. It consists of multiple acoustic transducers projecting upwards into the water column. It can measure the currents at many depths, thus providing a profile of the ocean currents.

**ambient noise**

All-encompassing sound at a given place, usually a composite of sound from many sources near and far (ANSI S1.1-1994 R2004), e.g., shipping vessels, seismic activity, precipitation, sea ice movement, wave action, and biological activity.

**automated identification system (AIS)**

A radio-based tracking system whereby vessels regularly broadcast their identity, location, speed, heading, dimensions, class, and other information to nearby receivers.

**background noise**

Total of all sources of interference in a system used for the production, detection, measurement, or recording of a signal, independent of the presence of the signal (ANSI S1.1-1994 R2004). Ambient noise detected, measured, or recorded with a signal is part of the background noise.

**bandwidth**

The range of frequencies over which a sound occurs. Broadband refers to a source that produces sound over a broad range of frequencies (e.g., seismic airguns, vessels) whereas narrowband sources produce sounds over a narrow frequency range (e.g., sonar) (ANSI/ASA S1.13-2005 R2010).

**box-and-whisker plot**

A plot that illustrates the centre, spread, and overall range of data from a visual 5-number summary. The ends of the box are the upper and lower quartiles (25th and 75th percentiles). The horizontal line inside the box is the median (50th percentile). The whiskers and points extend outside the box to the highest and lowest observations, where the points correspond to outlier observations (i.e., observations that fall more than  $1.5 \times \text{IQR}$  beyond the upper and lower quartiles, where IQR is the interquartile range).

**broadband sound level**

The total sound pressure level measured over a specified frequency range. If the frequency range is unspecified, it refers to the entire measured frequency range.

**cavitation**

A rapid formation and collapse of vapor cavities (i.e., bubbles or voids) in water, most often caused by a rapid change in pressure. Fast-spinning vessel propellers typically cause cavitation, which creates a lot of noise.

**decade**

Logarithmic frequency interval whose upper bound is ten times larger than its lower bound (ISO 2006).

**decidecade**

One tenth of a decade (ISO 2017). Note: An alternative name for decidecade (symbol ddec) is “one-tenth decade”. A decidecade is approximately equal to one third of an octave ( $1 \text{ ddec} \approx 0.3322 \text{ oct}$ ) and for this reason is sometimes referred to as a “one-third octave”.

**decidecade band**

Frequency band whose bandwidth is one decidecade. Note: The bandwidth of a decidecade band increases with increasing centre frequency.

**decibel (dB)**

One-tenth of a bel. Unit of level when the base of the logarithm is the tenth root of ten, and the quantities concerned are proportional to power (ANSI S1.1-1994 R2004).

**EVDI**

Existing Vessel Design Index.

**far-field**

The zone where, to an observer, sound originating from an array of sources (or a spatially distributed source) appears to radiate from a single point. The distance to the acoustic far-field increases with frequency.

**frequency**

The rate of oscillation of a periodic function measured in cycles-per-unit-time. The reciprocal of the period. Unit: hertz (Hz). Symbol:  $f$ . 1 Hz is equal to 1 cycle per second.

**harmonic**

A sinusoidal sound component that has a frequency that is an integer multiple of the frequency of a sound to which it is related. For example, the second harmonic of a sound has a frequency that is double the fundamental frequency of the sound.

**hertz (Hz)**

A unit of frequency defined as one cycle per second.

**hydrophone**

An underwater sound pressure transducer. A passive electronic device for recording or listening to underwater sound.

**LLI**

Lloyd List International

**mean-square sound pressure spectral density**

Distribution as a function of frequency of the mean-square sound pressure per unit bandwidth (usually 1 Hz) of a sound having a continuous spectrum (ANSI S1.1-1994 R2004). Unit:  $\mu\text{Pa}^2/\text{Hz}$ .

**median**

The 50th percentile of a statistical distribution.

**monopole source level (MSL)**

A source level that has been calculated using an acoustic model that accounts for the effect of the sea-surface and seabed on sound propagation, assuming a point-like (monopole) sound source. See related term: radiated noise level.

**multiple linear regression**

A statistical method that seeks to explain the response of a dependent variable using multiple explanatory variables.

**octave**

The interval between a sound and another sound with double or half the frequency. For example, one octave above 200 Hz is 400 Hz, and one octave below 200 Hz is 100 Hz.

**parabolic equation method**

A computationally efficient solution to the acoustic wave equation that is used to model propagation loss. The parabolic equation approximation omits effects of back-scattered sound, simplifying the computation of propagation loss. The effect of back-scattered sound is negligible for most ocean-acoustic propagation problems.

**point source**

A source that radiates sound as if from a single point (ANSI S1.1-1994 R2004).

**power spectrum density**

Generic term, formally defined as power in W/Hz, but sometimes loosely used to refer to the spectral density of other parameters such as square pressure or time-integrated square pressure.

**PPA**

Pacific Pilotage Authority

**pressure, acoustic**

The deviation from the ambient hydrostatic pressure caused by a sound wave. Also called overpressure. Unit: pascal (Pa). Symbol:  $p$ .

**pressure, hydrostatic**

The pressure at any given depth in a static liquid that is the result of the weight of the liquid acting on a unit area at that depth, plus any pressure acting on the surface of the liquid. Unit: pascal (Pa).

**principal components analysis (PCA)**

PCA is a commonly used data reduction and interpretation technique. It takes high dimensional data (many variables) and projects them onto a smaller, more manageable space for analysis and visualization.

**propagation loss (PL)**

The decibel reduction in sound level between two stated points that results from sound spreading away from an acoustic source subject to the influence of the surrounding environment. Also referred to as transmission loss.

**radiated noise level (RNL)**

A source level that has been calculated assuming sound pressure decays geometrically with distance from the source, with no influence of the sea-surface and seabed. See related term: monopole source level.

**received level (RL)**

The sound level measured (or that would be measured) at a defined location.

**sound**

A time-varying pressure disturbance generated by mechanical vibration waves travelling through a fluid medium such as air or water.

**sound pressure level (SPL)**

The decibel ratio of the time-mean-square sound pressure, in a stated frequency band, to the square of the reference sound pressure (ANSI S1.1-1994 R2004).

For sound in water, the reference sound pressure is one micropascal ( $p_0 = 1 \mu\text{Pa}$ ) and the unit for SPL is dB re  $1 \mu\text{Pa}^2$ :

$$L_p = 10 \log_{10}(p^2/p_0^2) = 20 \log_{10}(p/p_0)$$

Unless otherwise stated, SPL refers to the decibel level of the root-mean-square (rms) sound pressure.

**source level (SL)**

The sound level measured in the far-field and scaled back to a standard reference distance of 1 metre from the acoustic centre of the source. Unit: dB re  $1 \mu\text{Pa} \cdot \text{m}$  (pressure level) or dB re  $1 \mu\text{Pa}^2 \cdot \text{s} \cdot \text{m}$  (exposure level).

**spectral density level**

The decibel level ( $10 \cdot \log_{10}$ ) of the spectral density of a given parameter such as SPL or SEL, for which the units are dB re  $1 \mu\text{Pa}^2/\text{Hz}$  and dB re  $1 \mu\text{Pa}^2 \cdot \text{s}/\text{Hz}$ , respectively.

**spectrum**

An acoustic signal represented in terms of its power, energy, mean-square sound pressure, or sound exposure distribution with frequency.

**speed over ground (SOG)**

The speed of a vessel relative to the surface of the earth.

**speed through water (STW)**

The speed of a vessel relative to the water.

**ULS**

Underwater Listening Station.

**VFPA**

Vancouver Fraser Port Authority.

## Literature Cited

- [ISO] International Organization for Standardization. 2006. *ISO 80000-3:2006 Quantities and units – Part 3: Space and time*. <https://www.iso.org/standard/31888.html>.
- [ISO] International Organization for Standardization. 2017. *ISO 18405:2017. Underwater acoustics – Terminology*. Geneva. <https://www.iso.org/standard/62406.html>.
- Ainsworth, L.M., R. Routledge, and J. Cao. 2011. Functional Data Analysis in Ecosystem Research: The Decline of Oweekeno Lake Sockeye Salmon and Wannock River Flow. *Journal of Agricultural, Biological, and Environmental Statistics* 16(2): 282-300. <https://doi.org/10.1007/s13253-010-0049-z>.
- ANSI S1.1-1994. R2004. *American National Standard Acoustical Terminology*. American National Standards Institute, NY, USA.
- ANSI/ASA S1.13-2005. R2010. *American National Standard Measurement of Sound Pressure Levels in Air*. American National Standards Institute and Acoustical Society of America, NY, USA.
- ANSI/ASA S12.64/Part 1. 2009. *American National Standard Quantities and Procedures for Description and Measurement of Underwater Sound from Ships Part 1: General Requirements*. American National Standards Institute and Acoustical Society of America, NY, USA.
- Bedford Institute of Oceanography. 2015. *WebTide Tidal Prediction Model (v0.7.1)* (webpage). Government of Canada. <http://www.bio-lob.gc.ca/science/research-recherche/ocean/webtide/index-en.php>.
- Environment Canada. 2020. *Marine Weather* (webpage). [https://weather.gc.ca/mainmenu/marine\\_menu\\_e.html](https://weather.gc.ca/mainmenu/marine_menu_e.html).
- Hannay, D.E., X. Mouy, and Z. Li. 2016. An automated real-time vessel sound measurement system for calculating monopole source levels using a modified version of ANSI/ASA S12.64-2009. *Canadian Acoustics* 44(3). <https://jcaa.caa-aca.ca/index.php/jcaa/article/view/3002>.
- Johnson, R.A. and D.W. Wichern. 2007. *Applied Multivariate Statistical Analysis*. 6th edition. Pearson Prentice Hall, Upper Saddle River.
- Lewis, E.V. 1988. *Principles of Naval Architecture*, Volume 1: Stability and Strength. The Society of Naval Architects and Marine Engineers, Jersey City.
- MacGillivray, A.O. and Z. Li. 2016. *Seaspan Ferries Vessel Noise Analysis*. Document Number 01300, Version 1.0. Technical report by JASCO Applied Sciences for Vancouver Fraser Port Authority.
- MacGillivray, A.O., H. Frouin-Mouy, and J.E. Quijano. 2017. *BC Ferries Vessel Noise Analysis: Vessel Noise Analysis for Customers of Port of Vancouver*. Document Number 01449, Version 4.0. Technical report by JASCO Applied Sciences for Vancouver Fraser Port Authority ECHO Program.
- MacGillivray, A.O., Z. Li, D.E. Hannay, K.B. Trounce, and O. Robinson. 2019. Slowing deep-sea commercial vessels reduces underwater radiated noise. *Journal of the Acoustical Society of America* 146: 340-351. <https://doi.org/10.1121/1.5116140>.
- Ramsay, J. and B. Silverman. 2005. *Functional Data Analysis*. 2nd edition. Springer Series in Statistics.

Ross, D. and F.F. Alvarez. 1964. Radiated underwater noise of surface ships. *US Navy Journal of Underwater Acoustics* 14(331 ).

Ross, D. 1976. *Mechanics of Underwater Noise*. Pergamon Press, NY, USA.

Wittekind, D. and M. Schuster. 2016. Propeller cavitation noise and background noise in the sea. *Ocean Engineering* 120: 116-121.

## Appendix A. Description of Variables in Merged Database

Table A-1. Description of all the variables captured in the merged vessel noise database.

Variable	Description	Data source	Variable type	Included in MVA	Units	Notes
measurementId	The PortListen ID value for the ECHO measurement. Unique for every measurement. Contains the deployment ID of the measuring station, the MMSI of the recorded vessel, and the datetime of the closest approach.	ECHO	Operational	Not Included		
stationId	The ID of the station where the measurement was recorded	ECHO	Method	Not Included		
deploymentId	The deployment ID of the hydrophone recorder.	ECHO	Method	Not Included		Unique for every hydrophone deployment
mmsi	Maritime Mobile Service Identity. A nine digit code used by AIS to identify vessels.	ECHO	Design	Not Included		
imo	International Maritime Organization number. A seven digit number assigned to the hull of a ship. Generally given to ocean faring ships, so some port tugs do not have IMOs.	ECHO	Design	Not Included		
timestampCpa	Date and time of the closest point of approach of the vessel to the hydrophone, according to AIS.	ECHO	Operational	Not Included	Time (UTC)	
timestampAcousticCpa	Date and time of the closest point of approach of the vessel to the hydrophone as determined by an acoustic detector in PortListen.	ECHO	Operational	Not Included	Time (UTC)	
vesselName	Name of the vessel.	ECHO	Design	Not Included		
vesselType	Numerical AIS code for vessel type. The codes are specific to the vessel class and the cargo it carries.	ECHO	Design	Not Included	Double digit code	
jascoVesselClass	Class of the vessel, as determined from AIS and MarineTraffic.com, based on JASCO's naming scheme.	ECHO	Design	Not Included		Captured by category
shipLength	Length of the vessel from AIS.	ECHO	Design	Not Included	m	Superseded by Lloyd's
shipBreath	Breadth of the vessel from AIS (note typo in column name).	ECHO	Design	Not Included	m	Superseded by Lloyd's
staticDraught	Static draft of the vessel from AIS. This the draft of the vessel while not underway.	ECHO	Design	Not Included	m	Instead use actualVesselDraft

Variable	Description	Data source	Variable type	Included in MVA	Units	Notes
actualVesselDraft	Actual vessel draft from PPA, AIS, and summer draft, in that order.	ECHO	Operational	Independent	m	
distanceAtCpa	The horizontal distance between the vessel and the hydrophone at closest point of approach.	ECHO	Method	Not Included	m	Captured by surface.angle
sogMean	Mean speed over ground in the measurement window from AIS. This is the speed of vessel relative to the surface of the earth.	ECHO	Operational	Not Included	knots	Captured by sow
cogMean	Mean course over ground in the measurement window from AIS. Heading of vessel relative to earth's surface.	ECHO	Operational	Not Included	degrees	Captured by sow, wind.resistance
rotMean	Mean rate of turn of the vessel through the water in the measurement window from AIS.	ECHO	Operational	Not Included	degrees/min	Limited by measurement QC
trueHeadingMean	Mean heading in measurement window, counterclockwise from True North from AIS.	ECHO	Operational	Not Included	degrees	Captured by sow
sow	Speed through water. Calculated from speed over ground, course over ground, current speed, and current direction.	ECHO	Operational	Independent	knots	
qcStatus	Quality Check Status. Every measurement has been subjected to a manual review. Invalid measurements may be rejected for a variety of reasons.	ECHO	Method	Not Included		Only accepted measurements to be included in MVA
windSpeed	Wind speed at the time of measurement from the nearest met station.	ECHO	Operational	Not Included	knots	Captured by wind.resistance
windDirection	Direction of wind at the time of measurement from the nearest met station.	ECHO	Operational	Not Included	degrees	Captured by wind.resistance
currentSpeed	Speed of water current at time of measurement (measured or predicted, depending on location).	ECHO	Operational	Not Included	knots	Captured by sow
currentDirection	Direction of the water current (measured or predicted, depending on location).	ECHO	Operational	Not Included	degrees	Captured by sow
shaftRate	Rotational rate of the vessel's propellers. Estimated based on DEMON algorithm.	ECHO	Operational	Not Included	rpm	Insufficient data
monopoleSourceDepth	Depth of the representative monopole source for the vessel. Taken to be half the active draft of the vessel reported over AIS.	ECHO	Operational	Not Included	m	Captured by draft

Variable	Description	Data source	Variable type	Included in MVA	Units	Notes
vesselDwt	Dead weight tonnage from AIS. A measure of the weight of cargo a ship can carry (not its own weight)	ECHO	Design	Not Included	tons	Superseded by Lloyd's
vesselYearBuilt	Year the vessel was built from AIS.	ECHO	Design	Not Included	years	Superseded by Lloyd's
category	ECHO vessel category.	ECHO	Design	Independent		To be verified against Lloyd's list type (TYPE.LLI)
kDWT	Kilo dead weight tonnage from AIS (DWT/1000).	ECHO	Design	Not Included	kilotons	Superseded by Lloyd's
stw.mps	Speed through water (MKS).	ECHO	Operational	Not Included	m/s	Captured by sow
sogMean.mps	Mean speed over ground (MKS).	ECHO	Operational	Not Included	m/s	Captured by sow
windSpeed.mps	Wind speed (MKS).	ECHO	Operational	Not Included	m/s	Captured by wind.resistance
surface.angle	The depression angle from vessel to the hydrophone (calculated). Measured with respect to the sea surface.	ECHO	Method	Independent	degrees	
hydrophone.depth	Depth of the hydrophone below mean sea level.	ECHO	Method	Not Included	m	Captured by surface.angle
wind.resistance	Resistance on the vessel due to the wind. Calculated from windspeed, wind direction, speed over ground and course over ground.	ECHO	Operational	Independent	m <sup>2</sup> /s <sup>2</sup>	
Job.ID.PPA	Pilot job ID from the PPA lots. Unique for each trip.	PPA	Operational	Not Included		
Vessel.PPA	Vessel name according to PPA.	PPA	Design	Not Included		
DWT.PPA	Deadweight tonnage according to PPA.	PPA	Design	Not Included	tons	Superseded by Lloyd's
GRT.PPA	Gross tonnage according to PPA.	PPA	Design	Not Included	tons	Superseded by Lloyd's
LOA.PPA	Overall Length of a vessel according to PPA.	PPA	Design	Not Included	m	Superseded by Lloyd's
Beam.PPA	Width at the widest point of a vessel, according to PPA.	PPA	Design	Not Included	m	Superseded by Lloyd's
S.Draft.PPA	Maximum Draft/draught of the vessel according to PPA.	PPA	Operational	Not Included	m	Superseded by Lloyd's
Actual.Draft.PPA	The actual draft of the vessel logged by the pilot. Measured by the pilot visually or with software.	PPA	Operational	Not Included	m	Not always equal to AIS draft (actualVesselDraft)

Variable	Description	Data source	Variable type	Included in MVA	Units	Notes
Type.PPA	Class of the vessel, based on PPA's naming scheme.	PPA	Design	Not Included		To be verified against ECHO type (category)
PILOT_RPM_1.PPA	RPM of the vessel propeller as measured by the pilot. Not measured for a majority of the PPA data set.	PPA	Operational	Not Included	rpm	Not enough data
PILOT_RPM_2.PPA	RPM of the vessel propeller as measured by the pilot. Not measured for a majority of the PPA data set.	PPA	Operational	Not Included	rpm	Not enough data
PILOT_ECHO.PPA	Value stating whether or not the vessel took part in the ECHO slowdown trial.	PPA	Operational	Not Included		Not enough data
First.Pilot.StartBW.PPA	The time when the pilot on the vessel began their bridge watch.	PPA	Operational	Not Included	time (UTC)	
First.Pilot.StopBW.PPA	The time when the pilot on the vessel completed their bridge watch.	PPA	Operational	Not Included	time (UTC)	
VesselName.EVDI	Vessel name from ECHO	EVDI	Design	Not Included		
VesselClass.EVDI	Vessel class from ECHO	EVDI	Design	Not Included		
GHG.Rating	GHG Emissions Rating. A letter grade scale comparing the CO2 efficiency of vessels with a similar size and type. The scale indicates the number of standard deviations from the mean score for the vessel class. D is the centre.	EVDI	Design	Independent		
EVDI	Existing Vessel Design Index. A measure of a ships CO <sub>2</sub> emissions.	EVDI	Design	Not Included	grams CO <sub>2</sub> per tonne nautical mile	Captured by GHG.Rating
vessel.ID.lloyds	Matching ID number in the Lloyd's List database.	LLOYDS	Design	Not Included		
IMO.LLI	IMO according to Lloyds List's database.	LLOYDS	Design	Not Included		
MMSI.LLI	MMSI according to Lloyds List's database.	LLOYDS	Design	Not Included		
TYPE.LLI	A Lloyds List code signifying the vessel type.	LLOYDS	Design	Independent		Subtype of Category
VESSEL.TYPE.LLI	The vessel type, according to Lloyds.	LLOYDS	Design	Not Included		Unabbreviated TYPE.LLI
GROSS.LLI	Gross tonnage, according to Lloyds.	LLOYDS	Design	Independent	tonnes	
DRAFT.LLI	Maximum Draft of the vessel according to Lloyds. Measured at Summer load lines.	LLOYDS	Design	Independent	m	

Variable	Description	Data source	Variable type	Included in MVA	Units	Notes
LOA.LLI	Overall length of the vessel, according to Lloyds.	LLOYDS	Design	Independent	m	
YEAR.OF.BUILD.LLI	Year the vessel was built, from Lloyds.	LLOYDS	Design	Independent	years	
HULL.TYPE.LLI	A code signifying the type of Hull for the vessel. The code is only indicated when the hull differs from a standard mono hull.	LLOYDS	Design	Not Included		Insufficient data (blank entries not significant)
HULL.TYPE.DECODE.LLI	Text explaining the HULL.TYPE column code. DS = Double Side, DH = Double Hull, DB = Double Bottom. DS, DB and DH are typically for tankers.	LLOYDS	Design	Not Included		Insufficient data
HULL.MATERIAL.LLI	Material the vessel's hull is made from.	LLOYDS	Design	Not Included		Insufficient data (all steel)
PROPULSION.TYPE.LLI	Type of propulsion used to move the vessel.	LLOYDS	Design	Not Included		Insufficient data (all motor, except for two LNG)
FO.Capacity.LLI	Fuel Oil Capacity. A measure of the cubic metre capacity of the fuel tanks in the vessel.	LLOYDS	Design	Independent	m <sup>3</sup>	To be determined if 35% non-missing data is sufficient to impute remainder
SPEED.LLI	Maximum speed of the vessel, according to Lloyds. The speed the ship is designed to maintain, at the summer load waterline at maximum propeller RPM.	LLOYDS	Design	Independent	knots	May be combined with sww to calculate speed as % MCR
SPEED.TYPE.LLI	Acronyms denoting the type of speed measured in SPEED.LLI. AS = Average Speed, DS = Design Speed, SS = Service Speed and TS = Trial Speed.	LLOYDS	Design	Not Included		Insufficient data
DISPLACEMENT.LLI	Maximum displacement of the vessel, according to Lloyds. Measured at summer load line.	LLOYDS	Design	Independent	tonnes	
BREADTH.MOULDED.LLI	Maximum breadth of the vessel, measured at the moulded line of the frame.	LLOYDS	Design	Independent	m	
MainEngine_Type.LLI	Engine type. DSE = Diesel Electric, DSL = Diesel, GST = Gas Turbine	LLOYDS	Design	Independent		May only be possible to include for Cruise vessels
Main.Engine_Designer.LLI	Designer of the engine installed in the vessel.	LLOYDS	Design	Not Included		May be included as independent factor

Variable	Description	Data source	Variable type	Included in MVA	Units	Notes
MainEngine_Designation.LLI	Designation code of the engine	LLOYDS	Design	Not Included		May be related to EVDI
MainEngines_No.LLI	Number of main engines in the vessel.	LLOYDS	Design	Independent		
MainEngine_kW.LLI	Maximum rated power output of the main engines.	LLOYDS	Design	Independent	kilowatts	
MainEngine_RPM.LLI	Maximum rated RPM of the main engine.	LLOYDS	Design	Independent		
MainEngine_Cylinders.LLI	Number of cylinders in the main engine.	LLOYDS	Design	Independent		
MainEngine_StrokeType.LLI	Number of strokes the engine performs.	LLOYDS	Design	Independent		
PropellerType.LLI	The type of propeller. Az = Azimuth Drive, CP = Controllable Pitch, DP = Directional Pitch, FP = Fixed Pitch, RP = Rudder Pitch, Z = Z type	LLOYDS	Design	Independent		
No_of_propulsion_units.LLI	Number of propulsive engines. Corresponds to number of propellers.	LLOYDS	Design	Independent		
AuxiliaryEngine_kW.LLI	Maximum rated power output of the auxiliary engines.	LLOYDS	Design	Independent	kilowatts	
TotalEngine_kW.LLI	Power output of the combined main and auxiliary engines.	LLOYDS	Design	Not Included	kilowatts	Equal to sum of Main and Aux engine kW
broadbandMsl	Broadband monopole source level (MSL) of the vessel measurement (20–63000 Hz).	ECHO	Operational	Dependent	dB re 1 $\mu$ Pa m	
broadbandRnl	Broadband radiated noise level (RNL) of the vessel measurement (20–63000 Hz).	ECHO	Operational	Dependent	dB re 1 $\mu$ Pa m	
RNL_10Hz	Radiated noise level for the 1/3-octave-band centred at 10 Hz.	ECHO	Operational	Dependent	dB re 1 $\mu$ Pa m	
RNL_13Hz	Radiated noise level for the 1/3-octave-band centred at 13 Hz.	ECHO	Operational	Dependent	dB re 1 $\mu$ Pa m	
RNL_16Hz	Radiated noise level for the 1/3-octave-band centred at 16 Hz.	ECHO	Operational	Dependent	dB re 1 $\mu$ Pa m	
RNL_20Hz	Radiated noise level for the 1/3-octave-band centred at 20 Hz.	ECHO	Operational	Dependent	dB re 1 $\mu$ Pa m	
RNL_25Hz	Radiated noise level for the 1/3-octave-band centred at 25 Hz.	ECHO	Operational	Dependent	dB re 1 $\mu$ Pa m	
RNL_31Hz	Radiated noise level for the 1/3-octave-band centred at 31 Hz.	ECHO	Operational	Dependent	dB re 1 $\mu$ Pa m	
RNL_40Hz	Radiated noise level for the 1/3-octave-band centred at 40 Hz.	ECHO	Operational	Dependent	dB re 1 $\mu$ Pa m	
RNL_50Hz	Radiated noise level for the 1/3-octave-band centred at 50 Hz.	ECHO	Operational	Dependent	dB re 1 $\mu$ Pa m	
RNL_63Hz	Radiated noise level for the 1/3-octave-band centred at 63 Hz.	ECHO	Operational	Dependent	dB re 1 $\mu$ Pa m	

Variable	Description	Data source	Variable type	Included in MVA	Units	Notes
RNL_80Hz	Radiated noise level for the 1/3-octave-band centred at 80 Hz.	ECHO	Operational	Dependent	dB re 1 µPa m	
RNL_100Hz	Radiated noise level for the 1/3-octave-band centred at 100 Hz.	ECHO	Operational	Dependent	dB re 1 µPa m	
RNL_125Hz	Radiated noise level for the 1/3-octave-band centred at 125 Hz.	ECHO	Operational	Dependent	dB re 1 µPa m	
RNL_160Hz	Radiated noise level for the 1/3-octave-band centred at 160 Hz.	ECHO	Operational	Dependent	dB re 1 µPa m	
RNL_200Hz	Radiated noise level for the 1/3-octave-band centred at 200 Hz.	ECHO	Operational	Dependent	dB re 1 µPa m	
RNL_250Hz	Radiated noise level for the 1/3-octave-band centred at 250 Hz.	ECHO	Operational	Dependent	dB re 1 µPa m	
RNL_315Hz	Radiated noise level for the 1/3-octave-band centred at 315 Hz.	ECHO	Operational	Dependent	dB re 1 µPa m	
RNL_400Hz	Radiated noise level for the 1/3-octave-band centred at 400 Hz.	ECHO	Operational	Dependent	dB re 1 µPa m	
RNL_500Hz	Radiated noise level for the 1/3-octave-band centred at 500 Hz.	ECHO	Operational	Dependent	dB re 1 µPa m	
RNL_630Hz	Radiated noise level for the 1/3-octave-band centred at 630 Hz.	ECHO	Operational	Dependent	dB re 1 µPa m	
RNL_800Hz	Radiated noise level for the 1/3-octave-band centred at 800 Hz.	ECHO	Operational	Dependent	dB re 1 µPa m	
RNL_1000Hz	Radiated noise level for the 1/3-octave-band centred at 1000 Hz.	ECHO	Operational	Dependent	dB re 1 µPa m	
RNL_1250Hz	Radiated noise level for the 1/3-octave-band centred at 1250 Hz.	ECHO	Operational	Dependent	dB re 1 µPa m	
RNL_1600Hz	Radiated noise level for the 1/3-octave-band centred at 1600 Hz.	ECHO	Operational	Dependent	dB re 1 µPa m	
RNL_2000Hz	Radiated noise level for the 1/3-octave-band centred at 2000 Hz.	ECHO	Operational	Dependent	dB re 1 µPa m	

Variable	Description	Data source	Variable type	Included in MVA	Units	Notes
RNL_2500Hz	Radiated noise level for the 1/3-octave-band centred at 2500 Hz.	ECHO	Operational	Dependent	dB re 1 $\mu$ Pa m	
RNL_3150Hz	Radiated noise level for the 1/3-octave-band centred at 3150 Hz.	ECHO	Operational	Dependent	dB re 1 $\mu$ Pa m	
RNL_4000Hz	Radiated noise level for the 1/3-octave-band centred at 4000 Hz.	ECHO	Operational	Dependent	dB re 1 $\mu$ Pa m	
RNL_5000Hz	Radiated noise level for the 1/3-octave-band centred at 5000 Hz.	ECHO	Operational	Dependent	dB re 1 $\mu$ Pa m	
RNL_6300Hz	Radiated noise level for the 1/3-octave-band centred at 6300 Hz.	ECHO	Operational	Dependent	dB re 1 $\mu$ Pa m	
RNL_8000Hz	Radiated noise level for the 1/3-octave-band centred at 8000 Hz.	ECHO	Operational	Dependent	dB re 1 $\mu$ Pa m	
RNL_10000Hz	Radiated noise level for the 1/3-octave-band centred at 10 kHz.	ECHO	Operational	Dependent	dB re 1 $\mu$ Pa m	
RNL_12500Hz	Radiated noise level for the 1/3-octave-band centred at 1.25 kHz.	ECHO	Operational	Dependent	dB re 1 $\mu$ Pa m	
RNL_16000Hz	Radiated noise level for the 1/3-octave-band centred at 16 kHz.	ECHO	Operational	Dependent	dB re 1 $\mu$ Pa m	
RNL_20000Hz	Radiated noise level for the 1/3-octave-band centred at 20 kHz.	ECHO	Operational	Dependent	dB re 1 $\mu$ Pa m	
RNL_25000Hz	Radiated noise level for the 1/3-octave-band centred at 25 kHz.	ECHO	Operational	Dependent	dB re 1 $\mu$ Pa m	
RNL_31500Hz	Radiated noise level for the 1/3-octave-band centred at 31 kHz.	ECHO	Operational	Dependent	dB re 1 $\mu$ Pa m	
RNL_40000Hz	Radiated noise level for the 1/3-octave-band centred at 40 kHz.	ECHO	Operational	Dependent	dB re 1 $\mu$ Pa m	
RNL_50000Hz	Radiated noise level for the 1/3-octave-band centred at 50 kHz.	ECHO	Operational	Dependent	dB re 1 $\mu$ Pa m	
RNL_63000Hz	Radiated noise level for the 1/3-octave-band centred at 63 kHz.	ECHO	Operational	Dependent	dB re 1 $\mu$ Pa m	

Variable	Description	Data source	Variable type	Included in MVA	Units	Notes
MSL_10Hz	Monopole source level for the 1/3-octave-band centred at 10 Hz.	ECHO	Operational	Dependent	dB re 1 µPa m	
MSL_13Hz	Monopole source level for the 1/3-octave-band centred at 13 Hz.	ECHO	Operational	Dependent	dB re 1 µPa m	
MSL_16Hz	Monopole source level for the 1/3-octave-band centred at 16 Hz.	ECHO	Operational	Dependent	dB re 1 µPa m	
MSL_20Hz	Monopole source level for the 1/3-octave-band centred at 20 Hz.	ECHO	Operational	Dependent	dB re 1 µPa m	
MSL_25Hz	Monopole source level for the 1/3-octave-band centred at 25 Hz.	ECHO	Operational	Dependent	dB re 1 µPa m	
MSL_31Hz	Monopole source level for the 1/3-octave-band centred at 31 Hz.	ECHO	Operational	Dependent	dB re 1 µPa m	
MSL_40Hz	Monopole source level for the 1/3-octave-band centred at 40 Hz.	ECHO	Operational	Dependent	dB re 1 µPa m	
MSL_50Hz	Monopole source level for the 1/3-octave-band centred at 50 Hz.	ECHO	Operational	Dependent	dB re 1 µPa m	
MSL_63Hz	Monopole source level for the 1/3-octave-band centred at 63 Hz.	ECHO	Operational	Dependent	dB re 1 µPa m	
MSL_80Hz	Monopole source level for the 1/3-octave-band centred at 80 Hz.	ECHO	Operational	Dependent	dB re 1 µPa m	
MSL_100Hz	Monopole source level for the 1/3-octave-band centred at 100 Hz.	ECHO	Operational	Dependent	dB re 1 µPa m	
MSL_125Hz	Monopole source level for the 1/3-octave-band centred at 125 Hz.	ECHO	Operational	Dependent	dB re 1 µPa m	
MSL_160Hz	Monopole source level for the 1/3-octave-band centred at 160 Hz.	ECHO	Operational	Dependent	dB re 1 µPa m	
MSL_200Hz	Monopole source level for the 1/3-octave-band centred at 200 Hz.	ECHO	Operational	Dependent	dB re 1 µPa m	
MSL_250Hz	Monopole source level for the 1/3-octave-band centred at 250 Hz.	ECHO	Operational	Dependent	dB re 1 µPa m	

Variable	Description	Data source	Variable type	Included in MVA	Units	Notes
MSL_315Hz	Monopole source level for the 1/3-octave-band centred at 315 Hz.	ECHO	Operational	Dependent	dB re 1 $\mu$ Pa m	
MSL_400Hz	Monopole source level for the 1/3-octave-band centred at 400 Hz.	ECHO	Operational	Dependent	dB re 1 $\mu$ Pa m	
MSL_500Hz	Monopole source level for the 1/3-octave-band centred at 500 Hz.	ECHO	Operational	Dependent	dB re 1 $\mu$ Pa m	
MSL_630Hz	Monopole source level for the 1/3-octave-band centred at 630 Hz.	ECHO	Operational	Dependent	dB re 1 $\mu$ Pa m	
MSL_800Hz	Monopole source level for the 1/3-octave-band centred at 800 Hz.	ECHO	Operational	Dependent	dB re 1 $\mu$ Pa m	
MSL_1000Hz	Monopole source level for the 1/3-octave-band centred at 1000 Hz.	ECHO	Operational	Dependent	dB re 1 $\mu$ Pa m	
MSL_1250Hz	Monopole source level for the 1/3-octave-band centred at 1250 Hz.	ECHO	Operational	Dependent	dB re 1 $\mu$ Pa m	
MSL_1600Hz	Monopole source level for the 1/3-octave-band centred at 1600 Hz.	ECHO	Operational	Dependent	dB re 1 $\mu$ Pa m	
MSL_2000Hz	Monopole source level for the 1/3-octave-band centred at 2000 Hz.	ECHO	Operational	Dependent	dB re 1 $\mu$ Pa m	
MSL_2500Hz	Monopole source level for the 1/3-octave-band centred at 2500 Hz.	ECHO	Operational	Dependent	dB re 1 $\mu$ Pa m	
MSL_3150Hz	Monopole source level for the 1/3-octave-band centred at 3150 Hz.	ECHO	Operational	Dependent	dB re 1 $\mu$ Pa m	
MSL_4000Hz	Monopole source level for the 1/3-octave-band centred at 4000 Hz.	ECHO	Operational	Dependent	dB re 1 $\mu$ Pa m	
MSL_5000Hz	Monopole source level for the 1/3-octave-band centred at 5000 Hz.	ECHO	Operational	Dependent	dB re 1 $\mu$ Pa m	
MSL_6300Hz	Monopole source level for the 1/3-octave-band centred at 6300 Hz.	ECHO	Operational	Dependent	dB re 1 $\mu$ Pa m	
MSL_8000Hz	Monopole source level for the 1/3-octave-band centred at 8000 Hz.	ECHO	Operational	Dependent	dB re 1 $\mu$ Pa m	

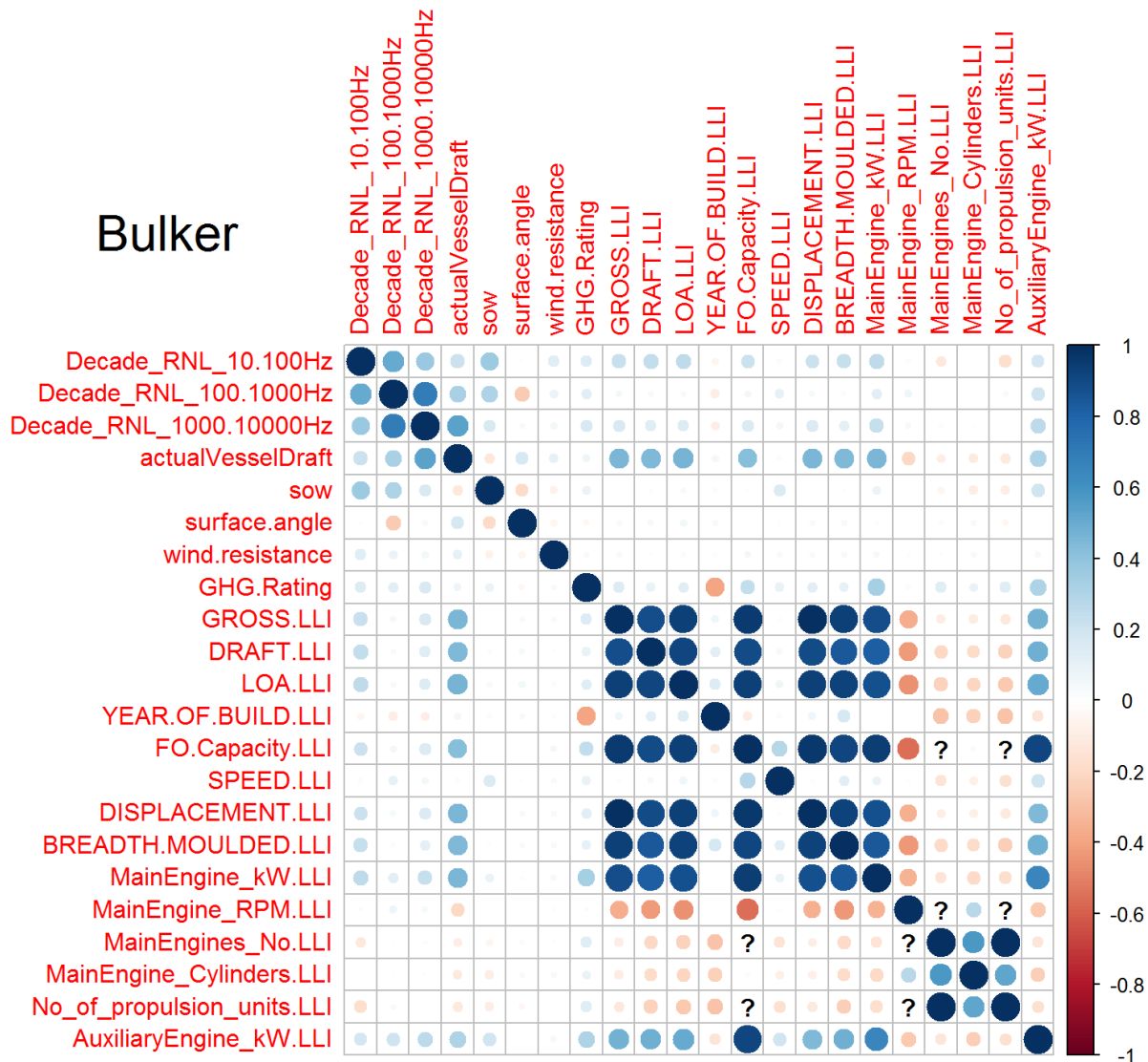
Variable	Description	Data source	Variable type	Included in MVA	Units	Notes
MSL_10000Hz	Monopole source level for the 1/3-octave-band centred at 10 kHz.	ECHO	Operational	Dependent	dB re 1 $\mu$ Pa m	
MSL_12500Hz	Monopole source level for the 1/3-octave-band centred at 1.25 kHz.	ECHO	Operational	Dependent	dB re 1 $\mu$ Pa m	
MSL_16000Hz	Monopole source level for the 1/3-octave-band centred at 16 kHz.	ECHO	Operational	Dependent	dB re 1 $\mu$ Pa m	
MSL_20000Hz	Monopole source level for the 1/3-octave-band centred at 20 kHz.	ECHO	Operational	Dependent	dB re 1 $\mu$ Pa m	
MSL_25000Hz	Monopole source level for the 1/3-octave-band centred at 25 kHz.	ECHO	Operational	Dependent	dB re 1 $\mu$ Pa m	
MSL_31500Hz	Monopole source level for the 1/3-octave-band centred at 31 kHz.	ECHO	Operational	Dependent	dB re 1 $\mu$ Pa m	
MSL_40000Hz	Monopole source level for the 1/3-octave-band centred at 40 kHz.	ECHO	Operational	Dependent	dB re 1 $\mu$ Pa m	
MSL_50000Hz	Monopole source level for the 1/3-octave-band centred at 50 kHz.	ECHO	Operational	Dependent	dB re 1 $\mu$ Pa m	
MSL_63000Hz	Monopole source level for the 1/3-octave-band centred at 63 kHz.	ECHO	Operational	Dependent	dB re 1 $\mu$ Pa m	
Decade_MSL_10.100Hz	Monopole source level for the decade band between 10 and 100 Hz.	ECHO	Operational	Not Included	dB re 1 $\mu$ Pa m	Calculated from 1/3-octave-band levels.
Decade_MSL_100.1000Hz	Monopole source level for the decade band between 100 and 1000 Hz	ECHO	Operational	Not Included	dB re 1 $\mu$ Pa m	Calculated from 1/3-octave-band levels.
Decade_MSL_1000.10000Hz	Monopole source level for the decade band between 1000 and 10000 Hz.	ECHO	Operational	Not Included	dB re 1 $\mu$ Pa m	Calculated from 1/3-octave-band levels.
Decade_RNL_10.100Hz	Radiated noise level for the decade band between 10 and 100 Hz.	ECHO	Operational	Not Included	dB re 1 $\mu$ Pa m	Calculated from 1/3-octave-band levels.

Variable	Description	Data source	Variable type	Included in MVA	Units	Notes
Decade_RNL_100.1000Hz	Radiated noise level for the decade band between 100 and 1000 Hz.	ECHO	Operational	Not Included	dB re 1 $\mu$ Pa m	Calculated from 1/3-octave-band levels.
Decade_RNL_1000.10000Hz	Radiated noise level for the decade band between 1000 and 10000 Hz.	Echo	Operational	Not Included	dB re 1 $\mu$ Pa m	Calculated from 1/3-octave-band levels.

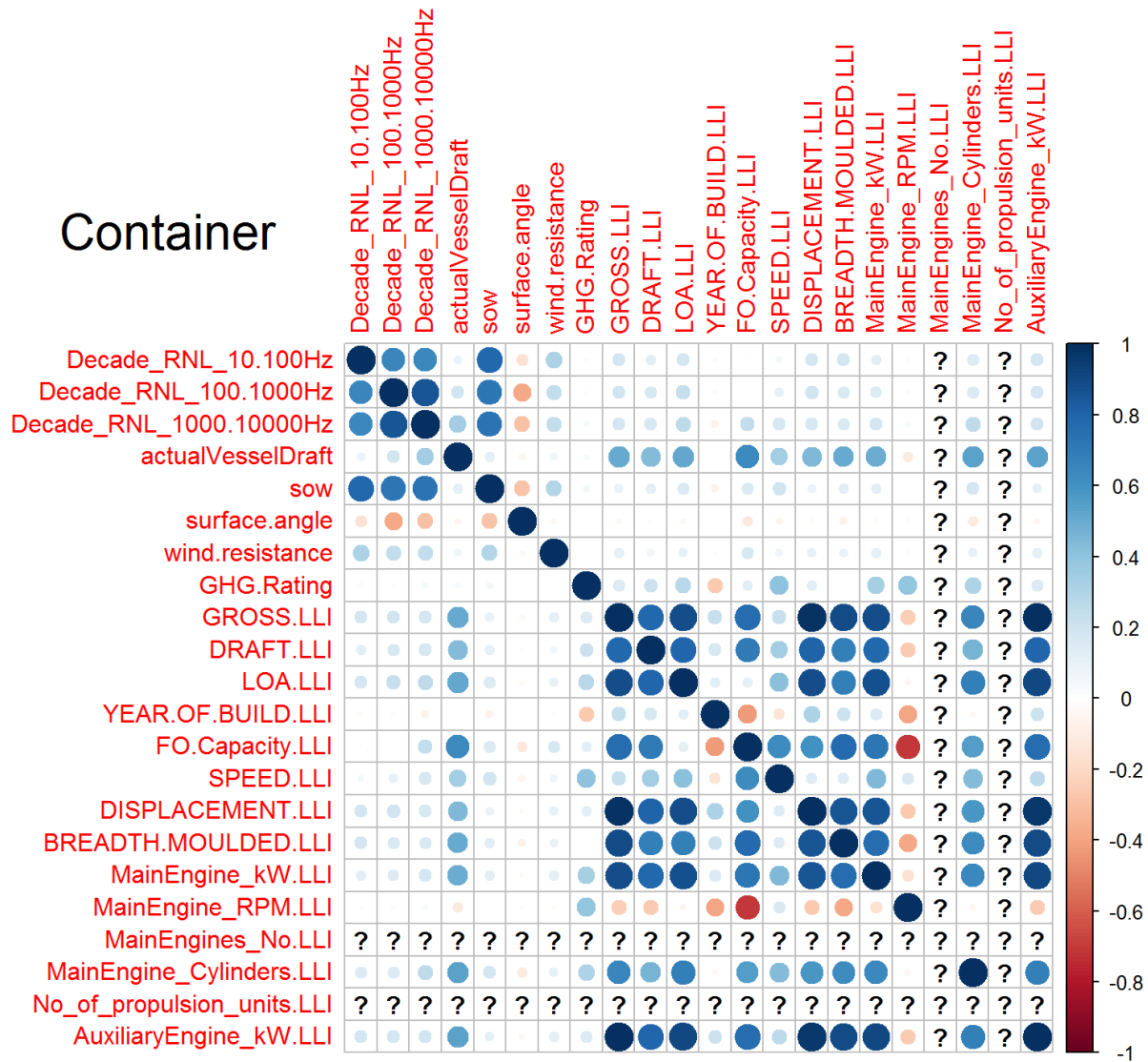
## Appendix B. Correlation Matrices

Correlation matrix plots in this appendix show correlations between pairs of variables in different vessel categories. The colored circles indicate the strength and magnitude of the correlation (blue = positive, red = negative, correlations along the diagonal are  $r=1$ ). The “?” indicates where the correlation cannot be computed between two variables (usually due to missing values, but sometimes due to a variable having a constant value). The first three rows and columns of the correlation matrix can be used to visually identify correlations between RNL and the predictor variables. Subsequent rows and columns can be used to visually identify correlations between pairs of predictors.

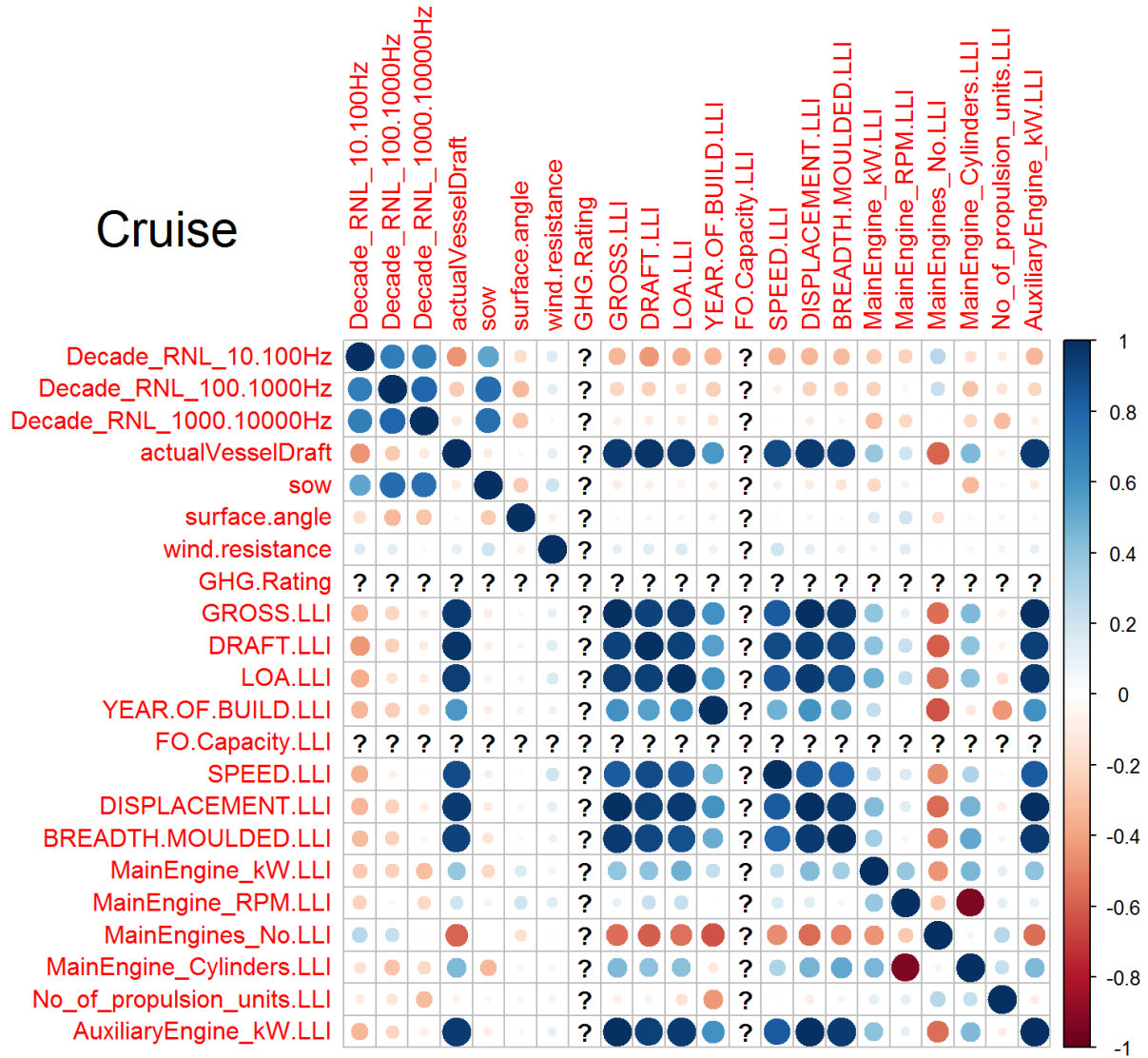
### B.1. Bulkers



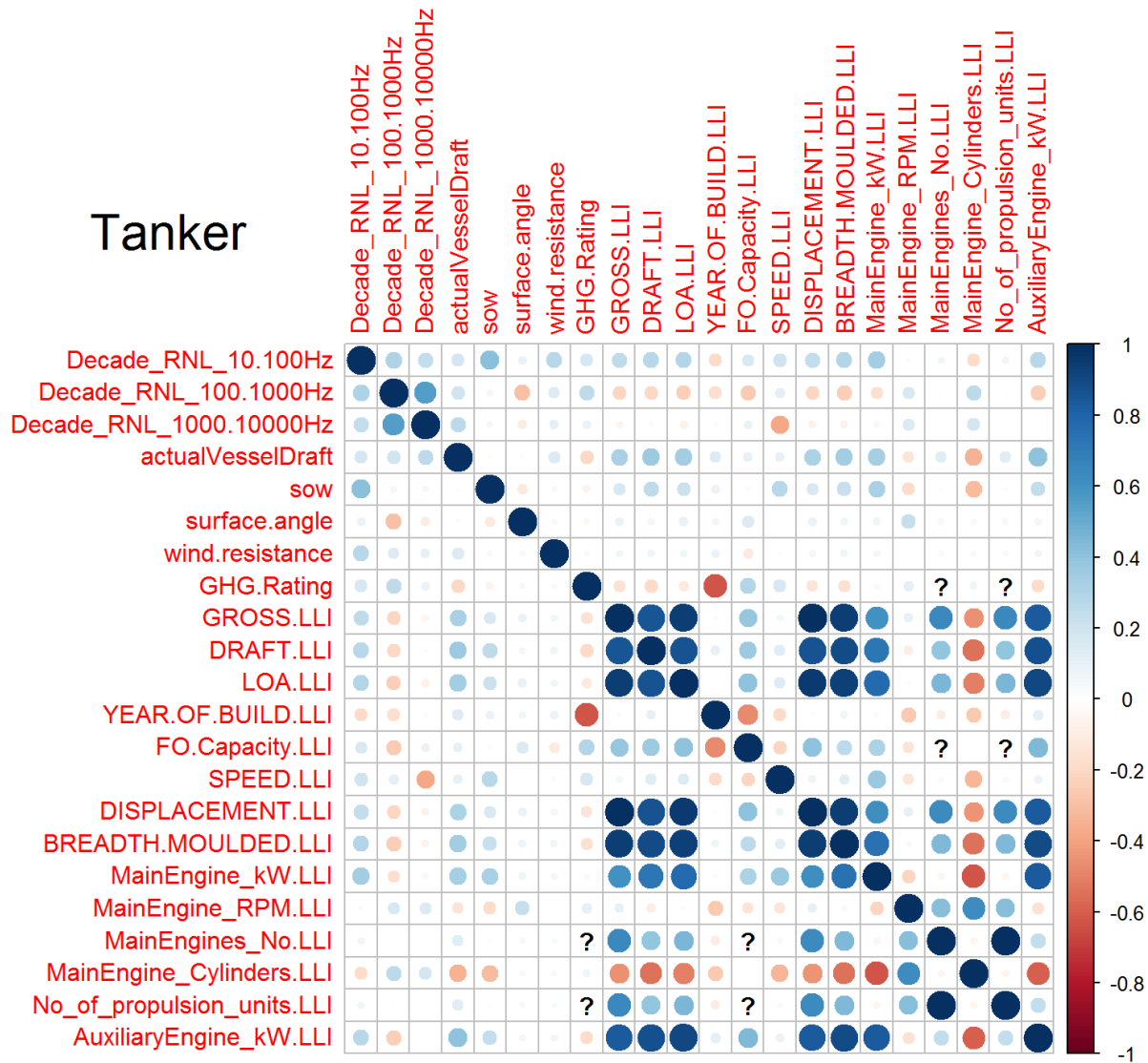
## B.2. Containers



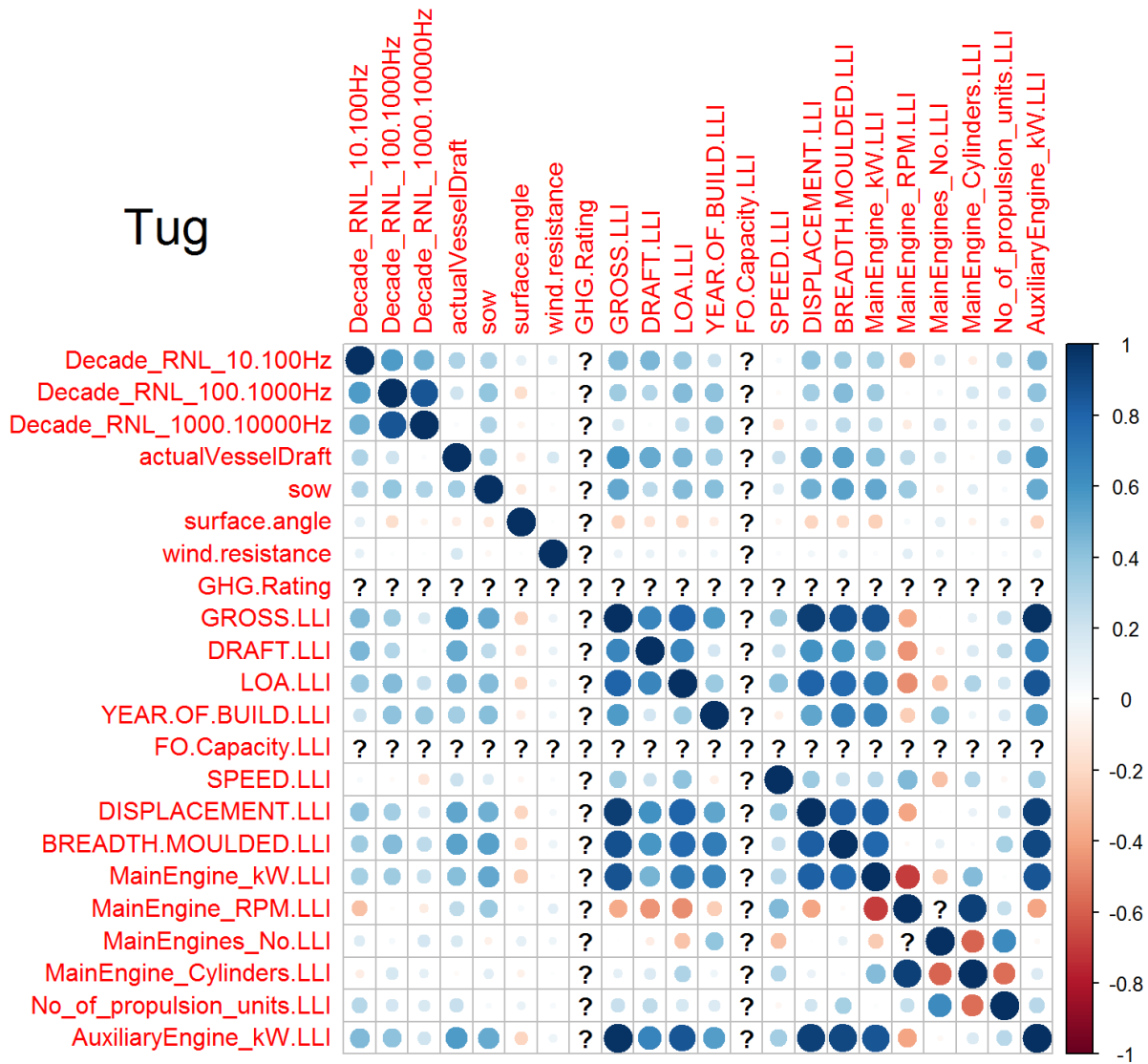
### B.3. Cruise



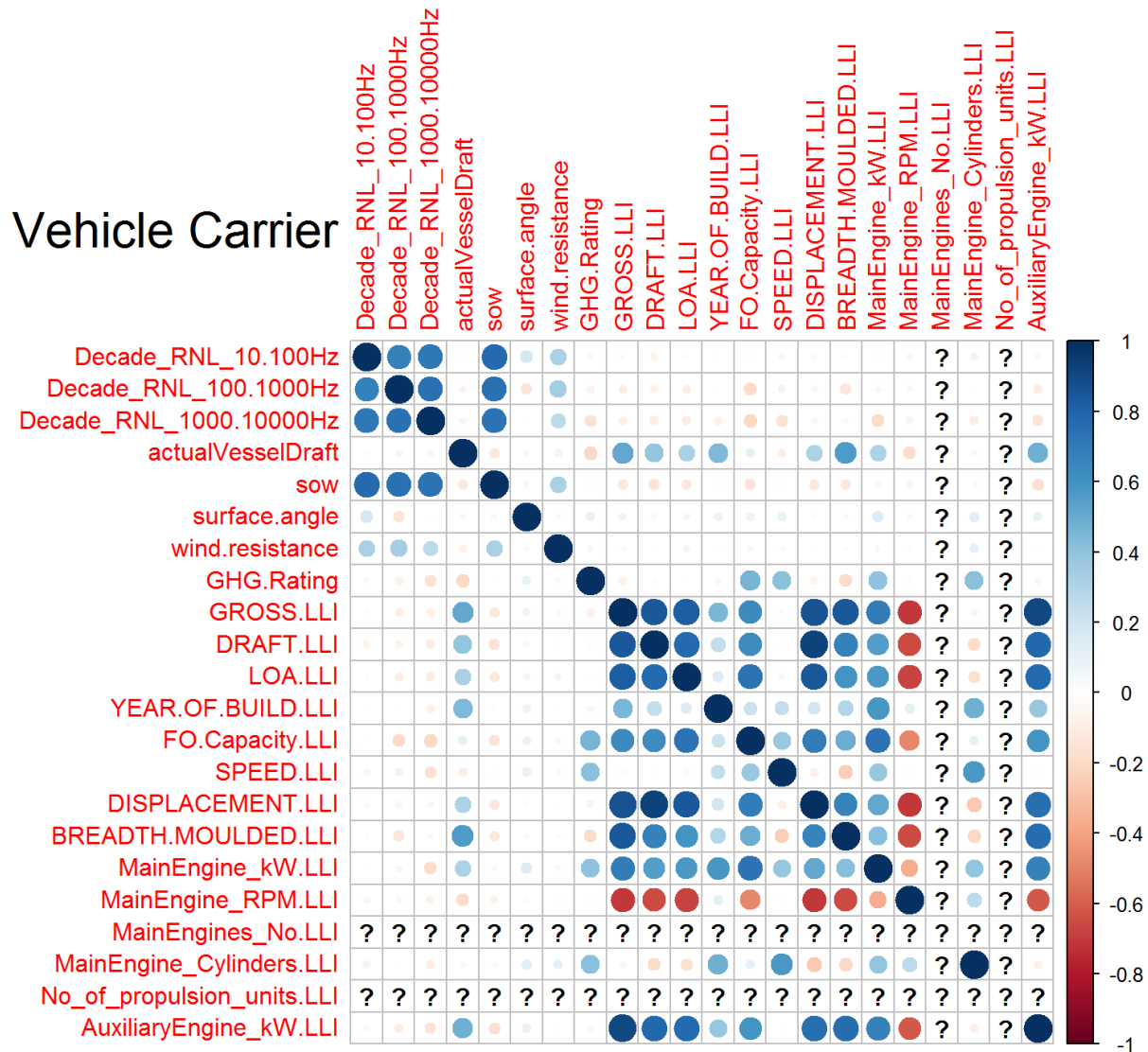
## B.4. Tanker



## B.5. Tugs



## B.6. Vehicle Carriers

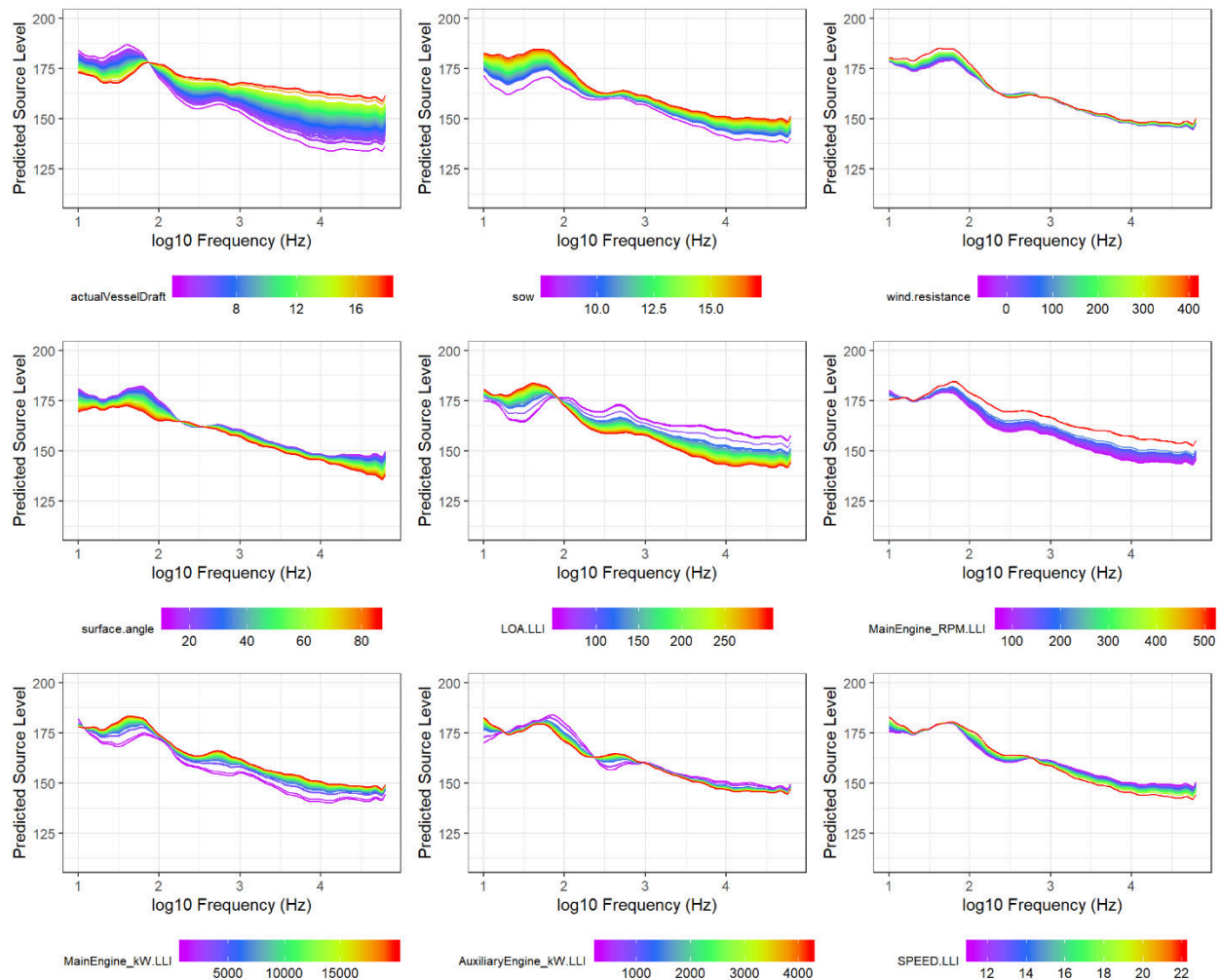


## Appendix C. Multiple-Predictor Functional Regression Results

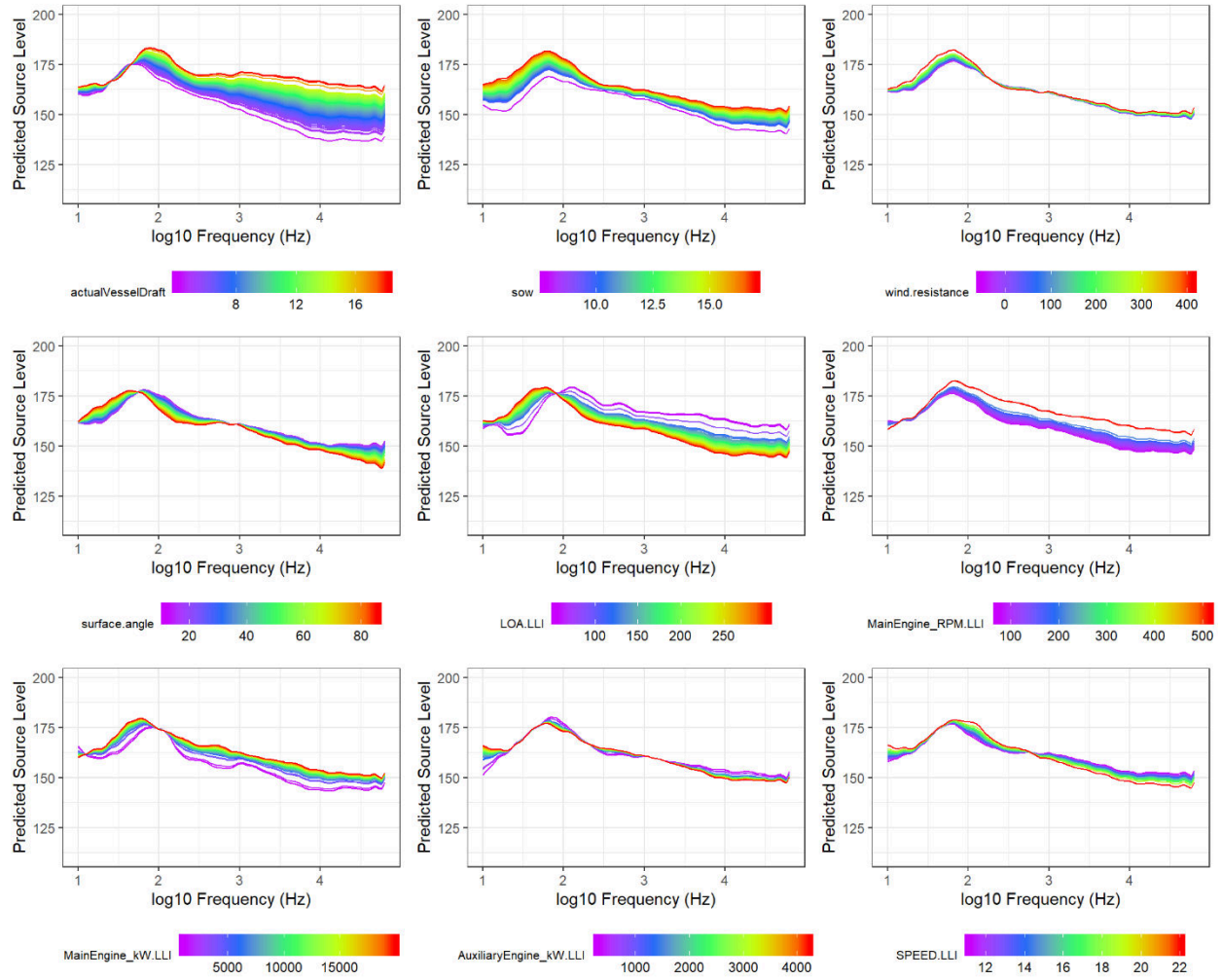
Plots in this appendix show the influence of individual predictors on source levels (dB re 1  $\mu$ Pa m) of an average vessel in each group. The curves show the predicted source levels obtained by changing the value of a single covariate (color-coded) while holding all other covariates at fixed average values. For covariates having more than 200 possible values in the data, 200 values were randomly selected, as well as the minimum and maximum value. Narrow groups of lines correspond to cases where there was very little variation with a given predictor.

### C.1. Bulkers and Tankers

#### C.1.1. MSL

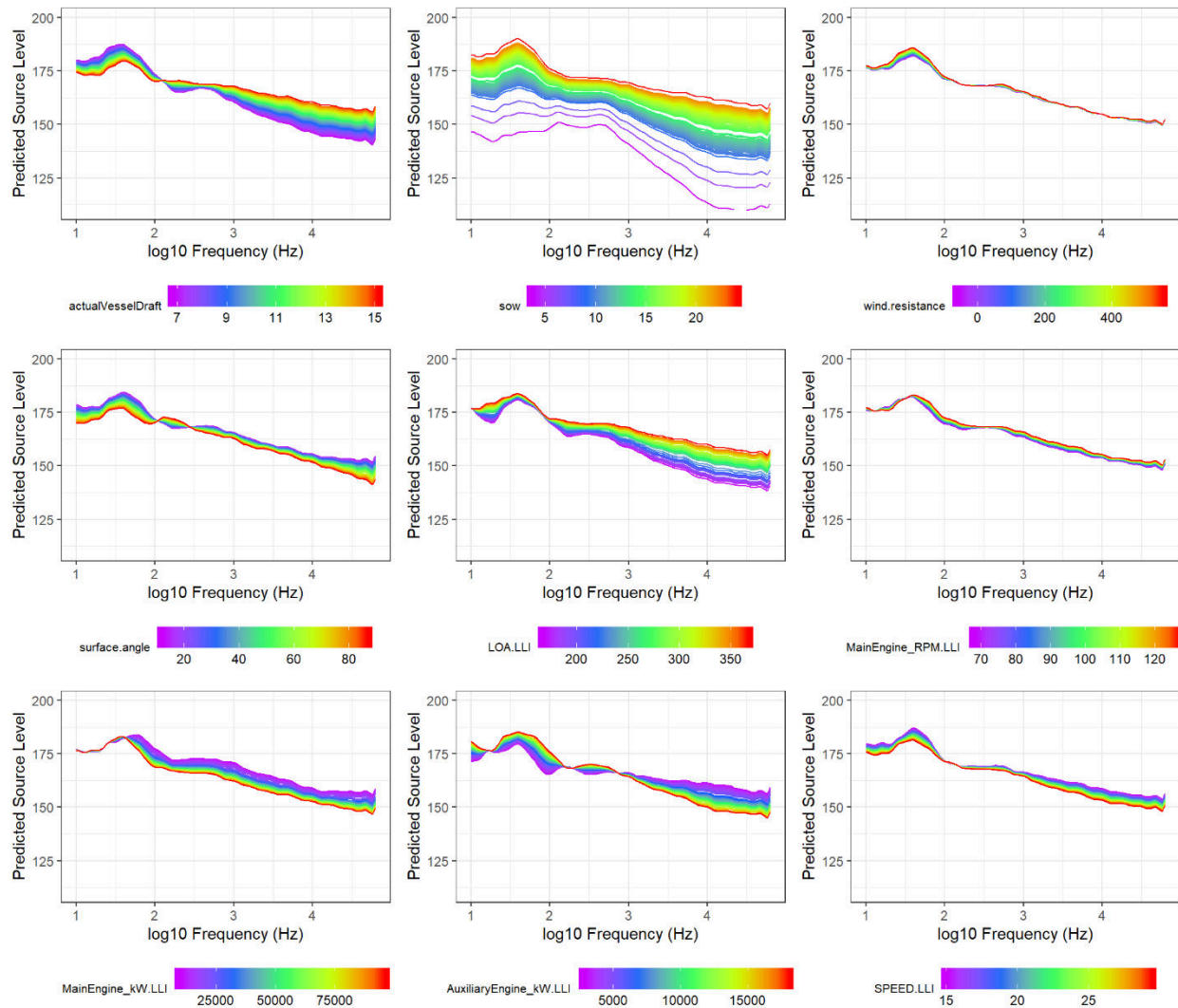


## C.1.2. RNL

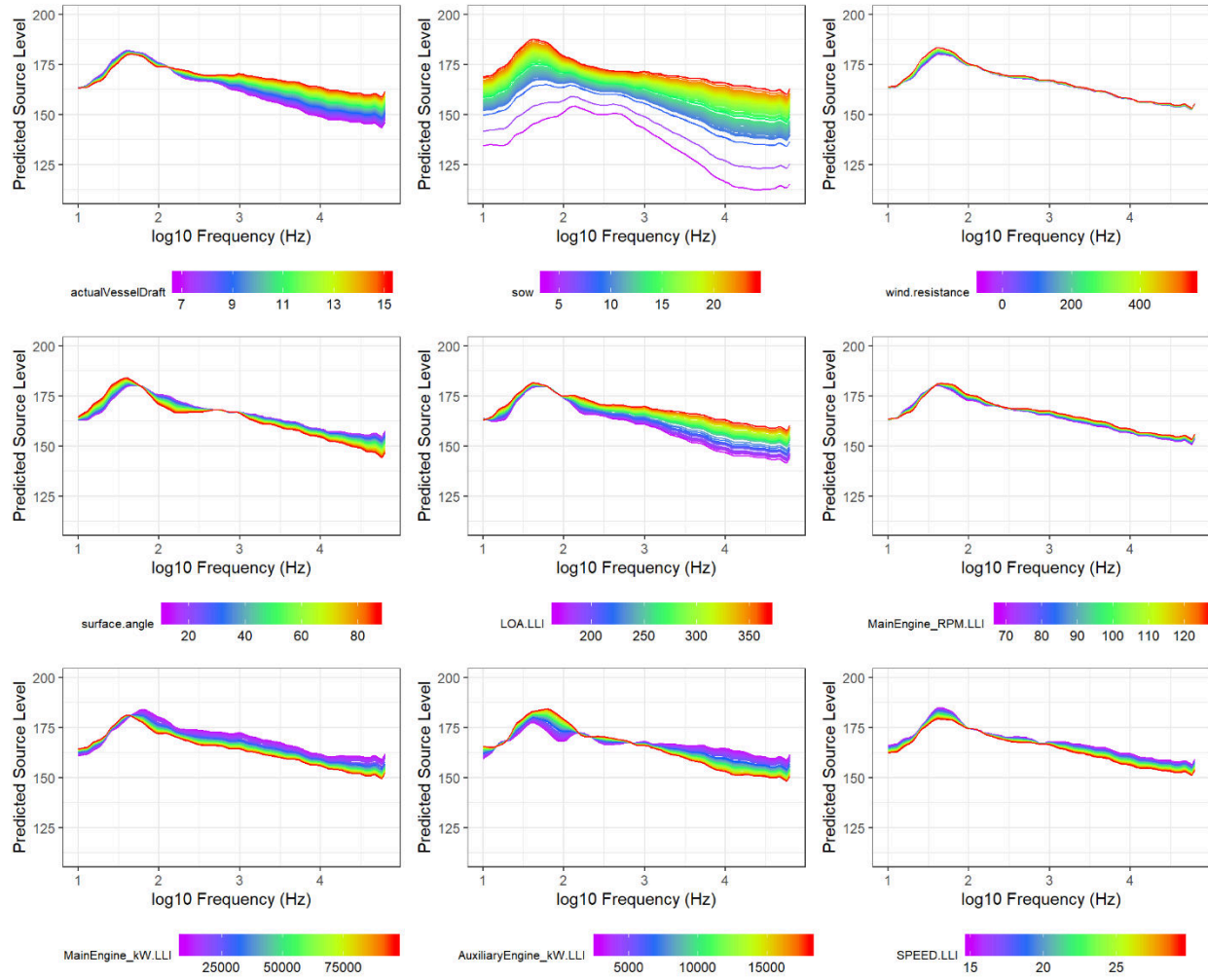


## C.2. Containers and Vehicle Carriers

### C.2.1. MSL

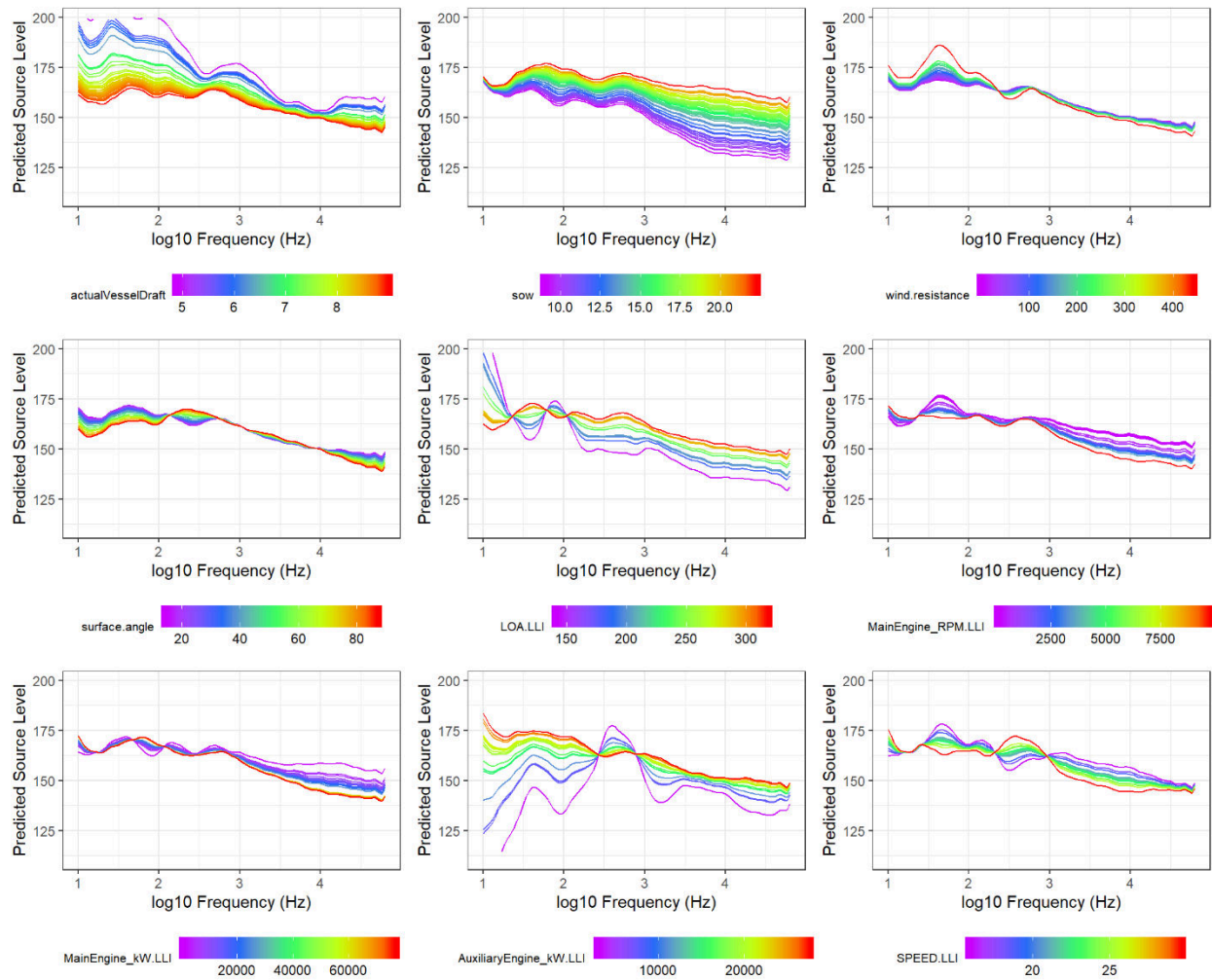


## C.2.2. RNL

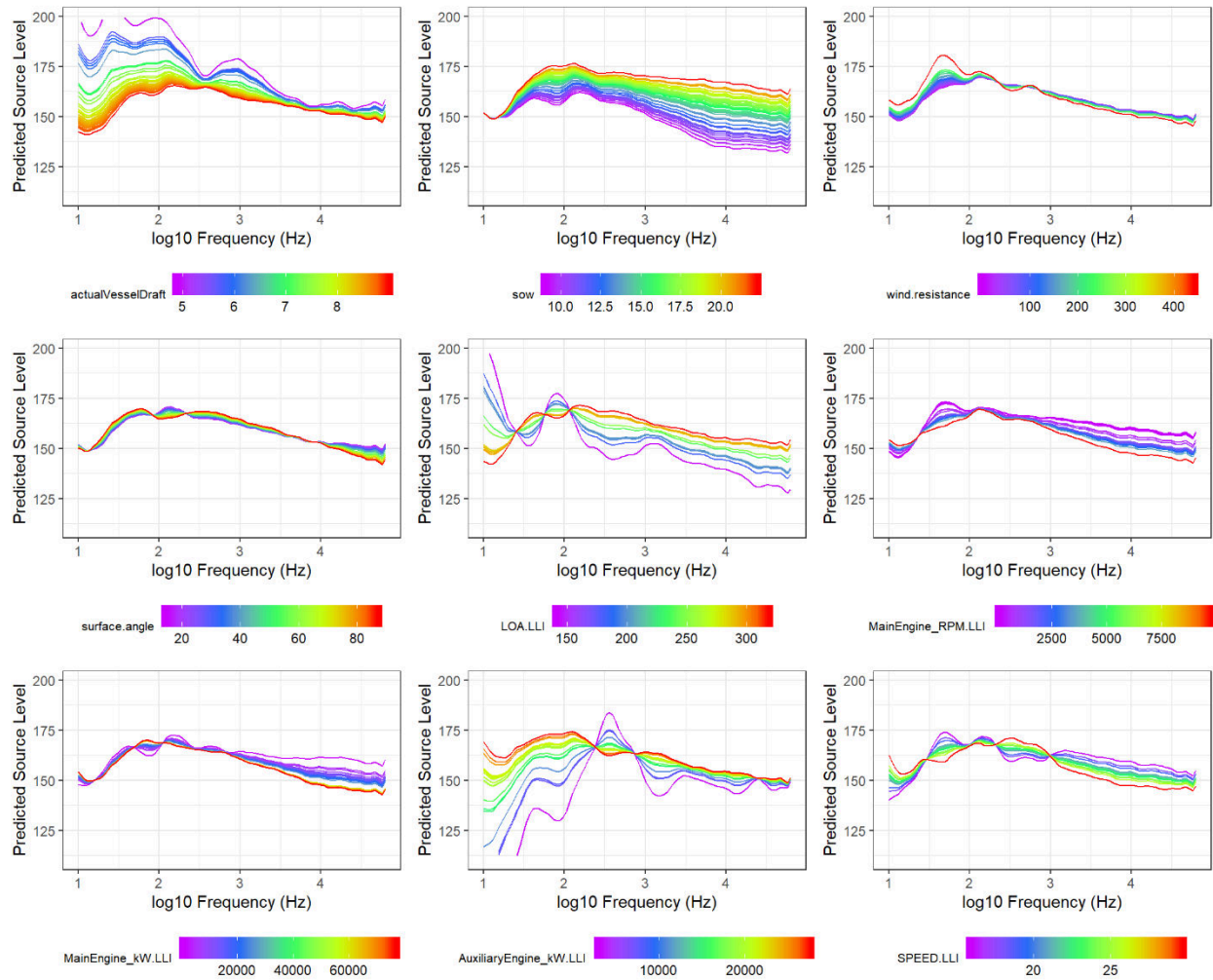


## C.3. Cruise

### C.3.1. MSL

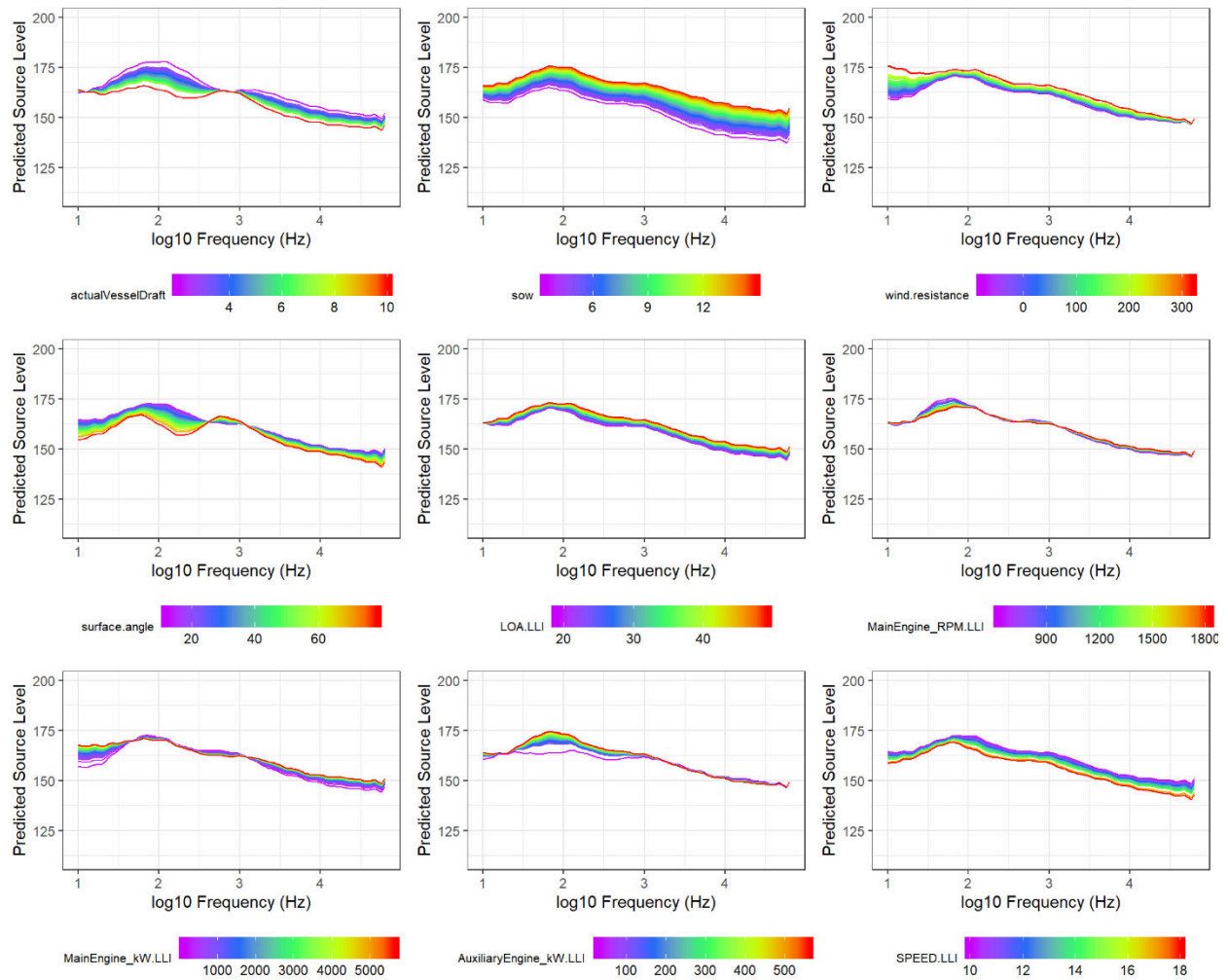


### C.3.2. RNL

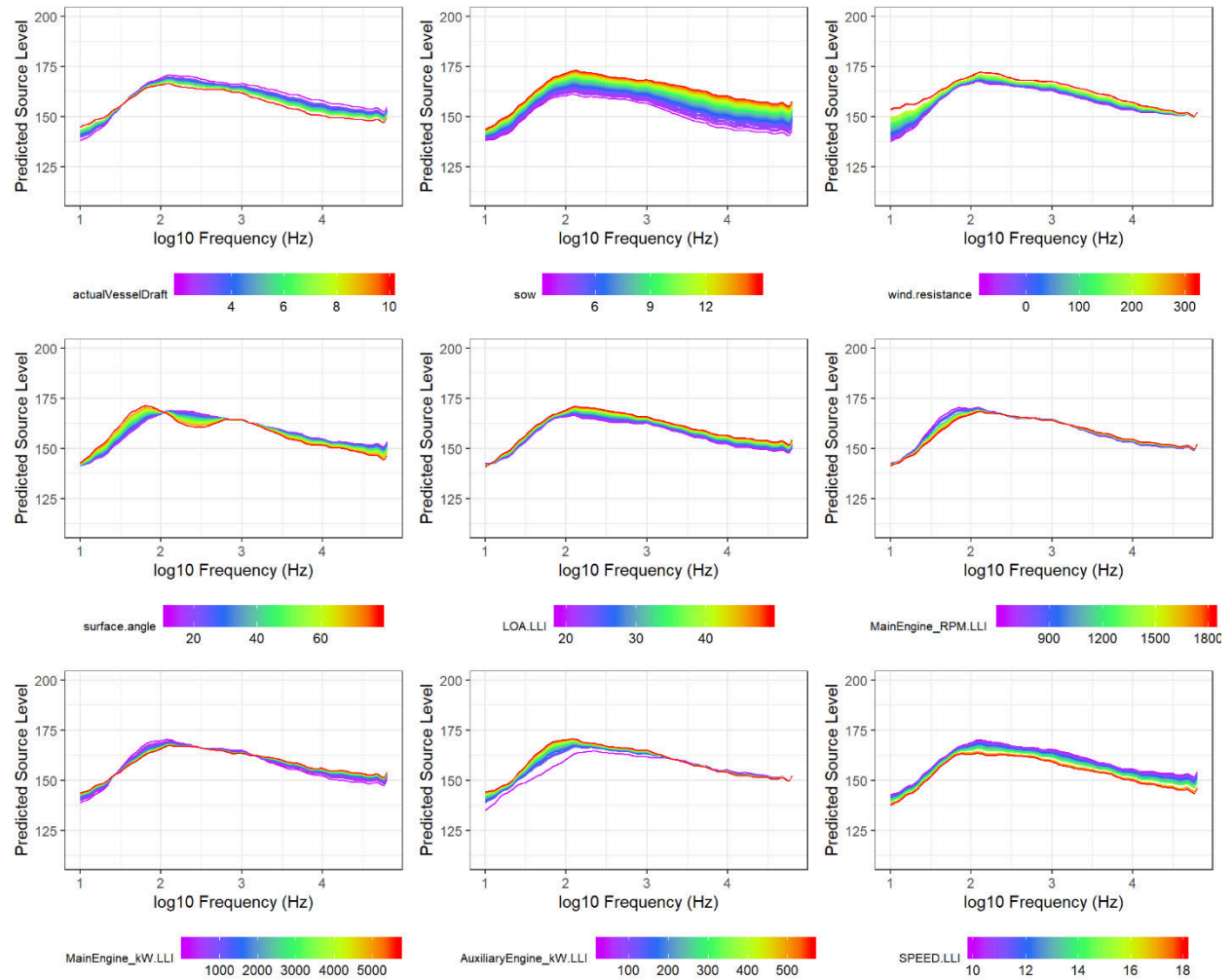


## C.4. Tugs

### C.4.1. MSL



## C.4.2. RNL



## Appendix D. Spectrum Plots

Plots in this appendix show radiated noise spectra for the five loudest and five quietest unique vessel measurements in each category, ranked according to their adjusted RNL (Table D-1). The spectrum levels for each vessel category are displayed using three different types of plots, to highlight features in different frequency ranges:

1. Source spectral density level in 0.125 Hz bins from 0–200 Hz on a linear frequency scale;
2. Source spectral density level in 1 Hz bins from 0–2000 Hz on a linear frequency scale;
3. Source spectral density level in 1 Hz bins from 1–20000 Hz on a logarithmic frequency scale.

The vessel identities in each category have been anonymized and are numbered in order of their ranked RNL (from loudest to quietest). The five loudest vessels are displayed using hot colors (red-orange) and the five quietest vessels are displayed using cool colors (green-blue).

Table D-1. Operating and design characteristics of the vessels shown in the spectrum plots (NA denotes missing data).

Vessel	STW (knots)	Actual draft (m)	Adjusted RNL* (dB re 1 $\mu$ Pa m)	Length (m)	Gross tonnage	Displacement (t)	Breadth (m)	Design speed (knots)	Main engines	Main engine power (kW)	Main engine RPM	Aux. engine power (kW)	Main engine cylinders
<i>Bulker (mean STW = 13.2 kn, mean actual draft = 8.3 m)</i>													
1	14.9	10.7	199.9	292	93695	202845	45.0	16.1	1	15965	91	2674	6
2	12.6	9.23	199.7	198	27192	57250	29.4	15.0	1	7548	104	3130	6
3	9.5	10.17	199.7	176	19831	38916	29.4	14.4	1	6840	129	1549	6
4	11.9	6.49	199.4	229	43827	92645	32.2	14.0	1	9401	127	2047	7
5	11.5	7.64	198.7	190	31532	65242	32.3	15.3	1	8890	116	1823	6
6	14.3	5.8	176.3	171	17977	36122	27.0	16.1	1	6150	136	1496	6
7	14.5	7.8	175.7	225	39736	87908	32.3	16.8	1	10320	89	1978	5
8	13.7	12.59	175.2	190	31781	64663	32.3	16.2	1	8170	96	1828	6
9	13.3	8.5	174.9	209	37158	68262	32.2	16.0	1	11300	105	4101	5
10	11.0	10.9	174.7	180	24785	47102	30.0	14.0	1	7548	NA	1675	NA
<i>Container (mean STW = 16.1 kn, mean actual draft = 10.5 m)</i>													
1	16.4	11.8	199.9	300	94402	145511	48.2	22.2	1	64271	84	12923	9
2	15.3	14.4	197.5	271	70262	105603	42.8	21.2	1	48590	80	10177	NA

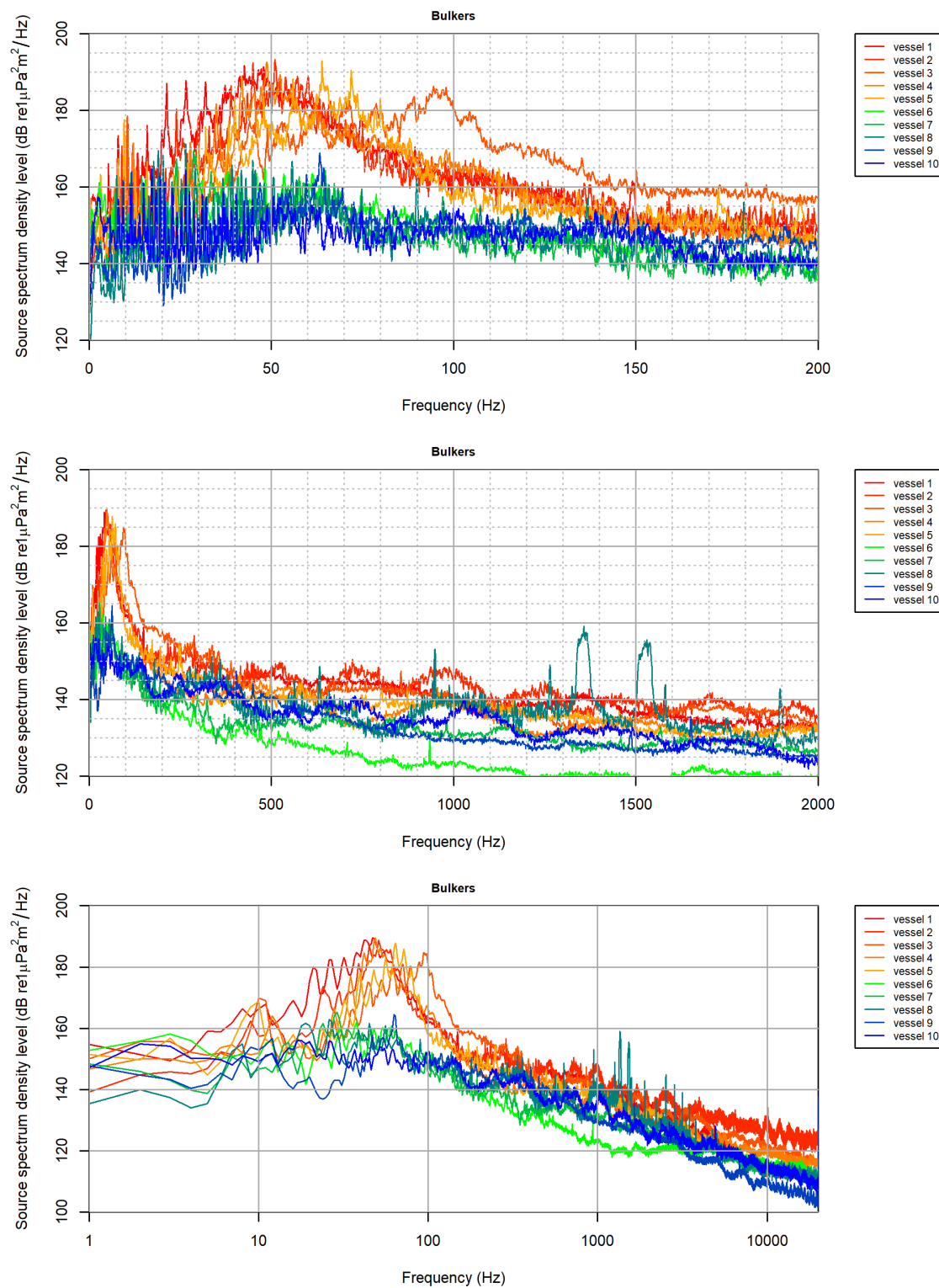
Vessel	STW (knots)	Actual draft (m)	Adjusted RNL* (dB re 1 µPa m)	Length (m)	Gross tonnage	Displacement (t)	Breadth (m)	Design speed (knots)	Main engines	Main engine power (kW)	Main engine RPM	Aux. engine power (kW)	Main engine cylinders
3	18.4	11.7	196.8	276	66199	91944	40.0	26.0	1	54942	102	9698	10
4	18.1	9.8	196.7	300	94402	145490	48.2	22.2	1	64271	84	12923	9
5	13.2	11.4	196.5	328	109712	153834	45.2	22.8	1	74101	84	14594	10
6	17.6	7.7	180.4	183	21583	39123	29.8	19.0	1	12408	105	3917	6
7	17.2	8.75	180.1	255	45169	77120	37.5	21.7	1	25040	95	7119	NA
8	13.5	12.25	180.0	285	68888	88269	40.0	24.5	1	49306	102	10016	12
9	20.1	9.15	179.4	260	39941	66091	32.3	24.5	1	37018	104	6445	8
10	12.8	8.77	178.4	294	54940	87354	32.2	23.5	1	45760	102	8341	9
<i>Cruise (mean STW = 14.4 kn, mean actual draft = 7.7 m)</i>													
1	20.1	8.58	196.4	290	108806	59576	36.0	24.3	2	19000	143	24832	16
2	11.9	8.2	191.8	285	86273	47964	32.3	21.9	1	13788	514	20148	12
3	8.7	8.2	191.0	294	83308	46142	32.3	21.5	5	11693	NA	19523	16
4	9.3	8	189.9	202	61396	34076	32.3	22.0	2	8759	130	14830	16
5	9.1	8.35	188.2	294	90228	52352	32.2	24.0	1	58799	NA	20978	NA
6	17.1	6.3	176.3	199	28890	16222	24.0	21.0	4	12410	160	7520	NA
7	14.9	7.46	175.6	250	68870	42014	32.2	22.8	NA	8821	NA	16447	12
8	11.2	6.98	172.6	196	43188	24496	29.2	19.0	2	6022	750	10803	12
9	14.9	5.8	165.2	181	30277	16974	25.5	18.0	4	4927	720	7845	12
10	10.8	4.9	158.3	142	10944	7192	18.0	16.0	2	1150	186	3137	NA
<i>Tanker (mean STW = 13.2 kn, mean actual draft = 8.3 m)</i>													
1	12.2	6.6	201.3	150	13472	25320	23.2	15.0	1	5922	173	1585	8
2	11.5	10.35	195.2	183	29527	58771	32.2	14.8	1	8684	127	2610	6
3	9.0	9.2	194.6	144	11880	22155	23.0	14.9	1	6300	500	1654	NA
4	11.4	9.35	194.4	148	12105	26214	24.2	17.0	1	6230	158	1671	7
5	13.3	7.2	193.6	183	30241	60807	32.2	15.0	1	9480	129	2650	6

Vessel	STW (knots)	Actual draft (m)	Adjusted RNL* (dB re 1 µPa m)	Length (m)	Gross tonnage	Displacement (t)	Breadth (m)	Design speed (knots)	Main engines	Main engine power (kW)	Main engine RPM	Aux. engine power (kW)	Main engine cylinders
6	14.4	5.1	178.3	170	19391	41733	26.6	16.6	1	7980	120	2183	6
7	12.0	11.7	177.9	183	29354	59900	32.2	14.5	1	8629	NA	2600	NA
8	12.5	10	177.9	181	26218	50180	32.0	15.0	1	8425	NA	2420	6
9	11.5	6	177.5	159	15591	31184	26.6	14.0	1	5792	NA	1739	NA
10	12.0	10.6	177.0	184	28326	61076	32.2	14.5	1	9671	NA	2706	NA
<i>Tug (mean STW = 8.3 kn, mean actual draft = 4.5 m)</i>													
1	5.6	3.6	192.8	34	444	813	10.6	10.5	NA	2621	750	312	NA
2	5.5	5.6	192.3	44	975	1573	11.9	14.0	2	2300	NA	499	16
3	7.3	4.6	190.4	36	199	411	8.0	11.5	NA	1641	NA	194	NA
4	11.4	6.7	189.0	40	1052	1807	12.8	13.4	2	3648	NA	522	NA
5	7.1	3	188.8	28	269	516	9.0	11.5	NA	1771	NA	232	NA
6	5.8	3	168.8	19	81	233	6.2	11.5	2	692	NA	113	NA
7	10.7	4.5	168.8	28	441	623	12.6	11.5	2	1839	NA	311	16
8	8.8	5	168.5	26	150	337	7.4	12.0	1	1081	NA	164	NA
9	5.8	5	167.8	30	358	649	8.8	12.0	NA	2144	NA	275	16
10	6.2	6	167.5	29	203	416	7.9	11.2	2	671	NA	196	NA
<i>Vehicle Carrier (mean STW = 16.1 kn, mean actual draft = 10.5 m)</i>													
1	15.1	9	199.9	188	46346	28222	31.2	20.3	1	11414	127	3474	8
2	15.6	9.05	193.2	200	64546	36974	35.4	20.0	1	13991	102	4385	NA
3	16.7	8.9	192.9	200	63007	38000	32.3	21.6	1	15540	104	4312	8
4	16.6	9.1	192.6	176	41009	24064	31.1	21.5	1	12640	127	3188	8
5	8.9	9.2	192.3	200	56973	32945	32.3	21.6	1	11935	127	4017	8
6	10.5	9.75	180.8	200	69931	36906	35.8	21.2	1	13750	105	4640	NA
7	19.0	8.95	180.4	189	49708	27039	32.3	19.8	1	11526	105	3649	5
8	12.5	7.65	179.8	200	52863	29663	32.2	21.8	1	11180	110	3811	8

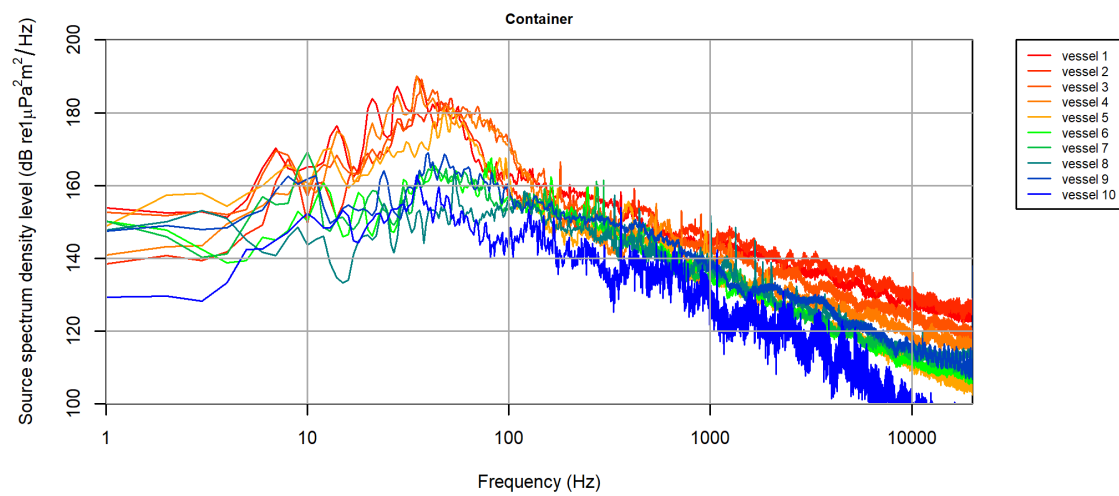
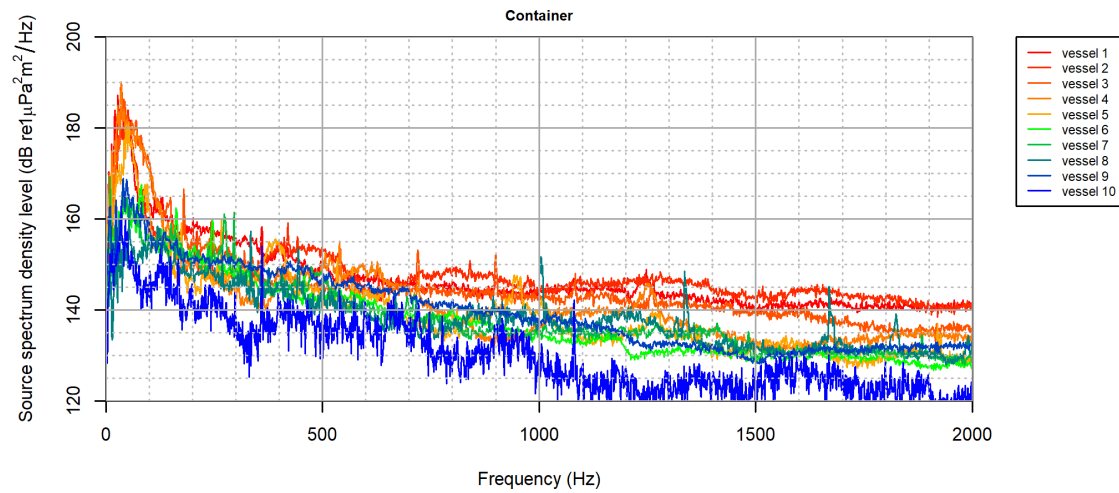
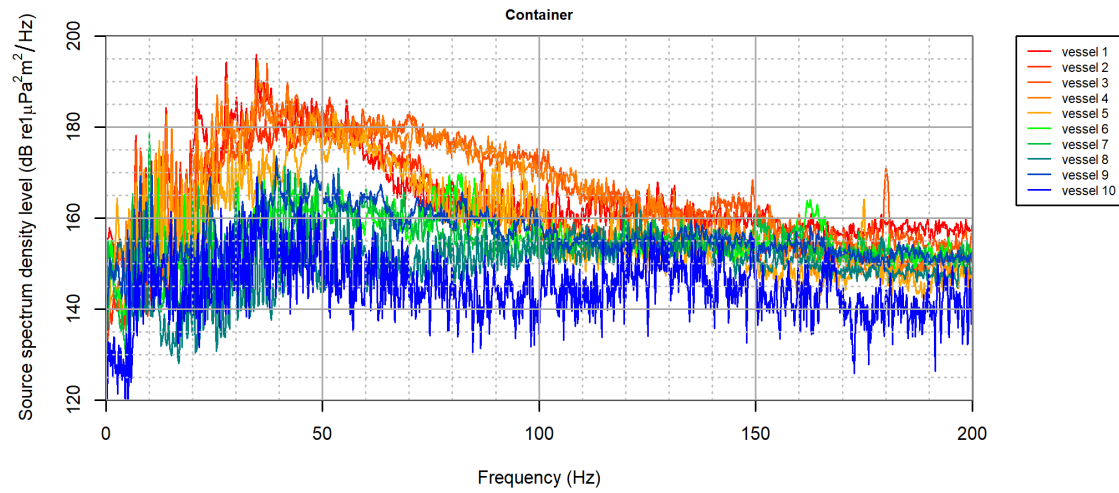
Vessel	STW (knots)	Actual draft (m)	Adjusted RNL* (dB re 1 $\mu$ Pa m)	Length (m)	Gross tonnage	Displacement (t)	Breadth (m)	Design speed (knots)	Main engines	Main engine power (kW)	Main engine RPM	Aux. engine power (kW)	Main engine cylinders
9	15.8	8.6	178.9	199	55598	37774	32.3	20.3	1	16584	NA	3949	8
10	15.2	8.8	177.2	176	41000	23962	31.1	20.8	1	12815	NA	3187	8

\* Adjusted RNL for each measurement was obtained by scaling the measured RNL according to the mean STW and actual draft (by vessel category group), using the multiple-variable functional regression model (Section 2.5.7).

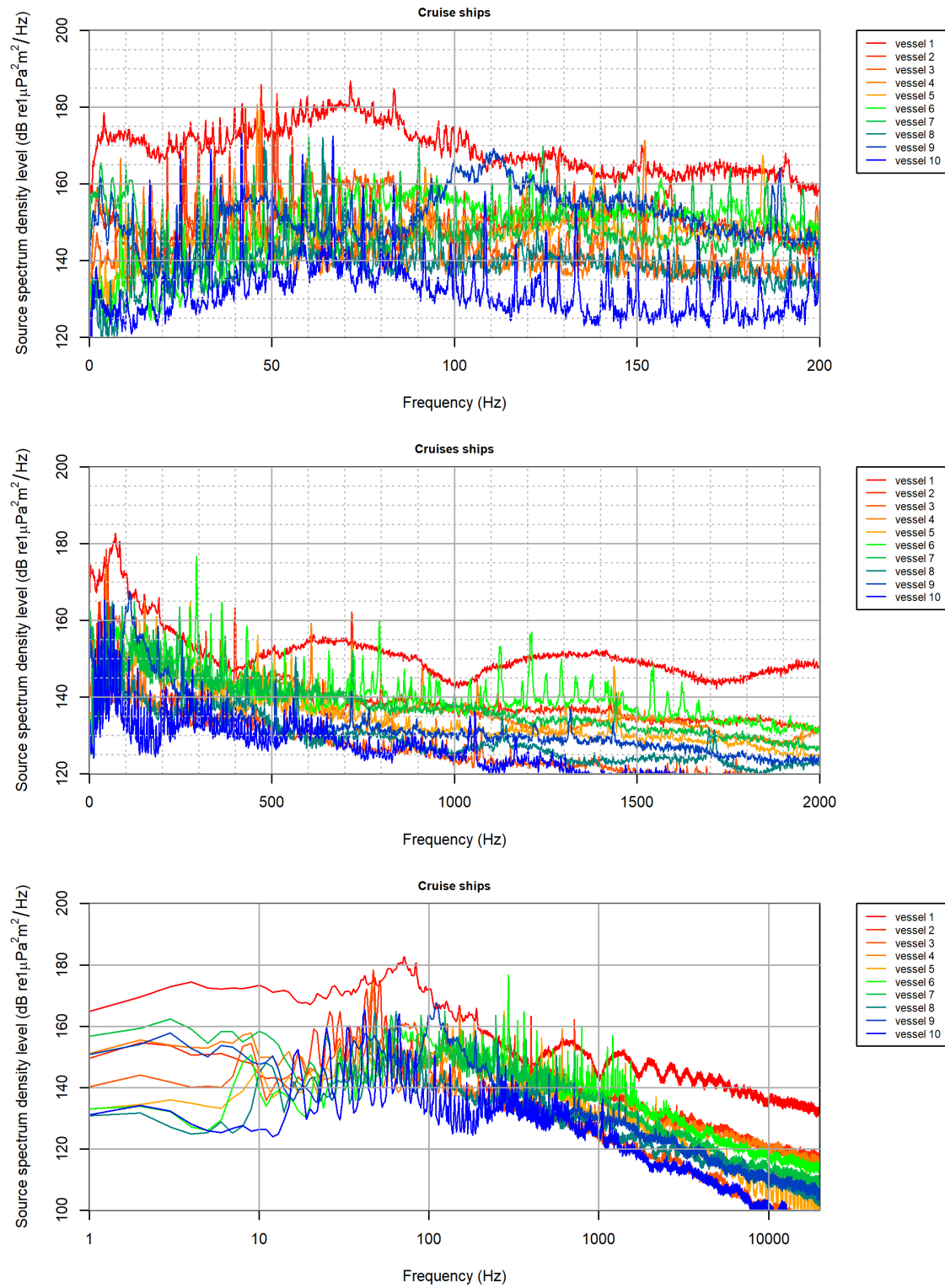
## D.1. Bulkheads



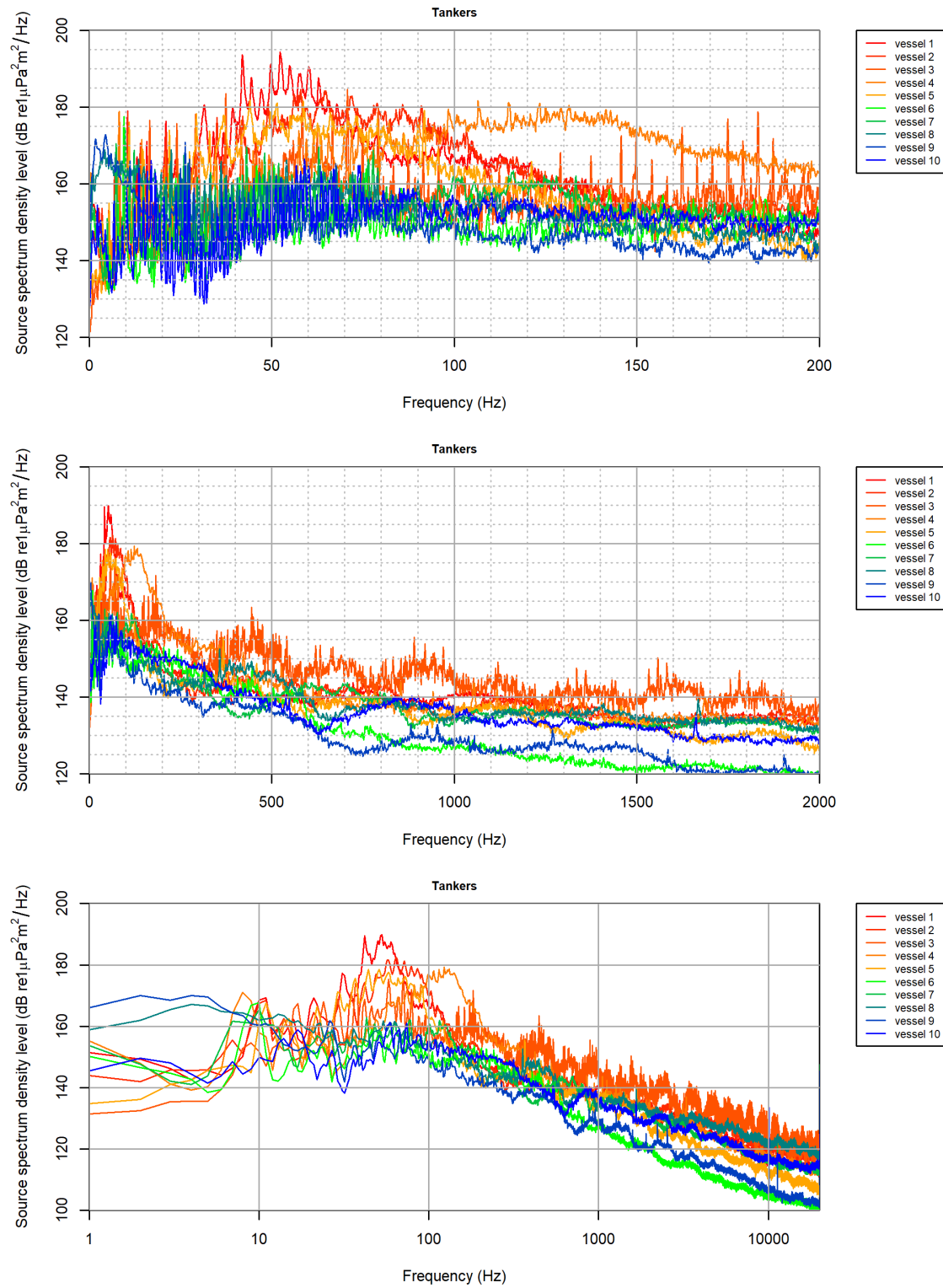
## D.2. Containers



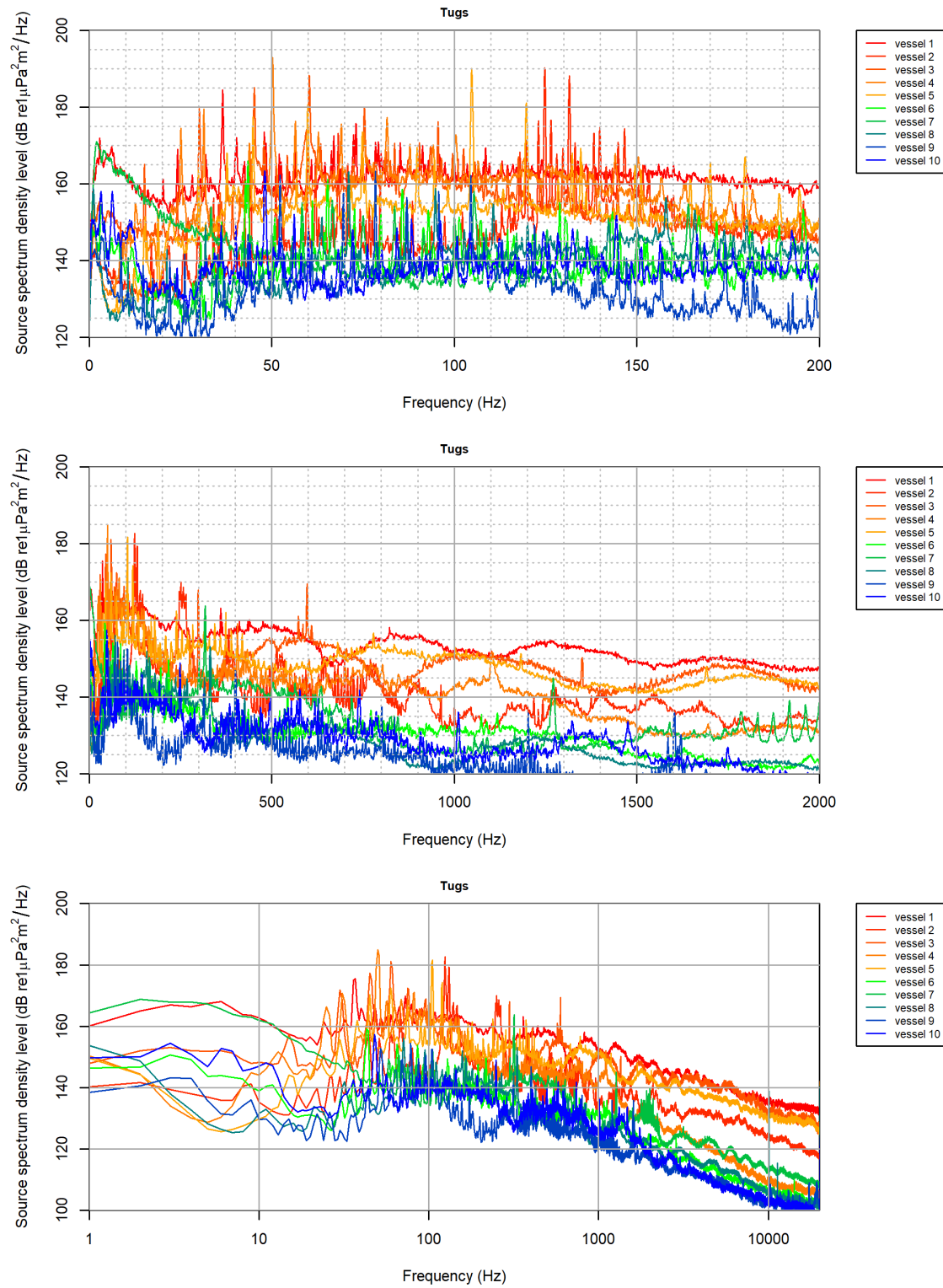
### D.3. Cruise



## D.4. Tankers



## D.5. Tugs



## D.6. Vehicle Carriers

